การแยกอิแนนทิโอเมอร์ของอิพอกไซด์ด้วยแก๊สโครมาโทกราฟี
ที่ใช้อนุพันธ์ของบีตาไซโคลเดกซ์ทรินเป็นเฟสคงที่

นางสาว จิราวิทย์ ญาณจินดา

ENANTIOMERIC SEPARATION OF EPOXIDES BY GAS CHROMATOGRAPHY USING DERIVATIZED β-CYCLODEXTRIN AS STATIONARY PHASE

Miss Jirawit Yanchinda

Thesis Title   Enantiomeric Separation of Epoxides by Gas Chromatography Using Derivatized β-Cyclodextrin as Stationary Phase

By   Miss Jirawit Yanchinda

Field of Study   Chemistry

Thesis Advisor   Assistant Professor Aroonsiri Shitangkoon, Ph.D.

Accepted by the Faculty of Science, Chulalongkorn University in Partial Fulfillment of the Requirements for the Master's Degree

…………………………………….. Dean of the Faculty of Science
(Professor Piamsak Menasveta, Ph.D.)

THESIS COMMITTEE

………………………………………….. Chairman
(Associate Professor Siri Varothai, Ph.D.)

………………………………….……. Thesis Advisor
(Assistant Professor Aroonsiri Shitangkoon, Ph.D.)

………………………………………….. Member
(Assistant Professor Tirayut Vilaivan, D.Phil.)

………………………………………….. Member
(Apichat Imyim, Ph.D.)

จิราวิทย์ ญาณจินดา: การแยกอิแนนทิโอเมอร์ของอิพอกไซด์ด้วยแก๊สโครมาโทกราฟีที่ใช้อนุพันธ์ของบีตาไซโคลเดกซ์ทรินเป็นเฟสคงที่. (ENANTIOMERIC SEPARATION OF EPOXIDES BY GAS CHROMATOGRAPHY USING DERIVATIZED β-CYCLODEXTRIN AS STATIONARY PHASE)

อาจารย์ที่ปรึกษา: ผศ.ดร.อรุณศิริ ชิตางกูร 142 หน้า. ISBN 974-17-6128-7

ได้ทำการแยกคู่อิแนนทิโอเมอร์ของแอโรมาติกอิพอกไซด์ด้วยแก๊สโครมาโทกราฟีที่มี เฮปตะคิส(2,3-ได-*O*-เมทิล-6-*O*-เทอร์ท-บิวทิลไดเมทิลไซลิล)ไซโคลมอลโตเฮปตะโอส (หรือ BSiMe) และเฮปตะคิส(2,3-ได-*O*-อะเซทิล-6-*O*-เทอร์ท-บิวทิลไดเมทิลไซลิล)ไซโคลมอลโตเฮปตะโอส (หรือ BSiAc) เป็นเฟสคงที่ชนิดไคร ลัล ได้ศึกษาผลของชนิดและตำแหน่งของหมู่แทนที่ของอนุพันธ์ของสไตรีนออกไซด์ ที่มีต่อค่ารีเทนชันและค่าการเลือกจำเพาะของอิแนนทิโอเมอร์ นอกจากนี้ ยังได้คำนวณค่าทางเทอร์โมไดนามิกส์ เพื่ออธิบายถึงแรงกระทำระหว่างอิแนนทิโอเมอร์กับเฟสคงที่และค่าการคัดเลือกจำเพาะสำหรับคู่อิแนนทิโอเมอร์ของอิพอกไซด์ที่นำมาศึกษา

อิแนนทิโอเมอร์ของอิพอกไซด์ทุกตัวสามารถแยกได้ด้วยเฟสคงที่ชนิดใดชนิดหนึ่งหรือทั้งสองชนิด พบว่าจำนวน, ชนิด, และตำแหน่งของหมู่แทนที่บนอิพอกไซด์มีผลต่อการคัดเลือกจำเพาะอย่างมากในทั้งสองคอลัมน์ ชนิดของหมู่แทนที่บนโมเลกุลของไซโคลเดกซ์ทริน (BSiMe เทียบกับ BSiAc) มีผลต่อค่าการคัดเลือกจำเพาะของอิแนนทิโอเมอร์ของอิพอกไซด์อย่างมากเช่นกัน ซึ่งคอลัมน์ทั้งสองนี้สามารถใช้เสริมกันได้เป็นอย่างดี เนื่องจากแนวโน้มของการแยกของทั้งสองคอลัมน์ค่อนข้างตรงกันข้าม

ภาควิชา	...............เคมี.............	ลายมือชื่อนิสิต	....
สาขาวิชา	...............เคมี.............	ลายมือชื่ออาจารย์ที่ปรึกษา	....
ปีการศึกษา	..............2547.............	ลายมือชื่ออาจารย์ที่ปรึกษาร่วม	....

JIRAWIT YANCHINDA: ENANTIOMERIC SEPARATION OF EPOXIDES BY GAS CHROMATOGRAPHY USING DERIVATIZED β-CYCLODEXTRIN AS STATIONARY PHASE. THESIS ADVISOR: ASSISTANT PROFESSOR AROONSIRI SHITANGKOON, Ph.D., 142 pp. ISBN 974-17-6128-7

Enantiomeric separations of aromatic epoxides were studied by means of capillary gas chromatography using heptakis(2,3-di-*O*-methyl-6-*O*-*tert*-butyldi methylsilyl)cyclomaltoheptaose (or BSiMe) and heptakis(2,3-di-*O*-acetyl-6-*O*-*tert*-butyldimethylsilyl)cyclomaltoheptaose (or BSiAc) as chiral stationary phases. The effects of substitution types and position of styrene oxide derivatives on retention and enantioselectivity have been investigated. Thermodynamic data on the interaction of enantiomers with chiral stationary phases were collected in detail in order to clarify the strength of analyte-stationary phase interaction and enantioselectivity towards the selected groups of epoxides

All epoxides with different substitution type and position were successfully separated with either BSiMe or BSiAc, or otherwise both of them. On both columns, the number, type, and position of analyte substitution have a strong influence on enantioselectivity. The type of substituent on cyclodextrin molecule (BSiMe vs. BSiAc) also affect enantioselectivity of epoxides greatly. Both columns can be used to compliment one another as their resolving abilities are quite opposite.

Department	.........Chemistry…..	Student's signature ....
Field of study	.........Chemistry…..	Advisor's signature ....
Academic year	.... 2004……..	Co-advisor's signature ....

ACKNOWLEDGEMENTS

CONTENTS

CONTENTS (Conts)

LIST OF TABLES

LIST OF FIGURES

LIST OF FIGURES (Cont.)

FIGURES   **PAGE**

LIST OF FIGURES (Cont.)

LIST OF ABBREVIATIONS AND SYMBOLS

BSiAc	=	heptakis(2,3-di-*O*-acetyl-6-*O*-*tert*-butyldimethylsilyl)cyclomalto heptaose
BSiMe	=	heptakis(2,3-di-*O*-methyl-6-*O*-*tert*-butyldimethylsilyl)cyclomalto heptaose
CD	=	cyclodextrin
°C	=	degree celsius
GC	=	gas chromatography
i.d.	=	internal diameter
K	=	distribution coefficient
k′	=	retention factor or capacity factor
m	=	meter
m	=	molality (mol/kg)
mm	=	millimeter
min	=	minute
N	=	number of theoretical plates
OV-1701	=	14% cyanopropylphenyl 86% dimethyl polysiloxane
R	=	universal gas constant (1.987 cal/mol$^.$K)
R^2	=	correlation coefficient
SN	=	separation number
T	=	absolute temperature (K)
t'_R	=	adjusted retention time
α	=	separation factor or selectivity
ΔH	=	enthalpy change
$\Delta(\Delta H)$	=	difference in enthalpy for an enantiomeric pair
ΔS	=	entropy change
$\Delta(\Delta S)$	=	difference in entropy for an enantiomeric pair
μm	=	micrometer

CHAPTER I

INTRODUCTION

Chirality has been of great interest because the majority of bioorganic molecules are chiral and, in nature, they exist in only one of the two possible enantiomeric forms, e.g. amino acids in the L-form and sugars in the D-form. Living organisms are composed of chiral biomolecules such as amino acids, sugars, proteins and nucleic acids and they show different biological responses to one of a pair of enantiomers in drugs, pesticides, or waste compounds, etc. [1-3]. Chirality is also a major concern in the modern pharmaceutical industries since enantiomers of a racemic drug may have different pharmaceutical activity. One enantiomer may produce the desired therapeutic activities, while the other may be inactive or introduce unwanted effects, such as ethambutol and levodopa. The (S,S)-form of ethambutol is an antituberculostatic agent but the (R,R)-form causes optical neuritis that can cause blindness [3]. The Parkinson's disease drug levodopa (Dopa) is marketed as an enantiomerically pure (S) form because the (R)-Dopa causes serious side-effect such as granulocytopenia (a loss of white blood cells that leaves patient prone to infections) [3]. In order to avoid any possible undesirable effects of enantiomer, there is a great need to develop new technologies that provide pure single enantiomers.
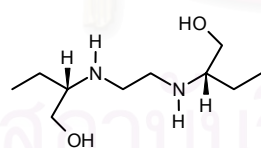
(S,S)-ethambutol: antituberculostatic   (R,R)-ethambutol: optical neuritis
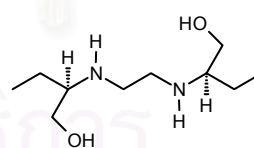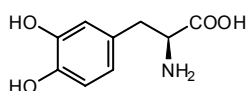
(S)-Dopa: anti-Parkinson   (R)-Dopa: granulocytopenia
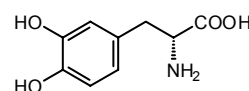
Figure 1.1   Chemical structures and biological activities of ethambutol and Dopa

There are two basic approaches to acquire purely single enantiomer of chiral compounds: asymmetric synthesis and separation of enantiomers. Currently, asymmetric synthesis is a topic that arouses a lot of interest and is dynamically developing. Chiral auxiliary or catalyst of high purity is generally utilized in the synthesis. As a consequence, enantiomeric separation techniques are highly required not only to resolve enantiomers but also to control and analyze enantiomeric purity of chiral reagents, auxiliary, catalysts and products in the asymmetric synthesis. Moreover, in principle, it should be the most cost-effective method for producing single-enantiomer products, because all the precursors are converting to desired enantiomers.

In general, chromatography and electrophoresis are used for the analysis of enantiomers due to their simplicity and efficiency. Today, complex mixtures are mostly resolved on capillary columns by direct gas chromatography (GC) owing to its high efficiency, sensitivity, and speed of analysis. There are a few preconditions connected to the use of GC technique, among which the thermostability of organic compounds and sufficient volatility of analytes are the most important ones. Primarily, the applications of enantioselective GC involve the accurate determination of enantiomeric ratio of chiral research chemicals, intermediates, metabolites, precursors drugs, pesticides, fungicides, herbicides, pheromones, flavors and fragrances [4].

The separation of optical isomers by GC can be accomplished by two approaches. The first approach involves the conversion of enantiomers into diastereomers, followed by separation with conventional stationary phases. The other and more preferable approach is based on the separation of enantiomers directly on chiral GC stationary phases. The most utilized type of chiral stationary phases nowadays is derived from cyclodextrins (CDs). The chiral discrimination ability of CD is based on the size of the CD cavity and the interactions between analytes and functional groups of CD. It is generally perceived that the resolution of chiral analytes occur through the intermediate formation of diastereomer between the chiral analyte and the CD molecule, whereby the interaction occurs both rapidly *via* fast kinetics and reversibly *via* distinct thermodynamics [5].

Undoubtedly knowledge about separation mechanisms is advantageous in designing and improving separation system. Indeed, the mechanistic aspects of enantioselective GC separation with CD derivatives as chiral stationary phases are extremely complicated and have not been entirely understood yet. In practical, selecting the most appropriate chiral stationary phase for the resolution of a group of chiral molecules with different chemical structures and molecular geometry is still a matter of trial and error process, and requires extensive experience.

Of all contributions to chiral recognition, analyte structure seems to be one of the crucial factors in chiral separation system. Nonetheless, only a few studies into the relationship between enantioselectivities of CD derivatives and chiral analytes were previously carried out [6-18]. Therefore, this research aims at systematic investigation into the influence of substituent type and position of styrene oxide on the enantiomeric separation. Epoxides were selected as the analytes of interest owing to their importance as chiral intermediate in the asymmetric synthetic pathway of pharmaceuticals, such as propanolol. Styrene oxide and its derivatives with various substituent types at *ortho*-, *meta*-, and *para*-positions are used as chiral analytes. They were separated by GC using heptakis(2,3-di-*O*-methyl-6-*O*-*tert*-butyldimethylsilyl) cyclomaltoheptaose (or BSiMe) and heptakis(2,3-di-*O*-acetyl-6-*O*-*tert*-butyldimethyl silyl)cyclomaltoheptaose (or BSiAc) as chiral selectors. Both derivatized β-CDs were separately dissolved in polysiloxane before using as chiral stationary phases. These two phases have been used successfully for chiral separation in GC [19-28]. Thermodynamic investigation was also performed in order to acquire greater insight about the interaction between epoxide analytes and CD derivatives. Hopefully, the interpretation of the data obtained from this work will provide some mechanistic knowledge about the influence of analyte structure on enantioselective selector-analyte binding interaction. This would enhance the possibility of selecting the most suitable chiral stationary phase and separation condition for the chiral recognition of these epoxide analytes, including other epoxides having similar structure to the test compounds.

CHAPTER II

THEORY

2.1   Gas chromatographic separation of enantiomers

Gas chromatographic method was considered one of the most valuable techniques for enantiomeric separation of volatile and thermally stable compounds. The separation could be accomplished by either indirect or direct approaches. In the indirect approach, a racemic mixture was reacted with a chiral reagent to form a pair of diastereomers. Since diastereomers possess different physical and chemical properties, they can be separated in an achiral environment using a nonchiral column [2]. The disadvantages of this method include long analysis time (sample preparation and identification); inconvenience (if the recover of pure enantiomers is needed after separation); the need for enantiomerically pure derivatizing agent; and possible biased results for enantiomeric composition due to partial racemization during derivatization [2]. Moreover, the derivatization process may cause discrimination due to kinetic resolution, incomplete recovery, decomposition, or loss during work-up, isolation, and sample handling [2, 29-30].

The direct enantiomer separation, a more effective and commonly used approach, is based on the formation of transient diastereomeric complexes between the enantiomers and the chiral molecule that is an integral part of the stationary phase. Several types of chiral selectors have been formally reported, i.e. amino acid and dipeptide derivatives, chiral transition metal complexes, and linear or cyclic carbohydrate derivatives [2, 29-31]. Among these, cyclodextrin derivatives are preferentially used as chiral selectors in direct gas chromatography.

2.2   Cyclodextrins and their derivatives

Cyclodextrins (CDs) are cyclic, $(1\rightarrow4)$-linked oligomers of α-D-glucopyranose, with each D-glucopyranosyl residue being in the $^4C_1$ conformation (Figure 2.1a). The three most important cyclodextrins consist of six, seven, and eight

α-D-glucopyranosyl residues, respectively. They are systematically named cyclomaltohexaose, cyclomaltoheptaose, and cyclomaltooctaose or, commonly known as alpha-, beta-, and gamma-cyclodextrins, respectively. Molecular dimension and some physical properties of three cyclodextrins are compared in Table 2.1.

(a)

(b)
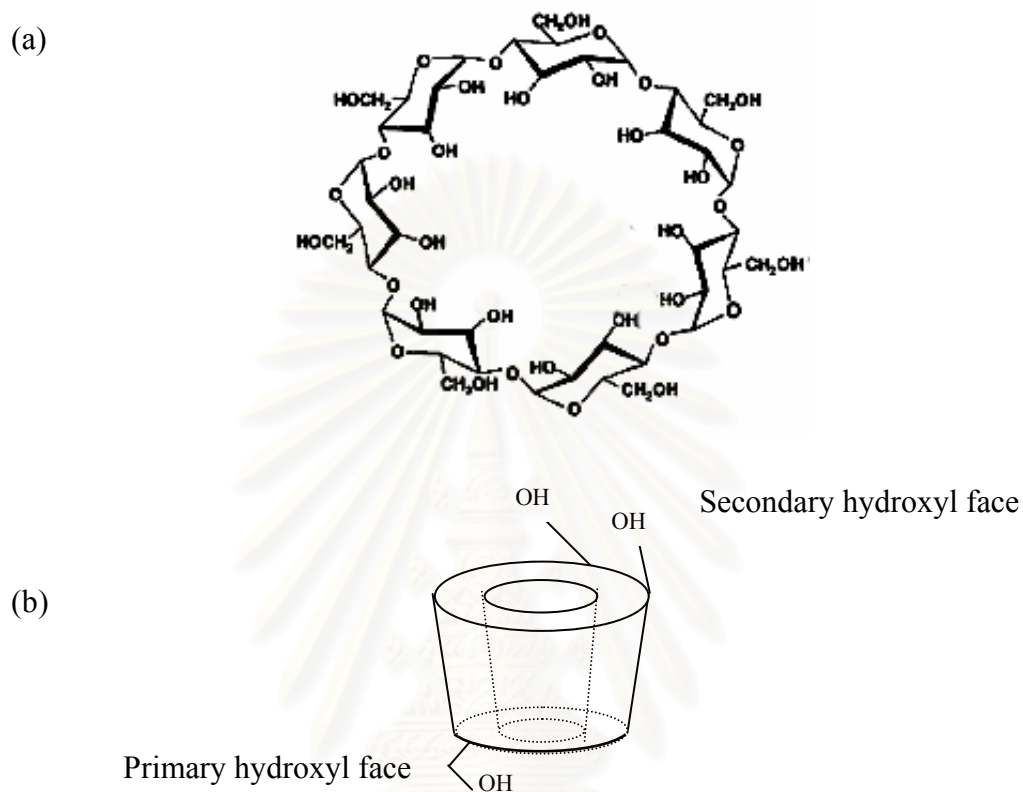
Figure 2.1 (a) Schematic structure of β-cyclodextrin [35].

(b) Schematic representation of hydroxyls located on the edge of β-cyclodextrin

Table 2.1   Molecular dimension and physical properties of cyclodextrins [36]

cyclodextrin	α	β	γ
number of glucose units	6	7	8
number of chiral centers	30	35	40
molecular weight	972.86	1135.01	1297.15
cavity diameter (Å)	4.7-5.3	6.0-6.5	7.5-8.3
volume of cavity (Å)^3	174	262	427
solubility in water (g/100 mL, 25 °C)	14.50	1.85	73.20
decomposition temperature (°C)	278	299	267

Native cyclodextrins possess two types of hydroxyls in their molecule: one is the secondary hydroxyl at the C2 and C3 chiral carbons of cyclodextrin along the large rim, the other is the primary hydroxyl at the C6 carbons along the small rim of cyclodextrin molecule. The molecule, in reality, is a doughnut or wreath-shaped truncated cone (Figure 2.1b). The outside of the molecule is hydrophilic while the inside is relatively hydrophobic. Because of their macrocyclic, conical structure and inherent chirality, CDs (as host molecules) are able to form diastereomeric complexes with a wide variety of guest molecules and the properties of encapsulated molecules, e.g. water solubilities, chemical stabilities, etc., are modified by this complex formation [34]. Consequently, CDs have turned out to be very versatile selectors for isomer and enantiomer separation [4, 28, 30-33].

2.3   Gas chromatographic separation of enantiomer with cyclodextrin derivatives

Based on previous studies [6-11, 25-27], the enantioseparation by GC using CD derivatives as chiral stationary phases is influenced by several parameters: chemistry of CD selector such as ring size, type and position of derivatization; CD concentration dissolved in polysiloxane matrix; polarity of polysiloxane matrix; chemical structure of enantiomers to be resolved; and separation temperature.

The CD ring size and the substituents of glucose units at C2, C3, and C6 positions considerably affect not only chemical and physical properties but also enantioselectivity of CD derivatives. Owing to the differences in the number of glucose units in their structure, α, β, and γ-CDs possess different cavity size. This affects inclusion-complexation mechanism of some analytes, which can completely or partly accommodate in the CD cavity.

Natural underivatized CDs were proved to be unfavorable for use as stationary phases in capillary GC because they are solid at room temperature, have limited operating temperature range and have low solubility in polysiloxane diluent. Therefore, they are unsuitable for coating capillary columns and give columns with very low efficiency. In addition, due to the presence of a large number of hydroxyl

groups, natural cyclodextrins can be chemically modified and accordingly yield numerous types of derivatives with improved physical and chemical properties such as water solubility and complexing behavior [36]. In general, substituents at chiral C2 and C3 positions are modified to small alkyl or acyl groups to increase enantioselectivity, while longer alkyl or bulky groups are substituted at C6 positions to change polarity, viscosity, or solubility in polysiloxane [28, 36]. However, it was recently reported that the bulky groups, such as *tert*-butyldimethylsilyl, at C6 position have an influence on the conformation of the CD ring, which in turn can impact on the enantioselectivity [4]. For most cyclodextrin derivatives that are still solid at room temperature and cannot be coated directly onto column wall, high efficient capillary columns can only be prepared by using cyclodextrin derivatives mixed in viscous polysiloxane as stationary phases. These columns were proved to be useful over a broad temperature range [28].

Enantioseparation of epoxides by GC using derivatized CDs as chiral stationary phases were reviewed as follow:

Li et al. [6] evaluated the performance of chiral GC stationary phase based on 2,6-di-*O*-pentyl-3-*O*-trifluoroacetyl (DP-TFA) liquid derivatives of α-, β-, and γ-CDs. More than 150 pairs of enantiomers, including chiral alcohols, diols, polyols, amines, amino alcohols, halohydrocarbons, lactones, α-halocarboxylic acid esters, carbohydrate, epoxides, nicotine compounds, pyrans and furans, were resolved on 10 m wall-coated fused silica capillary columns. Among three modified CDs, DP-TFA-γ-CD exhibited the broadest chiral selectivity for various types of aliphatic and aromatic epoxides, including glycidyl analogues and haloepihydrins.

Armstrong et al. [7] studied the effect of ring size on enantiomeric separation by using three types of (2,6-di-*O*-pentyl) derivative of α-, β- and γ-CDs. The largest number of compounds was separated on the derivatized β-CD column. Nonetheless, the dipentyl-α-CD was clearly superior at resolving a variety of epoxide racemates (such as 1,2-epoxyoct-7-ene; glycidyl isopropyl ether; limonene oxide; styrene oxide) and other cyclic ethers which were difficult to separate on larger CD stationary phases.
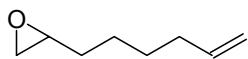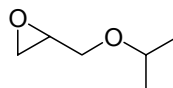
1,2-epoxyoct-7-ene   glycidyl isopropyl ether

Schurig et al. [8] studied the influence of substituent type on cyclodextrin ring based on heptakis(2,3,6-*O*-trimethyl)-β-cyclodextrin; heptakis(2,6-*O*-dimethyl-3-*O*-trifluoroacetyl)-β-cyclodextrin and heptakis(2,6-*O*-dimethyl-3-*O*-heptafluorobutyryl)-β-cyclodextrin in moderately polar polysiloxane OV-1701 on the separation of racemic methyl-substituted styrene oxides. The three phases showed different enantioselectivities. On heptakis(2,6-*O*-dimethyl-3-*O*-trifluoroacetyl)-β-cyclodextrin, three racemic methyl-substituted styrene oxides could be resolved. Nevertheless, styrene oxide could not be separated under similar condition.
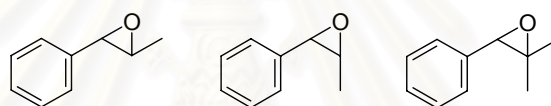
methyl-substituted styrene oxides

Reiher and Hamann [9] investigated the separation properties of perpentylated α-cyclodextrin for the enantioselective separation of aliphatic and aromatic epoxides. The results showed that both 1,2-aliphatic and 1,2-aromatic epoxides (i.e. 1,2-epoxyheptane; 1,2-epoxyheptane; 1,2-epoxyheptane; styrene oxide; 1,2-epoxy-3-phenylpropane) could not be separated. On the contrary, 2,3-epoxyoctane and 3,4-epoxy-4-methylpentan-2-one could be well resolved. This indicated that the asymmetric carbon of guest molecule must be in a position favorable for interaction with one of the chiral center of cyclodextrin.
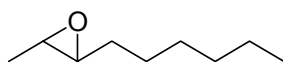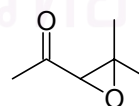
2,3-epoxyoctane   3,4-epoxy-4-methylpentan-2-one

Jung and Schurig [10] investigated the effect of chemical structure of analytes on selectivity. Different types of analytes, e.g. ketones, alcohols, epoxides, were examined on heptakis(2,6-di-*O*-methyl-3-*O*-trifluoroacetyl)-β-cyclodextrin

chemically bonded to polydimethylsiloxane (also known as Chirasil-Dex-TFA). For styrene oxide and methyl-substituted styrene oxides, they were resolved with high enantioselectivity on Chirasil-Dex-TFA.
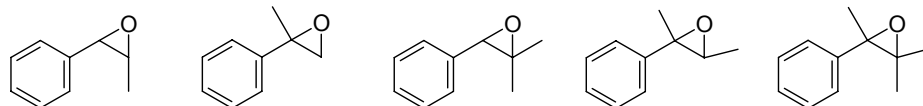
methyl-substituted styrene oxides

König and Gehrcke [11] studied the gas chromatographic separation of enantiomer of 20 aliphatic and aromatic epoxides on 2,6-di-*O*-methyl-3-*O*-pentyl-β-cyclodextrin mixed in polysiloxane. All of them could be separated and, among these, styrene oxide showed the highest enantioselectivity. For 1,2-epoxy alkanes, it was observed that enantioselectivity decreased as the alkyl chain length increased. The shortest aliphatic epoxide in this study, 1,2-epoxyhexane, was separated with the greatest enantioselectivity on this phase.

The (6-*O*-*tert*-butyldimethylsilyl) derivatives of β-cyclodextrin have been proved to be valuable chiral selectors and are widely used for enantiomer separation by GC. These derivatives have been used to separate variety classes of compounds. Their enantioselectivities as well as some selected applications were summarized as follow:

Klobes et al. [25] used heptakis(6-*O*-*tert*-butyldimethylsilyl-2,3-di-*O*-methyl)-β-cyclodextrin as chiral stationary phase to separate 9 compounds of technical toxaphene (CTTs). Eight enantiomers of CTTs could be resolved individually; however, several compounds coeluted when they were analyzed as a mixture. Technical toxaphene is synthetic pesticide containing several hundred polychlorinated bornanes most of which are chiral. So far, separation of CTT enantiomers has been achieved only on *tert*-butyldimethylsilyl derivatives of β-CD. It was believed that the bulky *tert*-butyldimethylsilyl groups influence the conformation of the CD molecule and, consequently, the enantioselectivity.
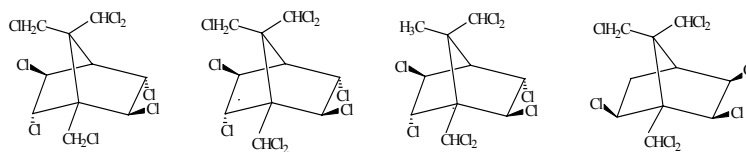
some compounds of technical toxaphene

Bicchi et al. [26] evaluated the enantioselectivity of 6-*O-tert*-butyldimethylsilyl and 6-*O-tert*-hexyldimethylsilyl-β-and γ-cyclodextrins with fragrance and pesticide racemates having different structures and volatilities. The 6-*O-tert*-butyldimethylsilyl-β-cyclodextrin was the most enantioselective for high-to-medium volatility racemates, while the 6-*O-tert*-hexyldimethylsilyl-γ-cyclodextrin was the most enantioselective for medium-to-low volatility enantiomers.

Ramos et al. [27] studied the separation of 2-acetyl-2-alkyl-γ-butyrolactone derivatives and their alcohol analogs by GC using 2,3-di-*O*-methyl-6-*O-tert*-butyldimethylsilyl-β-cyclodextrin as chiral stationary phase. This study suggested that chiral recognition for ketone derivatives depends more on the geometry than on the polarity of alkyl substituents of the butyrolactones. On the other hand, hydrogen bonds and steric effects are important factors on chiral recognition for alcohol derivatives.
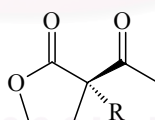
2-acetyl-2-alkyl-γ-butyrolactone derivatives

2.4 Thermodynamic investigation of enantiomer separation by gas chromatography

Variation of column temperature has played a major role on retention and enantioselectivity of chiral analytes on a CSP. An increase in temperature generally decreases the retention of analytes due to their lower affinity with the stationary phase and, consequently, they travel faster through the chromatographic

column. However, the enantioselectivity may either increase or decrease depending on the type of interaction mechanism. Thus, a change in temperature can be used to optimize enantioseparation. From the retention behavior and measurements of chromatographic parameters, thermodynamic parameters (e.g. enthalpy, entropy, Gibbs free energy, etc.), associated with the enantiomers and CSP can be obtained. Hopefully, some aspects on the mechanism involved in the enantioseparation could be realized.

Thermodynamic parameters responsible for chiral recognition in GC can be determined by two approaches. In *van't Hoff approach*, thermodynamic parameters are calculated through the relationship between natural logarithm of capacity factor (k′) or separation factor (α) versus the reciprocal of absolute temperature on a single chiral column. If the chiral selector were diluted in a medium, the calculated values would represent the interaction between analytes and the overall stationary phase. The other approach, described by Schurig et al. [37-39], is based on the determination of a retention increment accessible from the relative retention of enantiomers and reference standard on two columns: *a reference column* containing only the nonchiral stationary phase and *a chiral column* containing a chiral selector in the same stationary phase. In this case, thermodynamic parameters associated to the interaction only between analytes and chiral selector can be determined.

2.4.1   van't Hoff approach

Thermodynamic parameters are calculated from separation factor (α), which obtained from the enantiomer separation on a chiral column at given temperature. The difference in Gibbs's free energy, $\Delta(\Delta G)$, is directly calculated according to general equation (1):

$$- \Delta(\Delta G) = RT \cdot \ln \alpha = RT \cdot \ln(\frac{k_2'}{k_1'}) \qquad (1)$$

where   α   is the separation factor or selectivity and is calculated from the
ratio of k′ of two enantiomers.

k′   is the retention factor or capacity factor of each enantiomer and is calculated from solute retention time, $\dfrac{t_R - t_M}{t_M}$.

R   is the universal gas constant (1.987 cal/mol·K)

T   is the absolute temperature (K)

1,2   refer arbitrarily to the less and the more retained enantiomers, respectively

Combining equation (1) with the Gibbs-Helmholtz relationship, equation (2), leads to equation (3).

$$-\Delta(\Delta G) = -\Delta(\Delta H) + T \cdot \Delta(\Delta S) \tag{2}$$

$$RT \cdot \ln\alpha = -\Delta(\Delta H) + T \cdot \Delta(\Delta S) \tag{3}$$

From equation (3), the following equation can be rewritten

$$\ln\alpha = \frac{-\Delta(\Delta H)}{RT} + \frac{\Delta(\Delta S)}{R} \tag{4}$$

where $\Delta(\Delta H)$ is the difference in enthalpy values for enantiomeric pairs

          $\Delta(\Delta S)$ is the difference in entropy values for enantiomeric pairs

According to equation (4), the relationship between ln α and 1/T should be linear; therefore, $\Delta(\Delta H)$ and $\Delta(\Delta S)$ can be acquired from the slope and y-intercept of the plot. However, the calculations of thermodynamic parameters from van't Hoff plot of ln α versus 1/T is not possible, as a result of curvatures observed in many cases. This is due to the nonlinear dependence of selectivity on concentration of selectors in diluted system. Thus, this method is only valid for undiluted chiral selectors [39].

Alternatively, thermodynamic parameters can be calculated from retention factors instead of separation factors. Combination of equation (5) and (6)

results in equation (7), which shows that the relationship between ln k′ and 1/T is linear. Thermodynamic parameters of individual enantiomers can be obtained from van′t Hoff plot of ln k′ against 1/T. Subsequently, the differences in enthalpy and entropy of two enantiomers can be attained.

$$- \Delta G = RT \cdot \ln K = RT \cdot \ln(k' \cdot \beta) \tag{5}$$

$$\Delta G = \Delta H - T \cdot \Delta S \tag{6}$$

$$- \Delta H + T \cdot \Delta S = RT \cdot \ln(k' \cdot \beta)$$

$$\frac{-\Delta H}{RT} + \frac{\Delta S}{R} = \ln k' + \ln \beta$$

$$\ln k' = \frac{-\Delta H}{RT} + \frac{\Delta S}{R} - \ln \beta \tag{7}$$

where   K   is the distribution constant of chiral analyte (selectand) between the gas and the liquid phases.

β   is a constant called phase ratio (the ratio of mobile phase volume to stationary phase volume).

ΔH   is enthalpy change resulting from the interaction of the enantiomer with the stationary phase. ΔH value describes the degree of the strength of the interaction. The more negative the ΔH value, the higher the strength of the interaction and larger the retention in the column.

ΔS   is entropy change resulting from the interaction of the enantiomer with the stationary phase. ΔS value describes the degree to which the structure of the solute influences the interaction.

2.4.2 *Schurig approach*

This method, introduced by Schurig and co-workers [37-39], is based on the concept of the retention increment (R′), and thermodynamic parameters can be calculated according to equation (8).

$$-\Delta(\Delta G) = RT \cdot \ln\left(\frac{R_2'}{R_1'}\right) \tag{8}$$

The concept of the retention increment R′ has been developed to quantitatively differentiate between the physical non-enantioselective contributions to retention arising from achiral gas-liquid partitioning (achiral solvent: polysiloxane) and the chemical enantioselective contributions to retention arising from chiral molecular complexation, whereby only the latter contribution leads to the separation of enantiomers. R′ is proportional to the thermodynamic association constant K, according to the following equation.

$$R' = K \cdot m \tag{9}$$

where   K   is the association constant between chiral analyte (selectand) and a chiral selector in the stationary phase.

m   is molality (mol/kg) of the selector in achiral solvent

The determination of the retention increment relies on experimental values of relative adjusted retention data of the enantiomers and a reference standard (usually a small alkane) on an achiral reference column containing only polysiloxane ($r_\circ$) and a chiral column containing CD in polysiloxane (r). A relationship referring to the retention increment and relative retention data is defined by

$$R' = \frac{r - r_\circ}{r_\circ} \tag{10}$$

where $r = \dfrac{t'}{t'^*} = \dfrac{k'}{k'^*}$ for chiral column (cyclodextrin in polysiloxane)

$r_\circ = \dfrac{t'_\circ}{{t'_\circ}^*} = \dfrac{k'_\circ}{{k'_\circ}^*}$ for achiral reference column (only polysiloxane)

and $\quad t', t'^*$ are adjusted retention time of chiral analyte and a reference standard, respectively on the chiral column.

$t'_\circ, t'^*_\circ$ are adjusted retention time of chiral analyte and a reference standard, respectively on the achiral reference column.

k', k'^* are retention factors of chiral analyte and a reference standard, respectively on the chiral column.

$k'_\circ, k'^*_\circ$ are retention factors of chiral analyte and a reference standard, respectively on the achiral reference column.

By combining equation (8) with equation (2), $\Delta(\Delta H)$ and $\Delta(\Delta S)$ are obtainable from equation (11) by plotting $R \cdot \ln(\dfrac{R'_2}{R'_1})$ versus 1/T:

$$R \cdot \ln(\frac{R'_2}{R'_1}) = \frac{-\Delta(\Delta H)}{T} + \Delta(\Delta S) \tag{11}$$

Furthermore, applying equation (9) to the thermodynamic relationship in (5) results in

$$-\Delta G = RT \cdot \ln(\frac{R'}{m}) \tag{12}$$

$$\ln R' = \frac{-\Delta H}{RT} + \frac{\Delta S}{R} + \ln m \tag{13}$$

Thus, the thermodynamic parameters of individual enantiomers can be accessible from the plot of ln R′ against 1/T.

In *Schurig approach*, the chiral contribution from selector can be selectively determined through the concept of retention increment, R′. This eliminates the effects of the achiral polysiloxane (use as diluent) which contribute to the overall retention, but not the enantioselectivity. Moreover, the retention increment is linearly related to the concentration of chiral selector. Nevertheless, *van't Hoff approach* is still generally used as a first choice because of the simplicity and shorter analysis time.

CHAPTER III

EXPERIMENTAL

3.1   Synthesis of epoxide derivatives

3.1.1   General

Most of racemic epoxides were prepared from their corresponding ketones. All chemicals and solvents (reagent grade) were used as received. The progress of the reactions was followed by thin layer chromatography (TLC) on TLC aluminum sheets, silica gel 60 F_{254} (Merck) and detected under ultraviolet light at 254 nm. The products were purified, if necessary, by column chromatography with silica gel 60, particle size 40-63 μm (Merck). The structures of the synthesized epoxides were confirmed by ^{1}H-NMR spectroscopy (Varian Mercury Plus400 at 400 MHz) using deuterated chloroform (CDCl$_3$, 99.8%D, Aldrich) as solvent. All commercial epoxides and ketones used in this study are:

epoxides:
- benzyl glycidyl ether, 99% (Aldrich)
- epichlorohydrin, 99% (Aldrich)
- 1,2-epoxy-3-phenoxypropane, 99% (Aldrich)
- (2,3-epoxypropyl)benzene, 98% (Aldrich)
- styrene oxide, 97% (Fluka)

ketones:
- 3-acetylbenzonitrile, 97% (Aldrich)
- 4-acetylbenzonitrile, 98% (Fluka)
- 2′-bromoacetophenone, 99% (Aldrich)
- 3′-bromoacetophenone, 99% (Aldrich)
- 4′-bromoacetophenone, 98% (Aldrich)
- butyrophenone, 99% (Aldrich)
- 2′-chloroacetophenone, 97% (Aldrich)
- 3-chloroacetophenone, 97% (Fluka)
- 4′-chloroacetophenone, 97% (Aldrich)
- 2′,4′-dichloroacetophenone, 96% (Aldrich)

- 2′,5′-dichloroacetophenone, 98% (Aldrich)
- 3′,4′-dichloroacetophenone, 99% (Aldrich)
- 2′,4′-difluoroacetophenone, 98% (Aldrich)
- 2′,5′-difluoroacetophenone, 98% (Aldrich)
- 2′,6′-difluoroacetophenone, 97% (Aldrich)
- 3′,4′-difluoroacetophenone, 97% (Aldrich)
- 2′,4′-dimethylacetophenone, 96% (Aldrich)
- 2,5-dimethylacetophenone, 97% (Fluka)
- 3′,4′-dimethylacetophenone, 98% (Aldrich)
- 4′-ethylacetophenone, 97% (Aldrich)
- 2-fluoroacetophenone, 97% (Fluka)
- 3′-fluoroacetophenone, 99% (Aldrich)
- 4′-fluoroacetophenone, 99% (Aldrich)
- isobutyrophenone, 97% (Fluka)
- 3-methoxyacetophenone, 97% (Fluka)
- 2-methylacetophenone, 98% (Fluka)
- 3-methylacetophenone, 97% (Fluka)
- 4-methylacetophenone, 95% (Fluka)
- 4′-methylpropiophenone, 90% (Aldrich)
- 2-nitroacetophenone, 95% (Fluka)
- 3-nitroacetophenone, 98% (Fluka)
- 4-nitroacetophenone, 97% (Fluka)
- propiophenone, 99% (Aldrich)
- 2′,3′,4′,5′,6′-pentafluoroacetophenone, 97% (Aldrich)
- 2′,3′,4′,5′-tetrafluoroacetophenone, 99% (Aldrich)
- 2′,4′,5′-trifluoroacetophenone, 99% (Aldrich)
- 2′-(trifluoromethyl)acetophenone, 99% (Aldrich)
- 3′-(trifluoromethyl)acetophenone, 99% (Aldrich)
- 4-(trifluoromethyl)acetophenone, 98% (Fluka)

3.1.2 Synthesis of 4′-bromostyrene oxide (4Br)
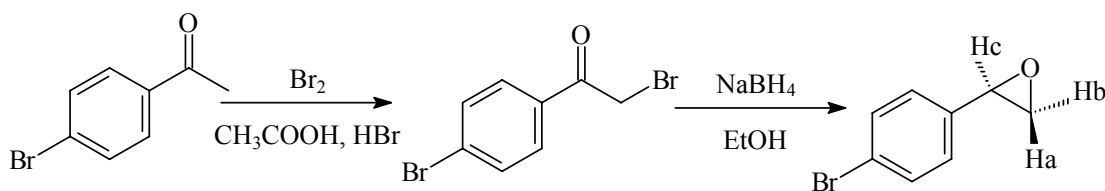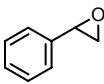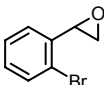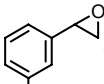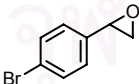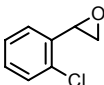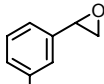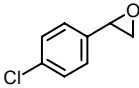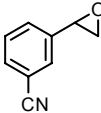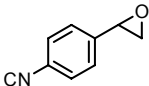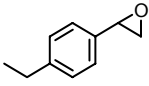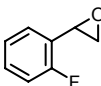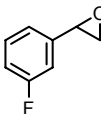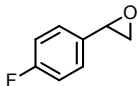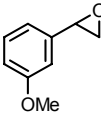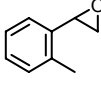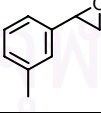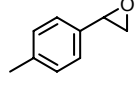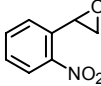
4′-Bromostyrene oxide (4Br): 4′-Bromoacetophenone (1.3933 g, 7 mmol) was placed in a 50 mL round bottom flask, equipped with a magnetic stirrer. To this flask, 1 mL of glacial acetic acid (Merck) and one drop of 48% hydrobromic acid (Fluka) were added all at once and the flask was cooled down to 20 °C in an ice bath. Bromine (0.515 mL, 1 eq) was added dropwise. After the reaction was complete (1-2 h), evidenced by disappearance of bromine color, the precipitate was filtered and washed several times with a solution of ethanol-water (1:1) until no acetic acid smell was present (~100 mL). The precipitate was then dissolved in 6 mL ethanol in a 50 mL round bottom flask. Sodium borohydride (0.2648 g, 1 eq) was added and stirring was continued. After the reaction was complete, water (10 mL) was added and the aqueous solution was extracted with dichloromethane (3 x 10 mL). The organic layer was then washed with water (2 x 10 mL) followed by 0.5% w/v citric acid solution (2 x 10 mL) to remove any remaining sodium borohydride. The organic layer was dried over anhydrous sodium sulfate, filtered and concentrated. The product was purified via flash column chromatography to afford 4′-bromostyrene oxide; 41.4% yield; R_f = 0.63 (hexane-CH_2Cl_2 1:1); ^{1}H-NMR (CDCl$_3$, 400 MHz): δ 2.79 (1H, dd, Ha of C$\underline{H}_2$O, J = 2.5 Hz, 5.4 Hz), 3.18 (1H, dd, Hb of C$\underline{H}_2$O, J = 4.0 Hz, 5.4 Hz), 3.82 (1H, t, Hc, C$\underline{H}$Ar), 7.10-7.58 (4H, m, Ar$\underline{H}$).
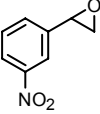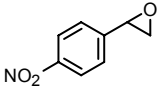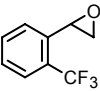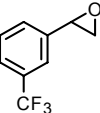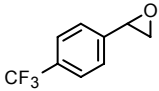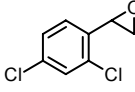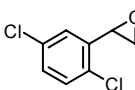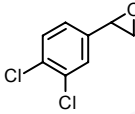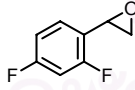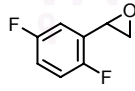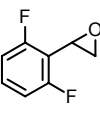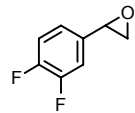
Most of epoxide derivatives were synthesized using the above procedure. However, during the bromination step, if the bromine color was still noticeable after 2 h, as for the synthesis of 2′-nitrostyrene oxide; 3′-cyanostyrene oxide; 2′,4′-difluorostyrene oxide; 2′,4′,5′-trifluorostyrene oxide; 2′,3′,4′,5′-tetrafluorostyrene oxide; and 2′,3′,4′,5′,6′-pentafluorostyrene
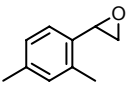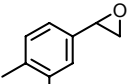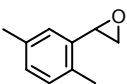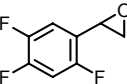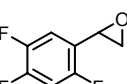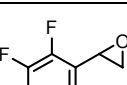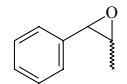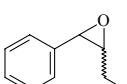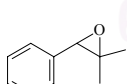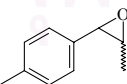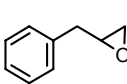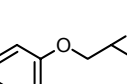
oxide, the reaction temperature was increased to 40 °C. If the precipitate was not formed after bromination as for the synthesis of, for example, disubstituted styrene oxides; methylstyrene oxide, the procedure was modified as followed. After the bromination was complete, saturated sodium hydrogen carbonate solution was added to the reaction mixture until pH 7.0 was reached. The aqueous solution was extracted with dichloromethane (3 x 10 mL), dried over sodium sulfate, and concentrated before redissolving in ethanol (6 mL). The reaction with NaBH$_4$ was then continued. All of synthesized epoxides could be obtained with at least 30% yield. All of the epoxide derivatives used in this study were shown in table 3.1.
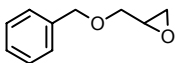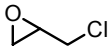
Table 3.1   Structure and abbreviation of all epoxide derivatives used in this study

structure	abbreviation	MW (g/mol)	compound
	1	120.10	styrene oxide
Monosubstituted styrene oxides			
	2Br	199.05	2′-bromostyrene oxide
	3Br	199.05	3′-bromostyrene oxide
	4Br	199.05	4′-bromostyrene oxide
	2Cl	154.60	2′-chlorostyrene oxide
	3Cl	154.60	3′-chlorostyrene oxide

structure	abbreviation	MW (g/mol)	compound
	4Cl	154.60	4′-chlorostyrene oxide
	3CN	145.16	3′-cyanostyrnene oxide
	4CN	145.16	4′-cyanostyrnene oxide
	4Et	148.21	4′-ethylstyrene oxide
	2F	138.14	2′-fluorostyrene oxide
	3F	138.14	3′-fluorostyrene oxide
	4F	138.14	4′-fluorostyrene oxide
	3OMe	150.18	3′-methoxystyrene oxide
	2Me	134.18	2′-methylstyrene oxide
	3Me	134.18	3′-methylstyrene oxide
	4Me	134.18	4′-methylstyrene oxide
	2NO	165.15	2′-nitrostyrene oxide

structure	abbreviation	MW (g/mol)	compound
	3NO	165.15	3′-nitrostyrene oxide
	4NO	165.15	4′-nitrostyrene oxide
	2CF	188.15	2′-(trifluoromethyl)styrene oxide
	3CF	188.15	3′-(trifluoromethyl)styrene oxide
	4CF	188.15	4′-(trifluoromethyl)styrene oxide
Disubstituted styrene oxides			
	24Cl	189.04	2′,4′-dichlorostyrene oxide
	25Cl	189.04	2′,5′-dichlorostyrene oxide
	34Cl	189.04	3′,4′-dichlorostyrene oxide
	24F	156.13	2′,4′-difluorostyrene oxide
	25F	156.13	2′,5′-difluorostyrene oxide
	26F	156.13	2′,6′-difluorostyrene oxide
	34F	156.13	3′,4′-difluorostyrene oxide

structure	abbreviation	MW (g/mol)	compound
	24Me	148.21	2′,4′-dimethylstyrene oxide
	34Me	148.21	3′,4′-dimethylstyrene oxide
	25Me	148.21	2′,5′-dimethylstyrene oxide
Other epoxides			
	TriF	174.12	2′,4′,5′-trifluorostyrene oxide
	TetraF	192.11	2′,3′,4′,5′-tetrafluorostyrene oxide
	PentaF	210.10	2′,3′,4′,5′,6′-pentafluorostyrene oxide
	2	134.18	phenylpropylene oxide
	3	148.21	phenylbutylene oxide
	4	148.21	phenylisopropylene oxide
	5	148.21	4′-methylphenylpropylene oxide
	6	134.18	(2,3-epoxypropyl)benzene
	7	150.18	1,2-epoxy-3-phenoxypropane

structure	abbreviation	MW (g/mol)	compound
	8	164.20	benzyl glycidyl ether
	9	92.52	epichlorohydrin

3.2   Gas chromatographic experiment

3.2.1   Preparation of capillary columns

Three 15m long, 0.25 mm i.d. deactivated fused-silica tubing (J&W Scientific) were coated statically [40] with 0.4% w/v solution of stationary phase to obtain a film of 0.25 μm thick. Three types of stationary phase used in this study are:

- polysiloxane OV-1701 (14% cyanopropylphenyl 86% dimethyl polysiloxane, Supelco) was used as reference stationary phase and as diluent for two solid cyclodextrin derivatives
- 30.0% heptakis(2,3-di-*O*-methyl-6-*O*-*tert*-butyldimethylsilyl)cyclo-maltoheptaose (or BSiMe) in OV-1701
- 33.5% heptakis(2,3-di-*O*-acetyl-6-*O*-*tert*-butyldimethysilyl)cyclo-maltoheptaose (or BSiAc) in OV-1701

Two cyclodextrin columns were prepared to contain identical molality of cyclodextrin derivatives. All columns were conditioned at 200 ºC until stable baseline was observed and overall column performance was determined by means of Grob test [41-42].

3.2.2   Gas chromatographic separation

All chromatographic analyses were performed on an Agilent 6890 gas chromatograph (Agilent Technologies) equipped with a split/splitless injector and a flame ionization detector (FID). Hydrogen was used as carrier gas at an average linear velocity of 50 cm/s. The split injector

and flame ionization detector temperatures were set at 250 °C. Each epoxide derivative was dissolved in hexane, except nitro- and cyano-substituted derivatives were dissolved in dichloromethane, to obtain a concentration of ~3-6 mg/mL. Approximately 0.2-0.4 μL of solution was injected with a split ratio of 100:1. Column efficiency was checked regularly at 200 °C with *n*-alkanes (retention factor, k′ >5; efficiency > 3000 plates/m).

3.2.3 Gas chromatographic determination of thermodynamic parameters

Each sample solution was injected at least in duplicate on three columns, a reference column and two cyclodextrin columns, at isothermal conditions in the temperature range of 60-200 °C at 10 °C interval. Retention times of the same analyte under the same condition from two consecutive runs were within ± 0.002 minutes. From the chromatograms obtained from the cyclodextrin columns, retention factors and enantioselectivities were calculated and used to determine thermodynamic parameters by means of *van't Hoff approach*. Relative retention of each compound, which obtained from reference column and cyclodextrin columns, were used to calculate the retention increment and the thermodynamic parameter were calculated by means of *Schurig approach*.

Thermodynamic data obtained by both methods were compared. These data were used as a tool for explaining the strength of interaction and enantioselectivity of epoxides studied on the two types of derivatized cyclodextrins. The differences and/or similarities in the thermodynamic parameters were discussed in terms of type and position of substituents.

CHAPTER IV

RESULTS AND DISCUSSION

4.1   Synthesis of styrene oxide derivatives

Most of styrene oxide derivatives used in this study were prepared by bromination of their corresponding ketones using liquid bromine to yield phenacyl bromide derivatives (I), followed by the ring closure reaction with sodium borohydride. BH_4^- serves as a base in an internal S_N2 reaction. An alkoxide ion acts as a nucleophile in displacing the neighboring bromine, in a 1-3-elimination reaction on an alcohol possessing a leaving group in the α-position, to yield an epoxide [43-44]. The identity of epoxide products was confirmed by ^{1}H-NMR for the chemical shift of OC$\underline{H}_2$ at ~2.7 ppm (dd) and ~3.2 ppm (dd); and of OC$\underline{H}$Ar at ~3.8-4.2 ppm (dd).
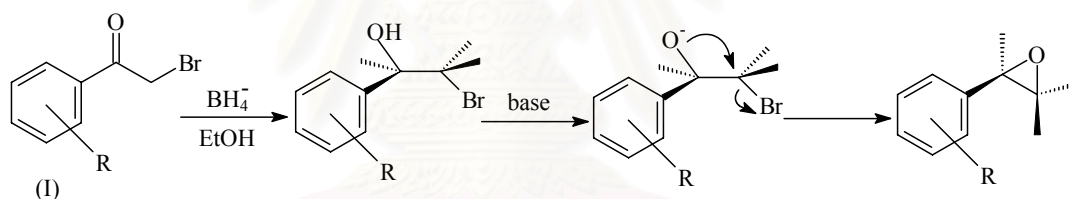
For the synthesis of styrene oxide derivatives with alkyl substitution on the side chain (compounds 2, 3, and 5), they exist in both *cis*- and *trans*-isomers. From ^{1}H-NMR spectra can be observed chemical shift from both *cis*- and *trans*-isomers, which are not chemical shift equivalent (~3.2 and 4.2 ppm for *cis*-isomer; ~3.0 and 3.6 ppm for *trans*-isomer). Considering ^{1}H-NMR coupling constant value (J) for C$\underline{H}$s belonging to the epoxy group of 4.1 Hz at 3.20 and 4.20 ppm (high intensity), it can be concluded that the major products of synthesized compounds **2**, **3**, and **5** are *cis*-isomer.

4.2 Determination of coated column performance

The quality of the columns prepared in this study was evaluated by means of Grob test [41-42]. Test chromatograms obtained from OV-1701, BSiMe and BSiAc columns are depicted in Figures 4.1-4.3, respectively. The Grob test mixture consists of twelve compounds of different functional group: *n*-decane (**C10**); *n*-undecane (**C11**); methyl decanoate (**E10**); methyl undecanoate (**E11**); methyl dodecanoate (**E12**); nonanal (**al**); 1-octanol (**ol**); 2,3-butanediol (**D**); 2,6-dimethyl phenol (**P**); 2,6-dimethylaniline (**A**); 2-ethylhexanoic acid (**S**); and dicyclohexylamine (**am**). Column efficiency was determined from the average separation number (SN) between **E10-E11** and **E11-E12** pairs. Column inertness was evaluated from the adsorption of alcohols (**ol** and **D**) and aldehyde (**al**). Acid-base characteristic of column was determined from the peak height ratio of **A** and **P** as well as the adsorption of strong acid and base (**S** and **am**).

According to Figure 4.1, OV-1701 column exhibited high efficiency with the average SN value of 28.6. This value is also in good agreement with the efficiency obtained by isothermally testing the column with *n*-alkanes in the temperature range of 60-200 °C (3000-4000 plates/meter). This indicated that OV-1701 column can be used efficiently at both high and low temperatures. Nevertheless, OV-1701 exhibited some adsorption towards **al** and **D**, but not **ol**, indicating that the separation of aldehydes and alcohols other than monoalcohols may not be appropriate. Considering **A** and **P** peak height, they are rather equivalent indicating the neutrality of the column. Nevertheless, this column is active to stronger acid (**S**) and base (**am**); and the analyses of underivatized carboxylic acids and amines are not recommended.

For BSiMe column (Figure 4.2), high efficiency (average SN = 28.4) was also observed over a wide temperature range. Column neutrality was good as indicated by the similar height of **A** and **P**. Slight adsorption of aldehyde (**al**) and alcohols (**ol**, **D**), but strong adsorption of **S** and **am**, were detected on this stationary phase. Interestingly, **D** was observed as two peaks of isomers indicating the ability of cyclodextrin to separate isomers. Additionally, the elution order of the test mixture on this column was different from that on OV-1701 column.
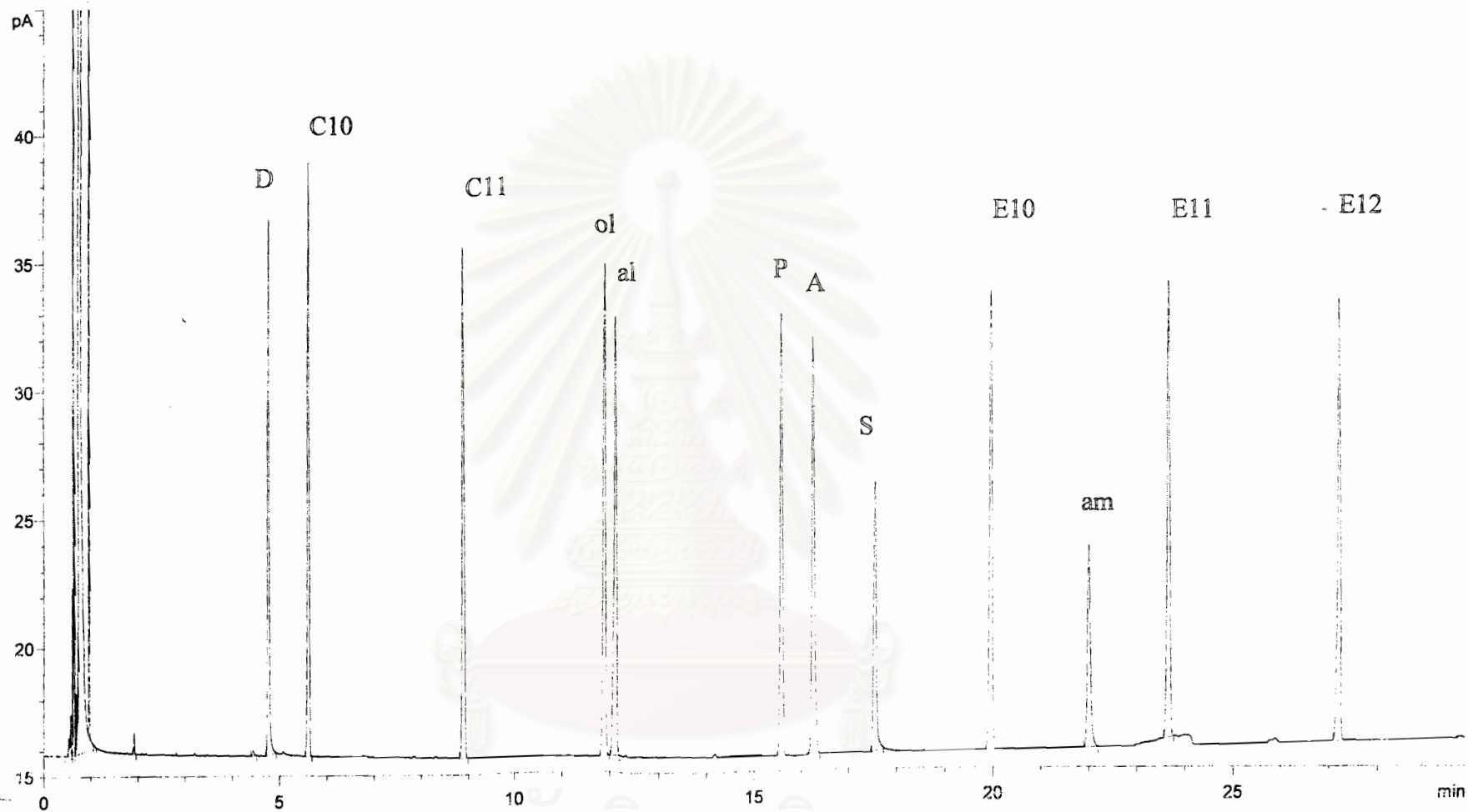
Figure 4.1   Chromatogram of Grob test on OV-1701 column (15.80 m x 0.25 mm i.d. x 0.25 μm film thickness); temperature program: 40 to 150 °C at 3.17 °C/min.
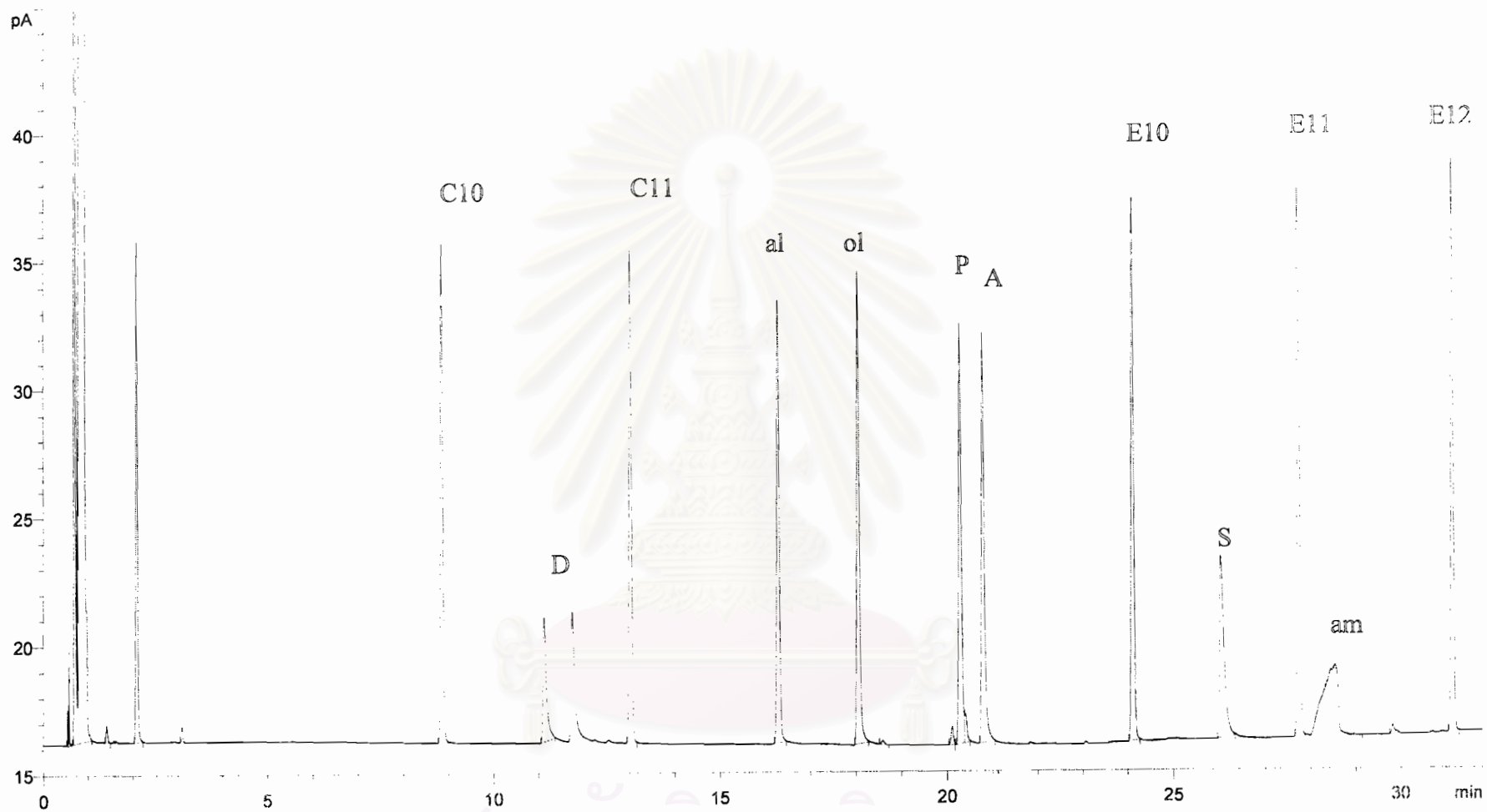
Figure 4.2   Chromatogram of Grob test on BSiMe column (15.75 m x 0.25 mm i.d. x 0.25 μm film thickness); temperature program: 40 to 150 °C at 3.17 °C/min.
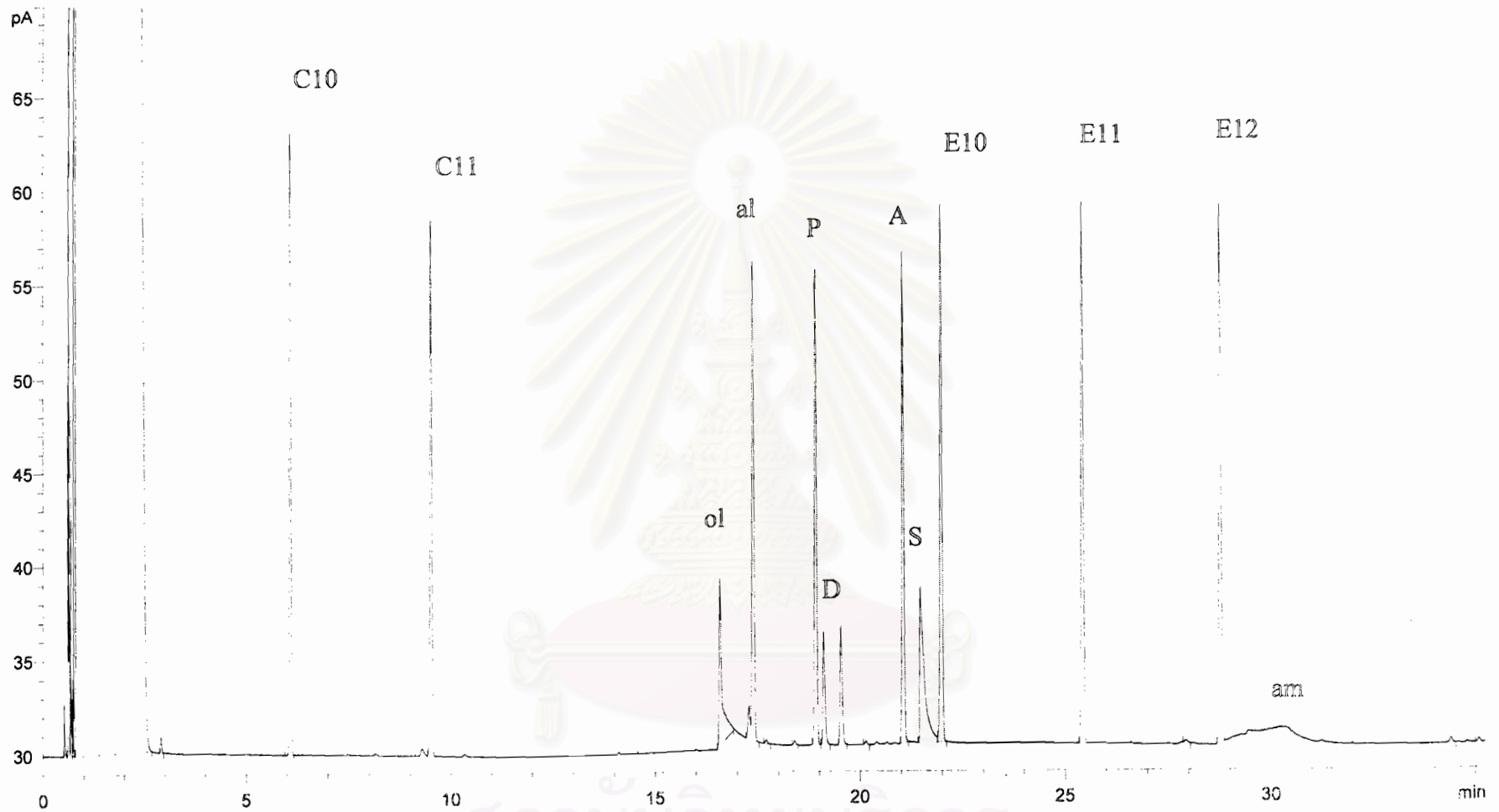
Figure 4.3   Chromatogram of Grob test on BSiAc column (16.00 m x 0.25 mm i.d. x 0.25 μm film thickness); temperature program: 40 to 150 °C at 3.12 °C/min.

As shown in Figure 4.3, BSiAc column also exhibited high efficiency with an average SN value of 28.7. Column neutrality was still good. However, this column is very active towards alcohols (**ol**, **D**), strong acid (**S**) and strong base (**am**), all peaks of which are poorly eluted or absent. As a result, BSiAc column is not suitable for analyzing alcohols, underivatized acids and amines. BSiAc also offered different selectivity from BSiMe, as different elution order of test compounds was noticed. Nevertheless, these three columns can be used efficiently for the analysis of epoxides, the compounds of interest in this study.

4.3   Gas chromatographic separation of styrene oxide derivatives

Separations of all analytes were performed isothermally in the temperature range of 60-200 °C at 10 °C intervals on three columns: OV-1701, BSiMe, and BSiAc columns. The retention factor (k′) and enantioselectivity (α) of racemic epoxides at 150 °C were calculated and shown in Figures 4.4-4.7

On OV-1701 column, the retention factors (k′) of epoxides varied noticeably depending on the type and number of substituents, except for positional isomers where similar retention was observed (Figure 4.4). Similar trends were also attained for the more retained enantiomers on the two chiral columns, BSiMe and BSiAc, but with higher retention values than on the nonchiral OV-1701 column (Figures 4.5-4.6). This suggested that CD derivatives were responsible for an increased retention in view of the fact that all three columns contain polysiloxane as a major component and have identical film thickness.

All racemic epoxides could be resolved into their enantiomers on at least one chiral column used. The enantioselectivities of epoxides on two chiral columns (Figure 4.7) displayed different trend and the values varied significantly depending upon the type, the number, and, more importantly, the position of substituents as demonstrated in Figure 4.8. It can be seen that, at 120 °C, the retention factors of all chloro-substituted styrene oxides are quite similar on the same column, with a slight increase in the order: *ortho- < meta- < para-*isomers. On the other hand, the enantioselectivities of isomers differ significantly and are greatly influenced by
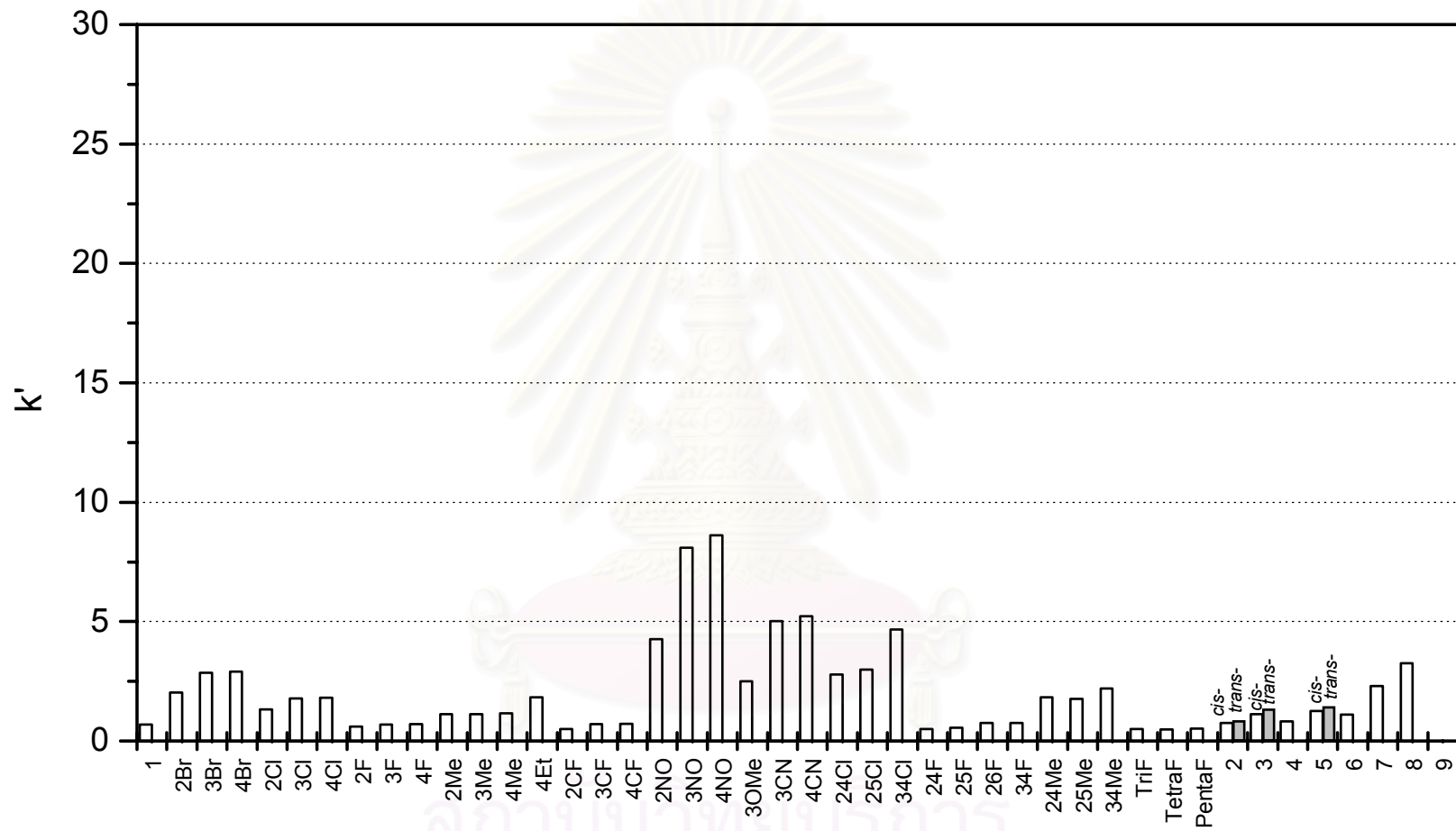
Figure 4.4   Retention factors (k′) of styrene oxide derivatives on OV-1701 phase at 150 °C.
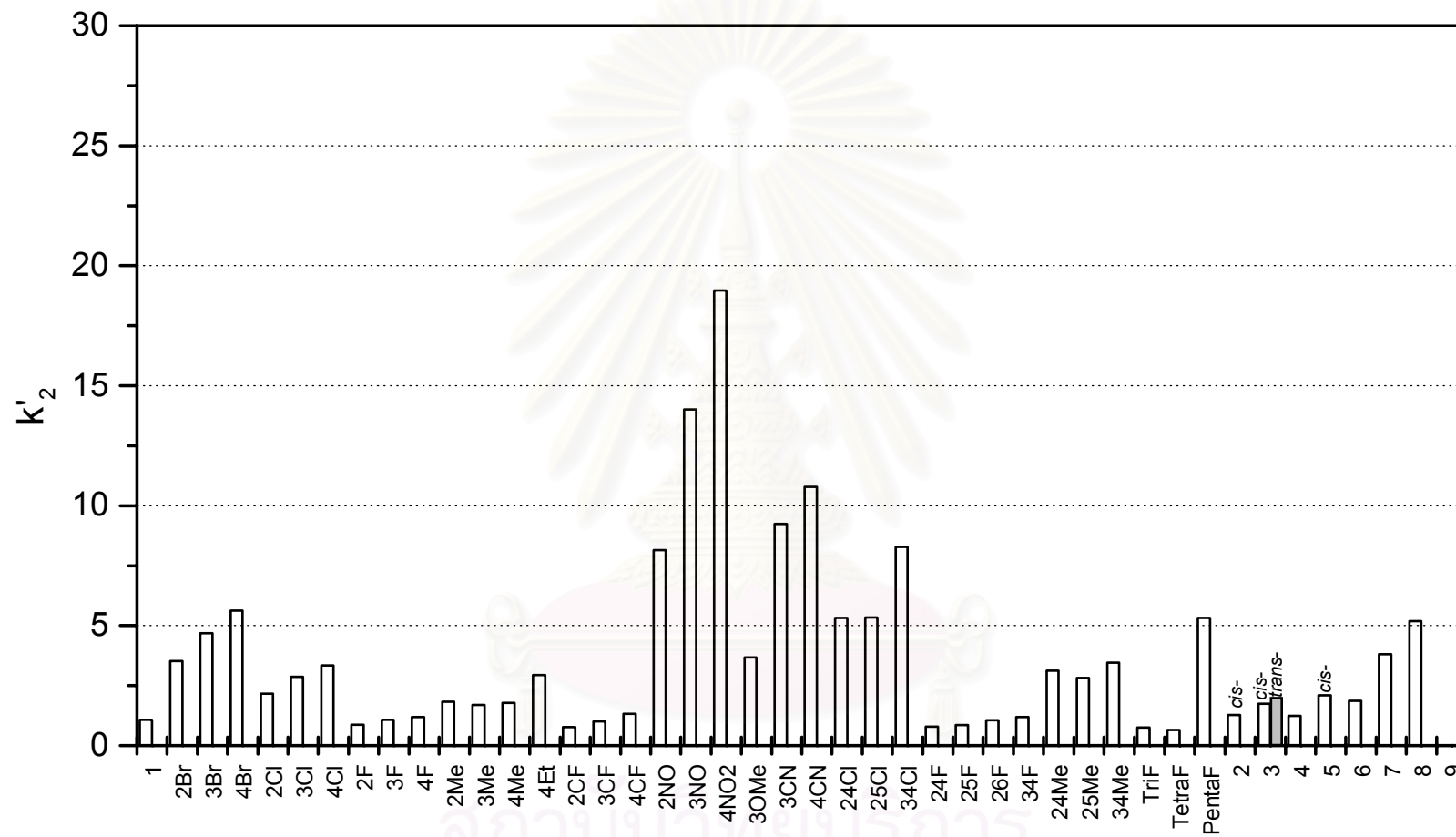
Figure 4.5   Retention factors (k_2') of the more retained enantiomers of styrene oxide derivatives on BSiMe phase at 150 °C.
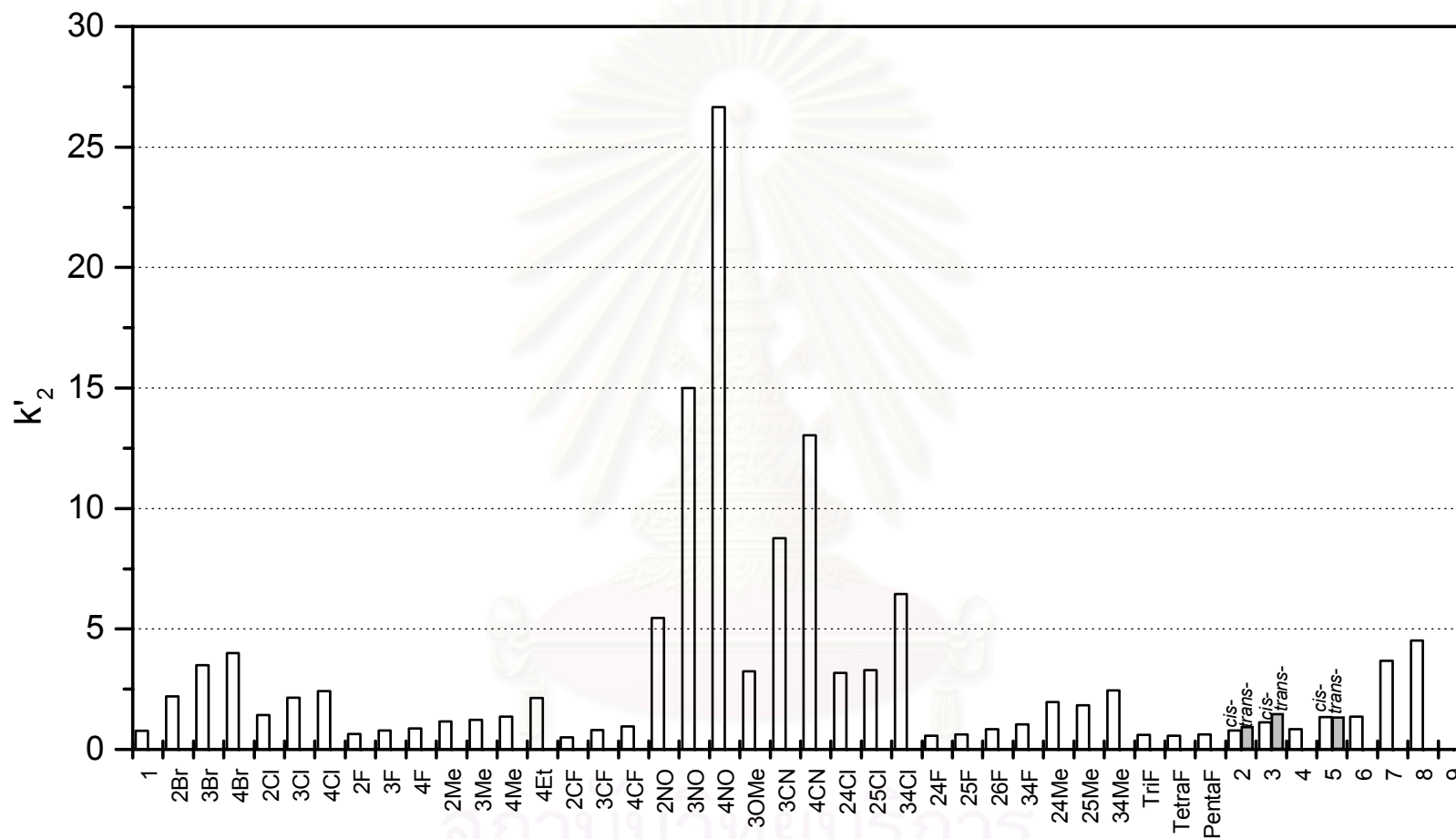
Figure 4.6   Retention factors (k_2') of the more retained enantiomers of styrene oxide derivatives on BSiAc phase at 150 °C.
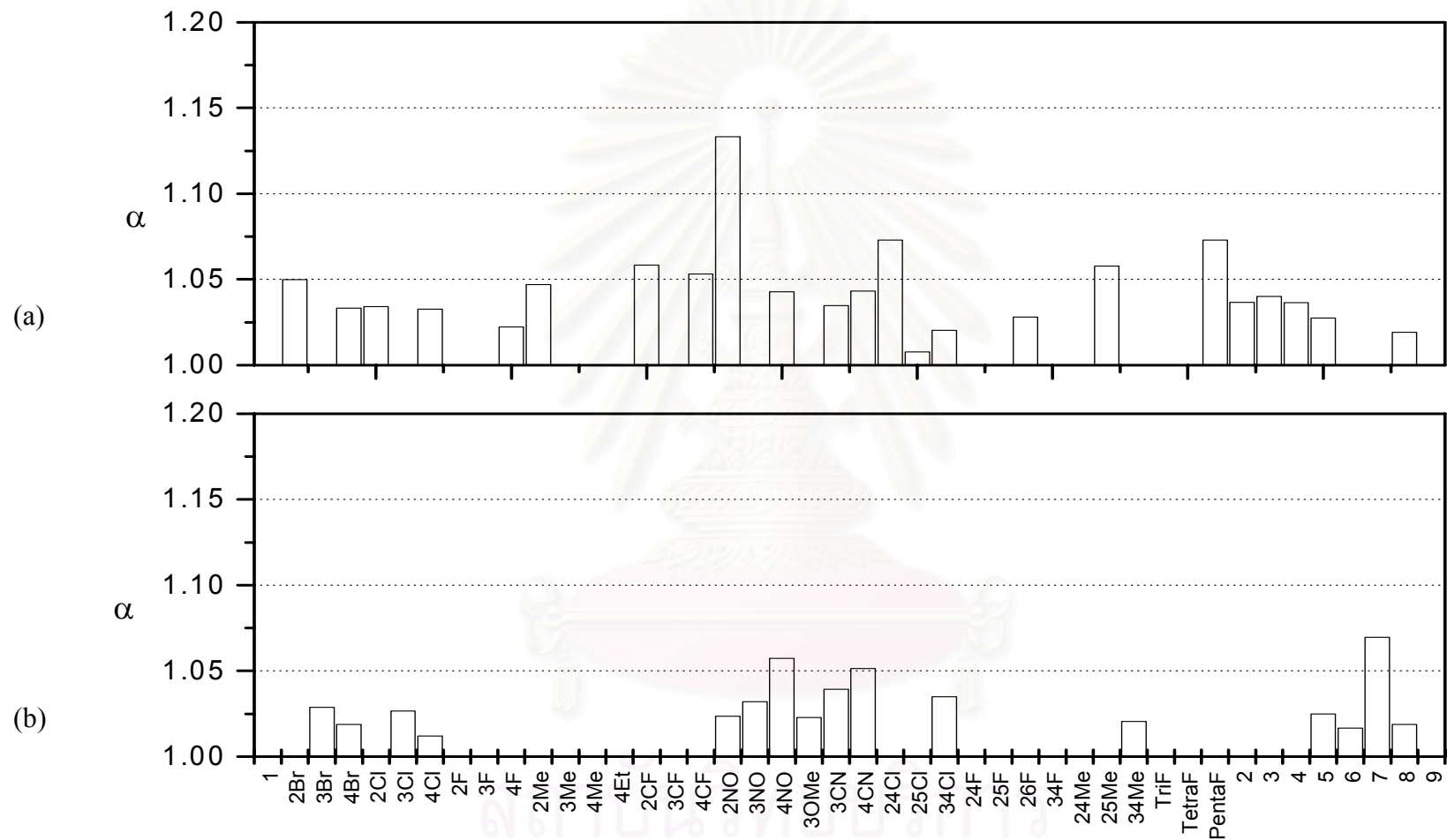
Figure 4.7   Separation factors (α) of the enantiomers of styrene oxide derivatives on (a) BSiMe and (b) BSiAc phases at 150 °C.

the substituent position as well as the type of cyclodextrin derivative. The BSiMe column was superior at resolving **2Cl** and **4Cl** enantiomers, but could not separate **3Cl** enantiomers. The BSiAc, on the contrary, was clearly excellent for the **3Cl** enantiomers.
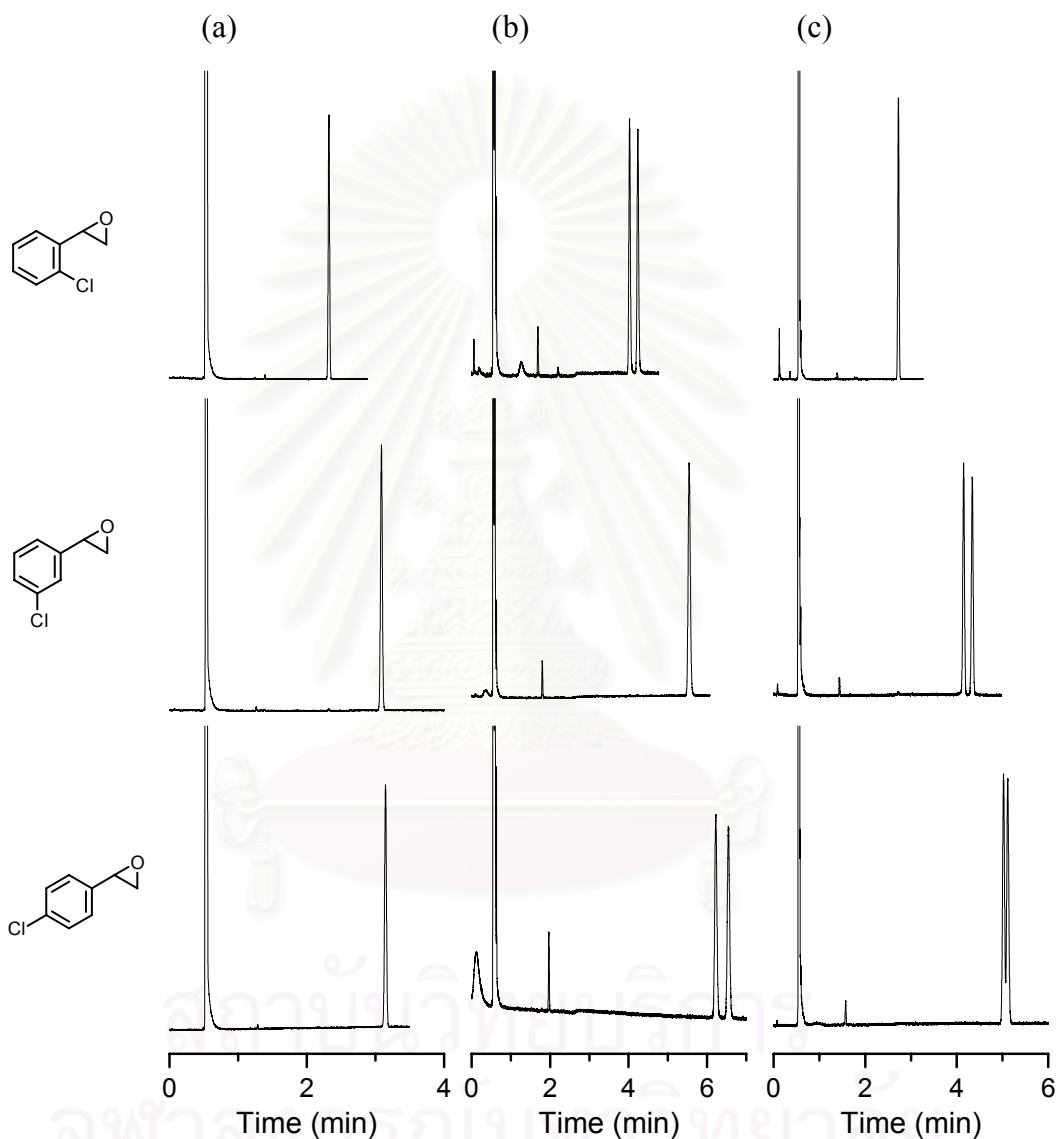
Figure 4.8   Chromatograms of three chloro-styrene oxides (top) **2Cl**; (middle) **3Cl**; and (bottom) **4Cl** on (a) OV-1701; (b) BSiMe; and (c) BSiAc phases at 120 °C.

Due to different physical property of analytes at a particular temperature, the retention and selectivity factors of analytes could not suitably reveal

the nature of interaction between analytes and cyclodextrin derivatives. Therefore, thermodynamic parameters (e.g. enthalpy and entropy) responsible for the interaction between analytes and gas chromatographic stationary phases, investigated over a temperature range, needed to be determined.

4.4   Thermodynamic investigation by *van't Hoff approach*

Thermodynamic parameters associated with the interactions between chiral epoxides and stationary phase could be acquired through the van't Hoff plot according to equation (7). All ln k′ vs. 1/T plots were linear, with almost all regression coefficients (R^2) values greater than 0.999. From these plots, enthalpy (ΔH) and entropy (ΔS) values for each enantiomer could be determined. When the enantiomers can be separated, the corresponding $\Delta(\Delta H)$ and $\Delta(\Delta S)$ values can be calculated from the relationship between ln α and 1/T. Theoretically, ln α vs. 1/T plots should be linear; however, nonlinear plots have been occasionally observed in the temperature range studied. Since there are various types of interactions involved in the complex formation between analyte and chiral stationary phase, e.g. van der Waals interactions, steric interactions, etc. [44-47]; the nonlinearity may possibly be indicative of a change in the interaction mechanism between analytes and chiral stationary phase as the temperature changed. Alternatively, the $\Delta(\Delta H)$ and $\Delta(\Delta S)$ values can also be calculated from the differences in ΔH and ΔS values of two enantiomers. As a result, the $\Delta(\Delta H)$ and $\Delta(\Delta S)$ values presented in this study were obtained from the latter approach, even though the values attained by both approaches were relatively similar.

4.4.1   Enthalpy change (-ΔH) and entropy change (-ΔS)
The enthalpy value (-ΔH) represented the strength of interaction between an analyte and stationary phase: the higher the value (more negative value), the higher the strength of interaction. On the other hand, the entropy value (-ΔS) denoted the loss of degree of freedom resulted from the interaction between the enantiomer and stationary phase. Enthalpy and entropy values of analytes on OV-1701 column were illustrated in Figures 4.9-4.10. The enthalpy values (-ΔH) of most analytes were very similar within 11.19 ± 1.06 kcal/mol. This suggested that major

contribution from analytes to interaction would come from the epoxy group and aromatic ring, as an aliphatic epoxide (compound **9**) gave the lowest value. In addition, analytes with large, electron-attracting group(s), i.e. cyano and nitro, and methoxy group tended to exhibit stronger interaction than other compounds. A slight increase in the interaction from *ortho-* < *meta-* ≈ *para*-isomers was also observed. A similar trend was noticed for the entropy values (Figure 4.10).

Enthalpy and entropy values of the more retained enantiomers of epoxides on BSiMe column exhibited larger values than those obtained from OV-1701 phase. However, similar trends to those obtained from OV-1701 phase were still noticed (Figures C12-C13, appendix C). Most retained enantiomers of analytes equally interacted to the stationary phase as their $-\Delta H_2$ values were within mean value ± standard deviation. Analytes with cyano, nitro, or methoxy group still exhibited stronger interaction than other compounds. Small aliphatic epoxides (compound **9**) interacted with the BSiMe the weakest. This indicated that aromatic epoxides interacted with the phase more strongly than aliphatic epoxides. Nonetheless, more variety of aliphatic epoxides should be studied before deduction can be drawn.

Enthalpy and entropy values of the more retained enantiomers of epoxides on BSiAc column exhibited larger values than those obtained from OV-1701 phase as well (Figures C16-C17, appendix C). The average $-\Delta H_2$ and $-\Delta S_2$ values attained from both BSiMe and BSiAc were relatively equivalent, supporting that the major contribution of analytes were from the epoxy group. Among all positional isomers of mono-substituted styrene oxides, the trend for the interaction between analytes and stationary phase was quite obvious and it increased in the order: *ortho* < *meta* < *para*. Interestingly, epichlorohydrin **(9)**, the only aliphatic epoxide used in this study, showed very strong interaction towards polar BSiAc phase (high $-\Delta H_2$ and $-\Delta S_2$ values). It was possible that strong dipole-dipole interactions between a small, polar epichlorohydrin and BSiAc brought about the increased $-\Delta H_2$ and $-\Delta S_2$ values compared to values from less polar BSiMe phase. Similar results were recognized for mono-substituted styrene oxides with cyano, nitro, or methoxy group as well.
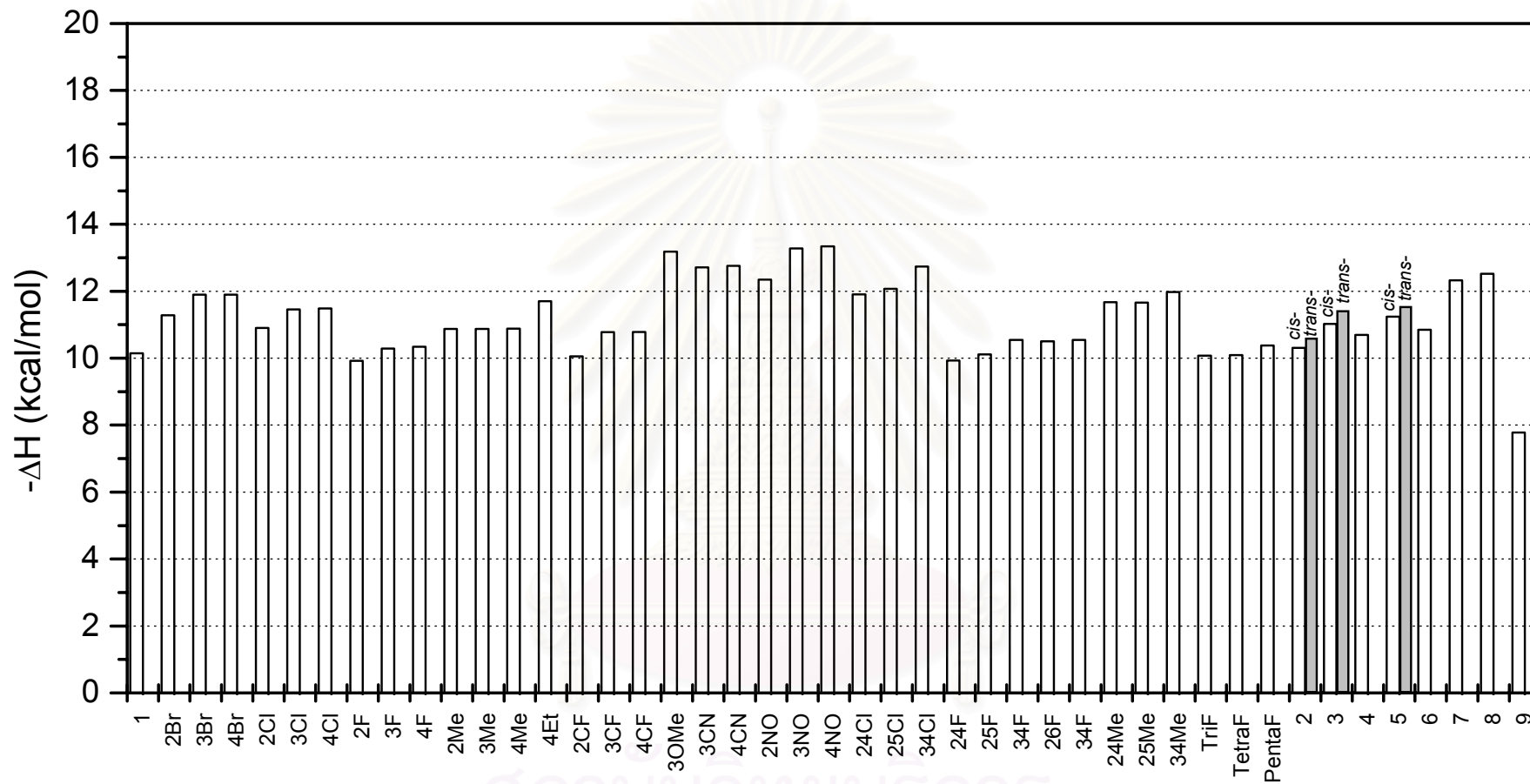
Figure 4.9   Enthalpy values (-ΔH, kcal/mol) of styrene oxide derivatives on OV-1701 phase obtained from *van't Hoff approach* ($\bar{x}$ = 11.19; SD = 1.06).
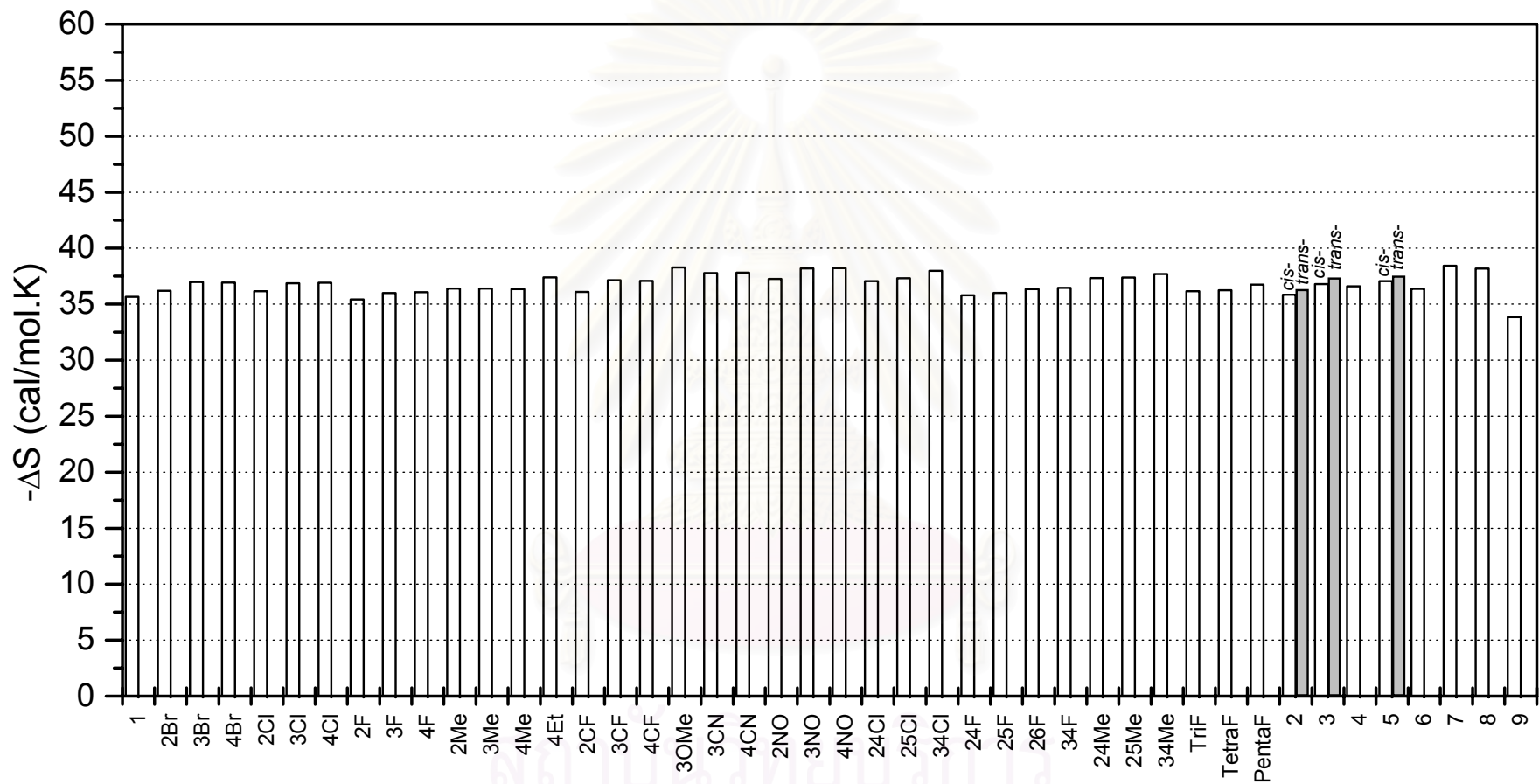
Figure 4.10   Entropy values (-ΔS, cal/mol·K) of styrene oxide derivatives on OV-1701 phase obtained from *van't Hoff approach* ($\bar{x} = 36.18$; SD = 0.88).

4.4.2 Enthalpy difference (-Δ(ΔH)) and entropy difference (-Δ(ΔS))

The -Δ(ΔH) and -Δ(ΔS) values of BSiMe column towards each epoxide analyte was considerably different, despite the fact that they both showed similar trend (Figures C14-C15, appendix C). From Figure 4.11, it was clearly observed that the position of analyte substitution played an essential role to enantioselectivity than the type of substitution. Using styrene oxide (compound **1**) as a reference, mono-substitution at position 2 (*ortho*) or 4 (*para*) on the aromatic ring seemed to promote enantiorecognition as seen from higher -Δ(ΔH) values, except for alkyl-substituted at *para*-position (compounds **4Me** and **4Et**). The effect was even more pronounced with trifluoromethyl and nitro groups at *ortho*-position, compounds **2CF** and **2NO**, respectively. Unfortunately, BSiMe showed poor or no enantiodifferentiation towards *meta*-substituted styrene oxides.

For di-substituted styrene oxides, the trend was not apparent as for the mono-substituted derivatives since there were only three types of substitution (chloro, fluoro, and methyl) and not all six isomers of each derivative could be prepared. Preliminary results (Figure 4.12) indicated that, for dichloro and difluoro derivatives, the substitution at *ortho*- and *para*-positions enhanced the enantiorecognition as -Δ(ΔH) values were in the order: (2,4; 2,6) > (2,5; 3,4). The -Δ(ΔH) values of 2,4- or 2,6-substituted derivatives were greater than the values of 2- or 4-substituted derivatives alone. The substitution at *meta*-position, even combined with substitution at *ortho*- or *para*-position, would reduce the enantiorecognition as demonstrated in Figure 4.13. The results for the dimethyl derivatives were not in agreement with those from dichloro- or difluoro-derivatives, as the only enantioseparation observed was from 2′,5′-dimethylstyrene oxide (**25Me**). The enantiomer separation of mono- and di-methylstyrene oxides was shown in Figure 4.14.

Figure 4.11   Difference in enthalpy values (-Δ(ΔH), kcal/mol) of the enantiomers of mono-substituted styrene oxide derivatives on BSiMe phase obtained from *van't Hoff approach*.

Figure 4.12   Difference in enthalpy values (-Δ(ΔH), kcal/mol) of the enantiomers of di-substituted styrene oxide derivatives on BSiMe phase obtained from *van't Hoff approach*.
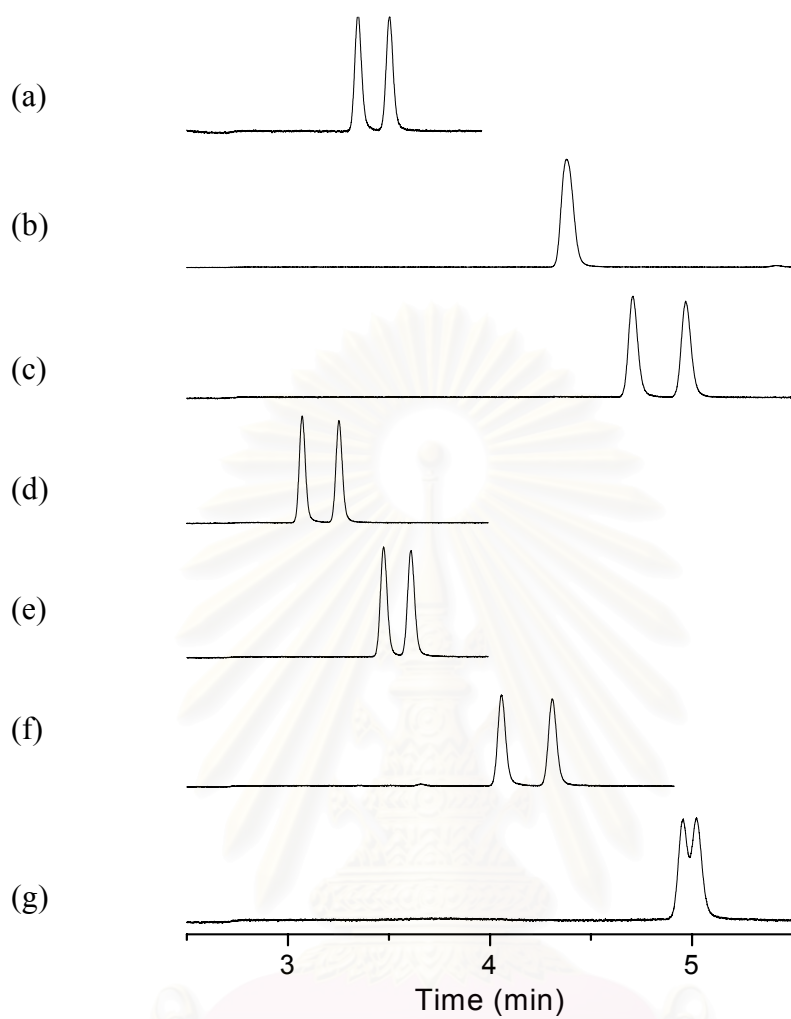
Figure 4.13   Chromatograms of mono- and di-fluorostyrene oxides (a) **2F**; (b) **3F**;
(c) **4F**; (d) **24F**; (e) **25F**; (f) **26F** and (g) **34F** on BSiMe phase at 100
°C
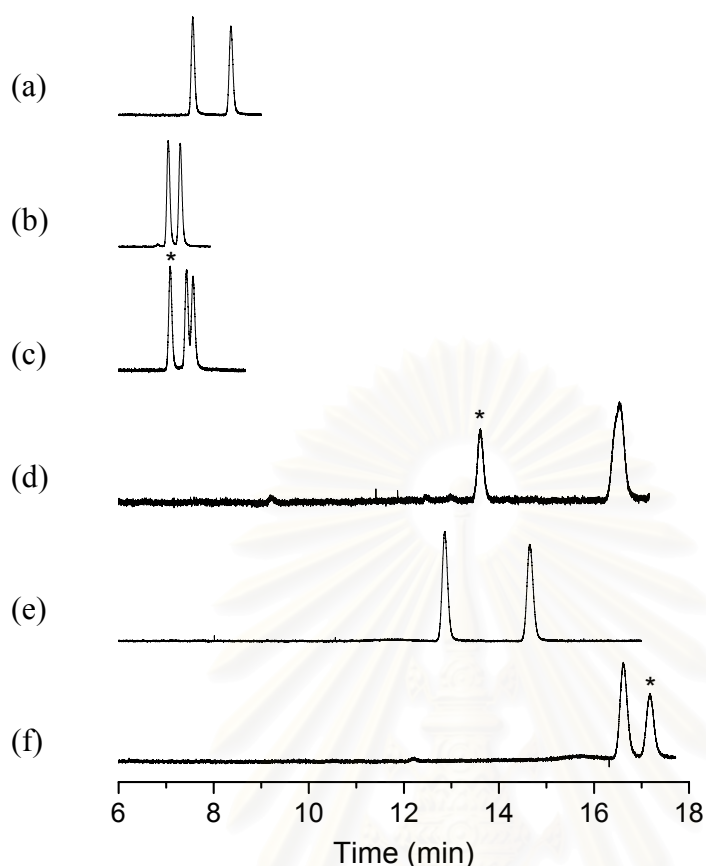
Figure 4.14   Chromatograms of mono- and di-methylstyrene oxides (a) **2Me**; (b) **3Me**; (c) **4Me**; (d) **24Me**; and (e) **34Me** on BSiMe phase at 100 °C. (* indicates contaminant peaks.)

The effect of number of substituents on an aromatic ring was also examined and demonstrated in Figure 4.15. When all aromatic protons of styrene oxide (**1**) were replaced with fluorine atoms as in **pentaF**, the enantiomers were perfectly separated in shorter analysis time (Figure 4.15b). Interestingly, 2′,4′,5′-trifluorostyrene oxide (**triF**) and 2′,3′,4′,5′-tetrafluoro styrene oxide (**tetraF**) decreased the enantiorecognition, as no separation was observed under the same condition. Since the number of tested compounds is limited, more analytes of this type should be investigated to reveal more meaningful information.
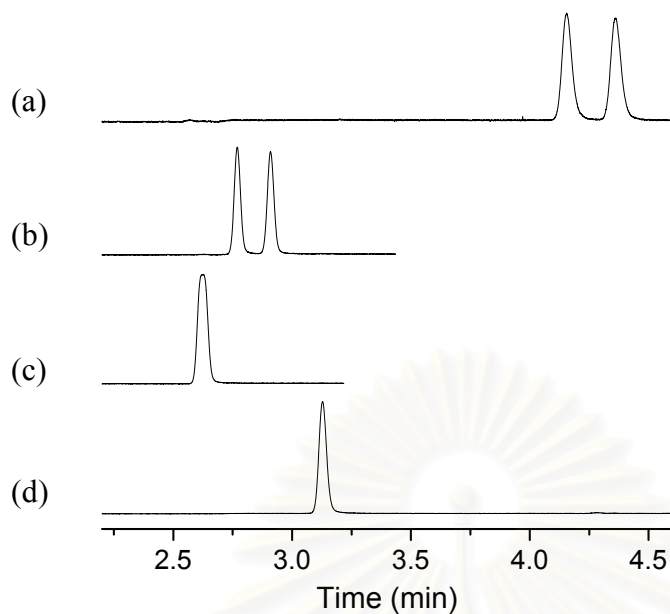
Figure 4.15   Chromatograms of styrene oxide and its fluoro-derivatives (a) **1**; (b)
pentaF; (c) **tetraF**; and (d) **triF** on BSiMe phase at 100 °C.

The enantiorecognition for styrene oxide derivatives with alkyl
substitution on the side chain (compounds **2**, **3**, **4**, and **5**) was relatively better than
that of styrene oxide (**1**). Compounds **2**, **3**, and **5** are present in both *cis-* and *trans-*
isomers; therefore, four peaks (enantiomers) should be observed in the chromatogram.
In all three cases, *cis-*isomers exhibited much higher $-\Delta(\Delta H)$ values than *trans-*
isomers (Figure 4.16). For epoxides that are isomers (**4Et**, **3**, **4**, **5**), changes in
substituent position can give rise to a significant change in separation selectivity. As
shown in Figure 4.17, enantiomers of all analytes could be separated at 110 °C, except
those of **4Et** which also displayed the longest retention time.
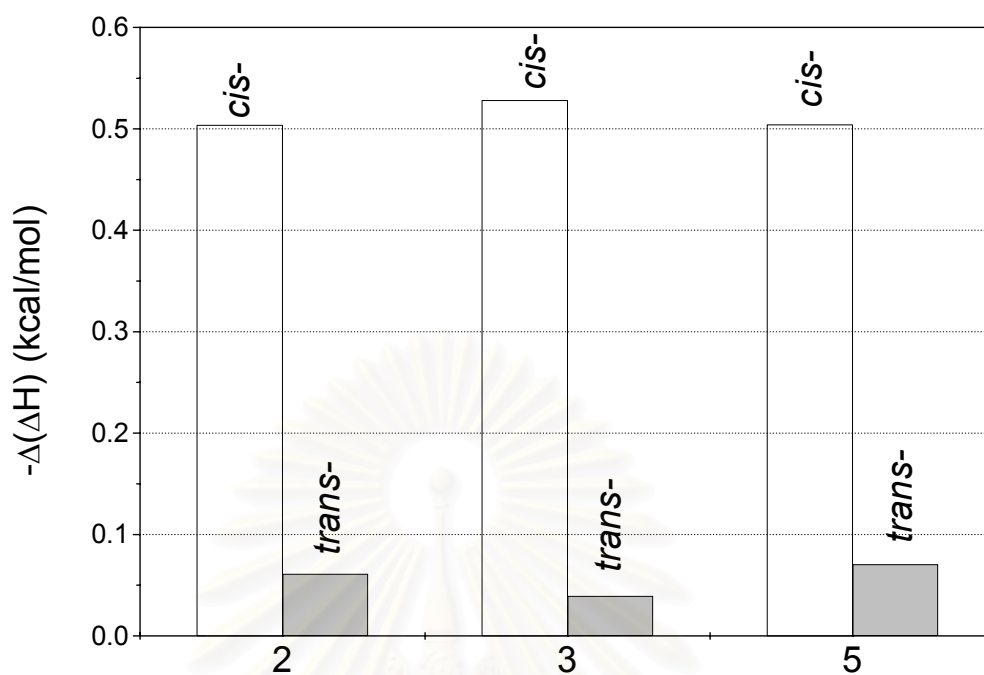
Figure 4.16   Difference in enthalpy values (-Δ(ΔH), kcal/mol) of the enantiomers of
styrene oxide derivatives **2**, **3**, and **5** on BSiMe phase obtained from
van't Hoff approach.
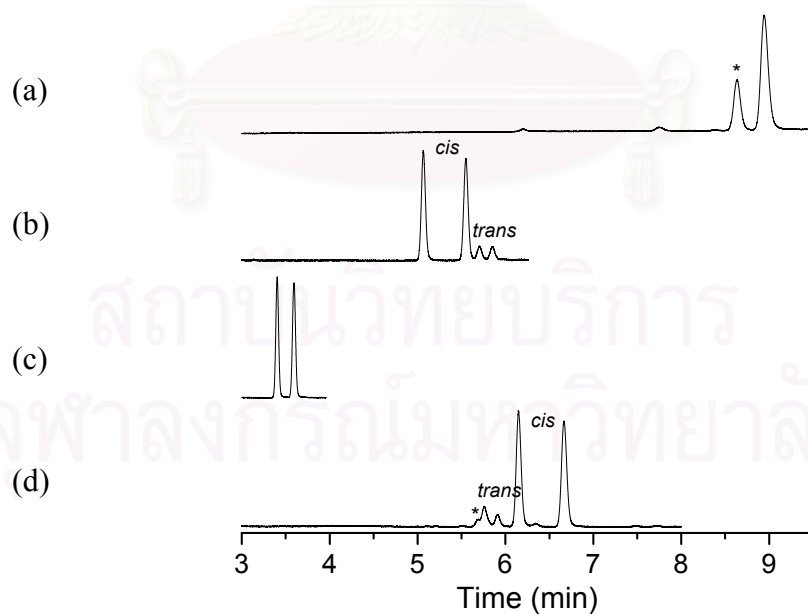
Figure 4.17   Chromatograms of (a) **4Et**; (b) **3**; (c) **4**; and (d) **5** on BSiMe phase at
110 °C. (* indicates contaminant peaks.)

Comparison of the enantioseparation of analytes **1**, **6**, **7**, and **8** revealed that the distance between the epoxy group, i.e. the chiral center, and the aromatic ring could affect the separation selectivity (Figure 4.18). The introduction of oxygen atom into a side chain could influence the enantiorecognition as well. Nevertheless, the effect cannot be generalized from the results obtained in this study due to the limited number of analytes.
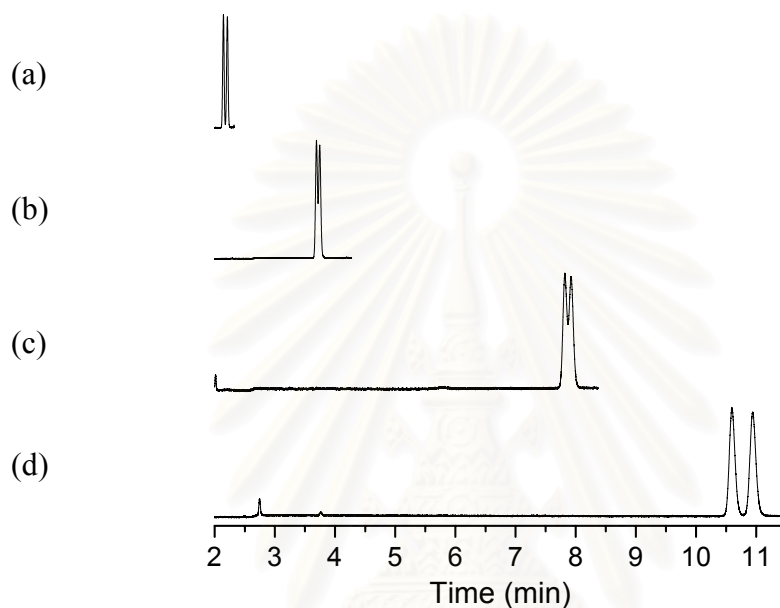
Figure 4.18   Chromatograms of (a) **1**; (b) **6**; (c) **7**; and (d) **8** on BSiMe phase at 120 °C.

The ability of BSiAc to separate enantiomers of aromatic epoxides was as well explored. The $-\Delta(\Delta H)$ and $-\Delta(\Delta S)$ values obtained from BSiAc column (Figures C18-C19, appendix C) were generally lower than those obtained from BSiMe column. Nonetheless, their tendencies were quite reverse. For enantiomers of mono-substituted aromatic epoxides, which were poorly or could not be separated on BSiMe column, they were well resolved on BSiAc column, particularly the *meta*-substituted derivatives (Figure 4.19). The $-\Delta(\Delta H)$ values for the group of halogen- and trifluoromethyl-substituted derivatives were in the order: (*ortho, para*) < *meta*. However, the enantiorecognition of BSiAc towards epoxides with methyl, cyano and nitro substituents was quite different and the highest $-\Delta(\Delta H)$ values were observed for *para*-substituted analytes.
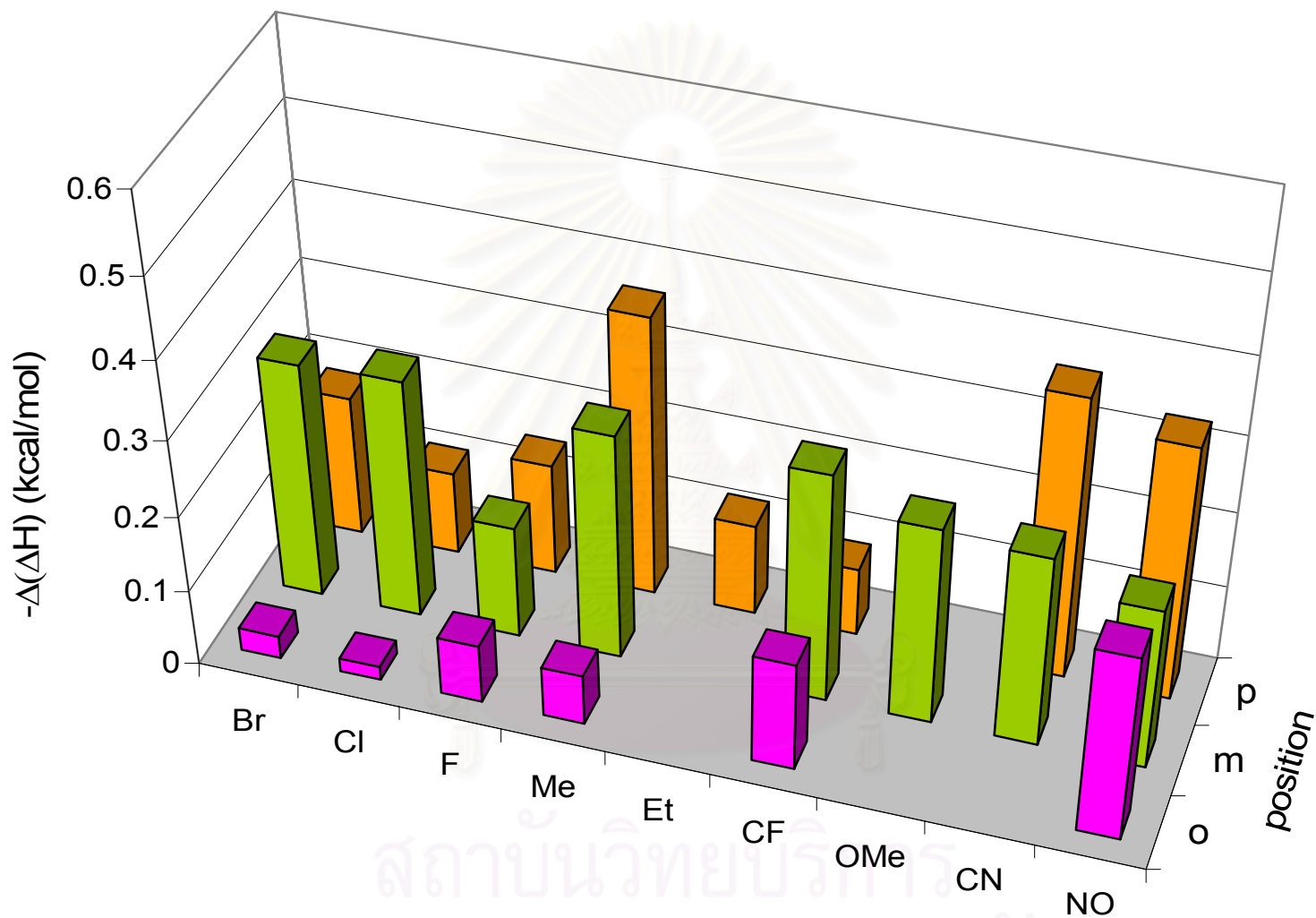
Figure 4.19   Difference in enthalpy values (-Δ(ΔH), kcal/mol) of the enantiomers of mono-substituted styrene oxide derivatives on BSiAc phase obtained from *van't Hoff approach*.

A comparison of the ln α vs. 1/T plots of all mono-fluorostyrene oxides indicated that temperature had strong effect on the enantioseparation of **2F** and **4F**, but showed a lesser influence on the separation of **3F** enantiomers (Figure 4.20). At temperatures above 85 °C, the enantioselectivity of **3F** was superior to **2F** and **4F**, but below 85 °C enantioselectivity of **3F** appeared to decline. A curved ln α vs. 1/T plot of **3F** also implied that epoxide **3F** tended to interact with the stationary phase by multiple mechanisms and no particular mechanism dominated [48]. Among all epoxides used in this study, only styrene oxide (**1**) and **3F**, separated with BSiAc column, exhibited separation selectivity maxima on ln α vs. 1/T plots.
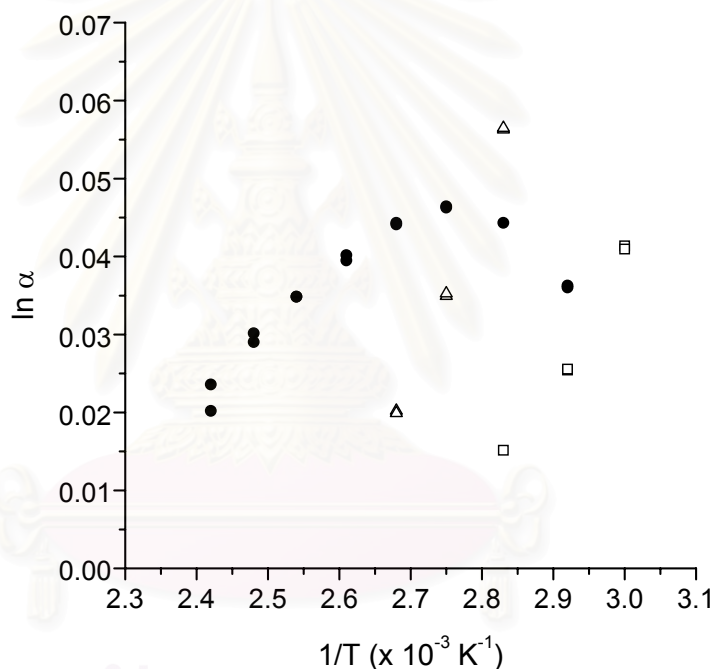
Figure 4.20   Plots of ln α vs. 1/T for the enantiomers of **2F** (□); **3F** (●); and **4F** (△) on BSiAc phase.

BSiAc also offered exciting results for di-substituted styrene oxides. Analytes that could not be enantioseparated successfully on BSiMe column could be well resolved on BSiAc column. The difference in polarity and size of CD substituents at C2 and C3 chiral carbons (BSiMe vs. BSiAc) would bring about the change in interaction strength and in molecular conformation and; consequently, the change in enantiorecognition of derivatized CDs. The generalized trend for di-substituted epoxides could not be introduced, since the enantiorecognition varied with both substitution type and position (Figure 4.21). Nevertheless, 3,4-substituted styrene oxides, regardless the type of substituent, demonstrated the highest enantioseparation among all di-substituted analytes tested on BSiAc column. The enantioseparation of three dichlorostyrene oxides, for example, on both columns was compared in Figure 4.22. These aforementioned results unquestionably suggested that substitution position on both analytes and cyclodextrins possess a major impact on enantioselectivity.

The effect of electronegative substituent on enantiodifferentiation was observed. The methyl- and trifluoromethyl-styrene oxides (**2Me**, **3Me**, **4Me** vs. **2CF**, **3CF**, **4CF**) showed different trend of separation selectivity on both columns (Figures 4.11 vs. 4.19). The number and position of analyte substituent on the separation of enantiomers was further demonstrated. It could be seen from the $-\Delta(\Delta H)$ values of mono-, di-, tri-, tetra- and penta-fluorostyrene oxides that enantiorecognition varied significantly on both columns.

For styrene oxide derivatives with alkyl substitution on the side chain (**2**, **3**, **4**, **5**, **6**, **7**, and **8**), the enantioseparation was much superior than that of styrene oxide **1** (Figure 4.23). Considering the enantiomer separation of *cis*- and *trans*-isomers of analytes **2**, **3**, and **5**, the separation was greatly improved on BSiAc column. Furthermore, the $-\Delta(\Delta H)$ values of both *cis*- and *trans*-isomers were relatively comparable. The enantiomer separation of phenylpropylene oxide (**2**) on BSiMe and BSiAc was compared in Figure 4.24. Interestingly, the elution order of *cis*-**2** and *trans*-**2** was different. On BSiMe column, *trans*-isomer eluted before *cis*-isomer, but the opposite was observed on BSiAc column.
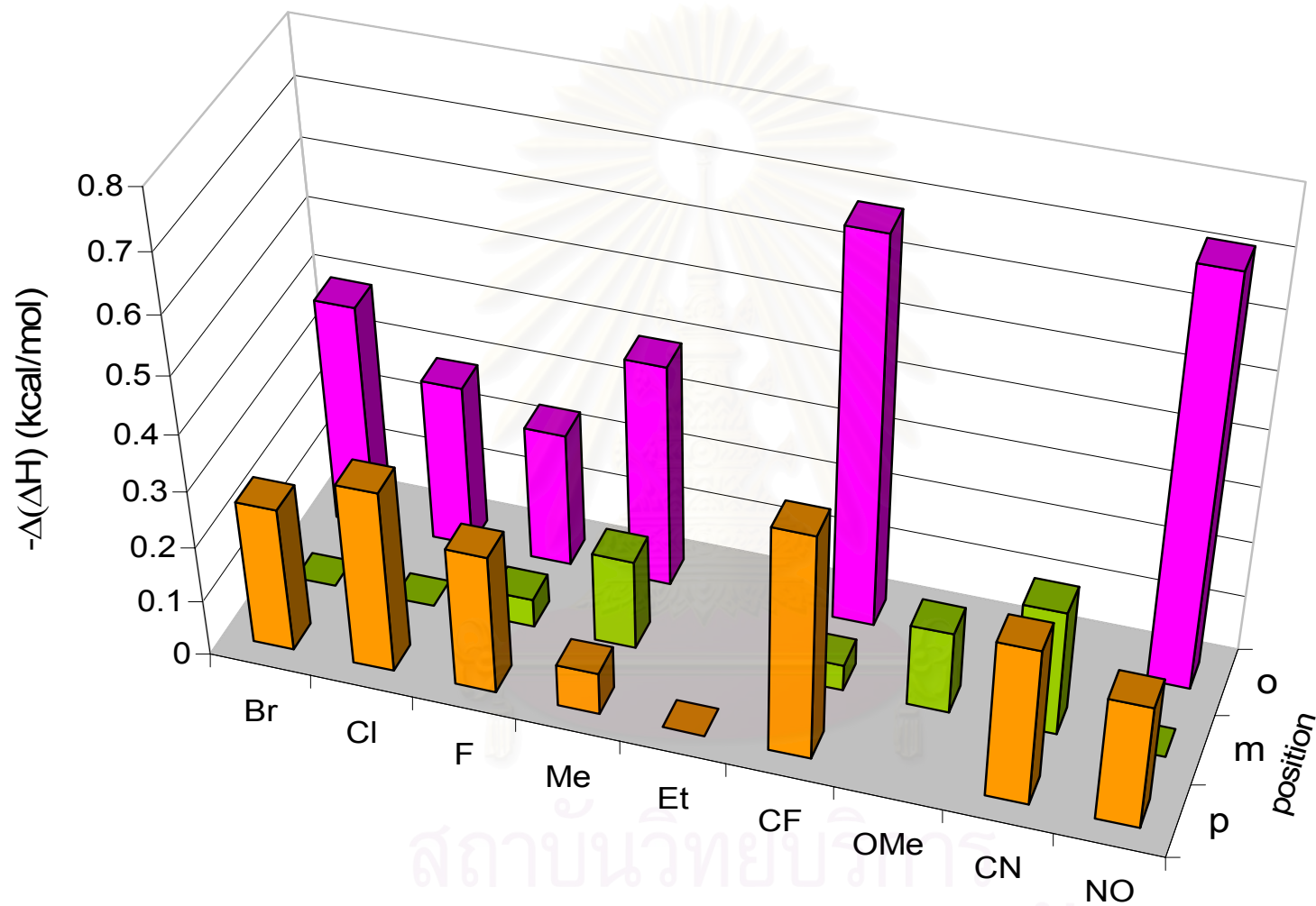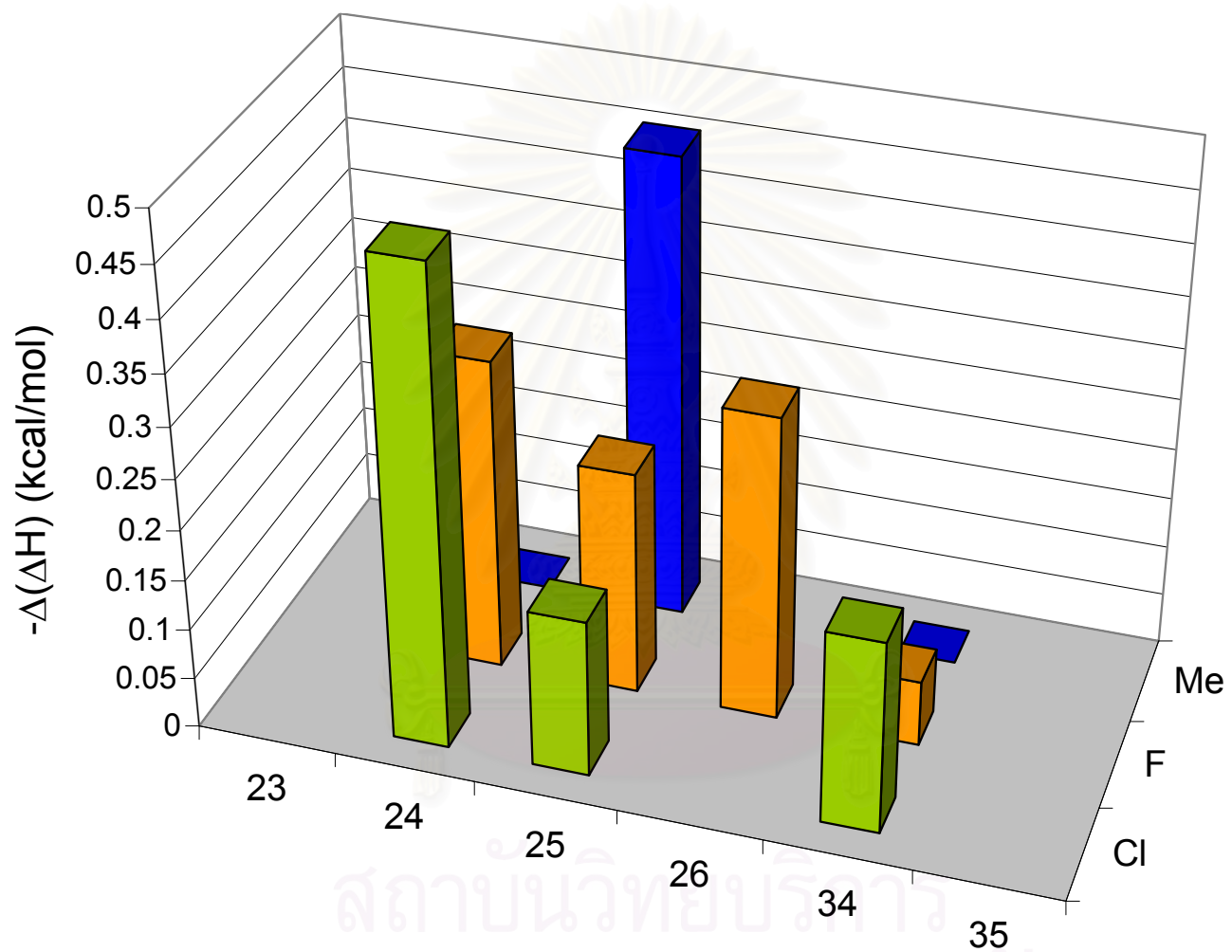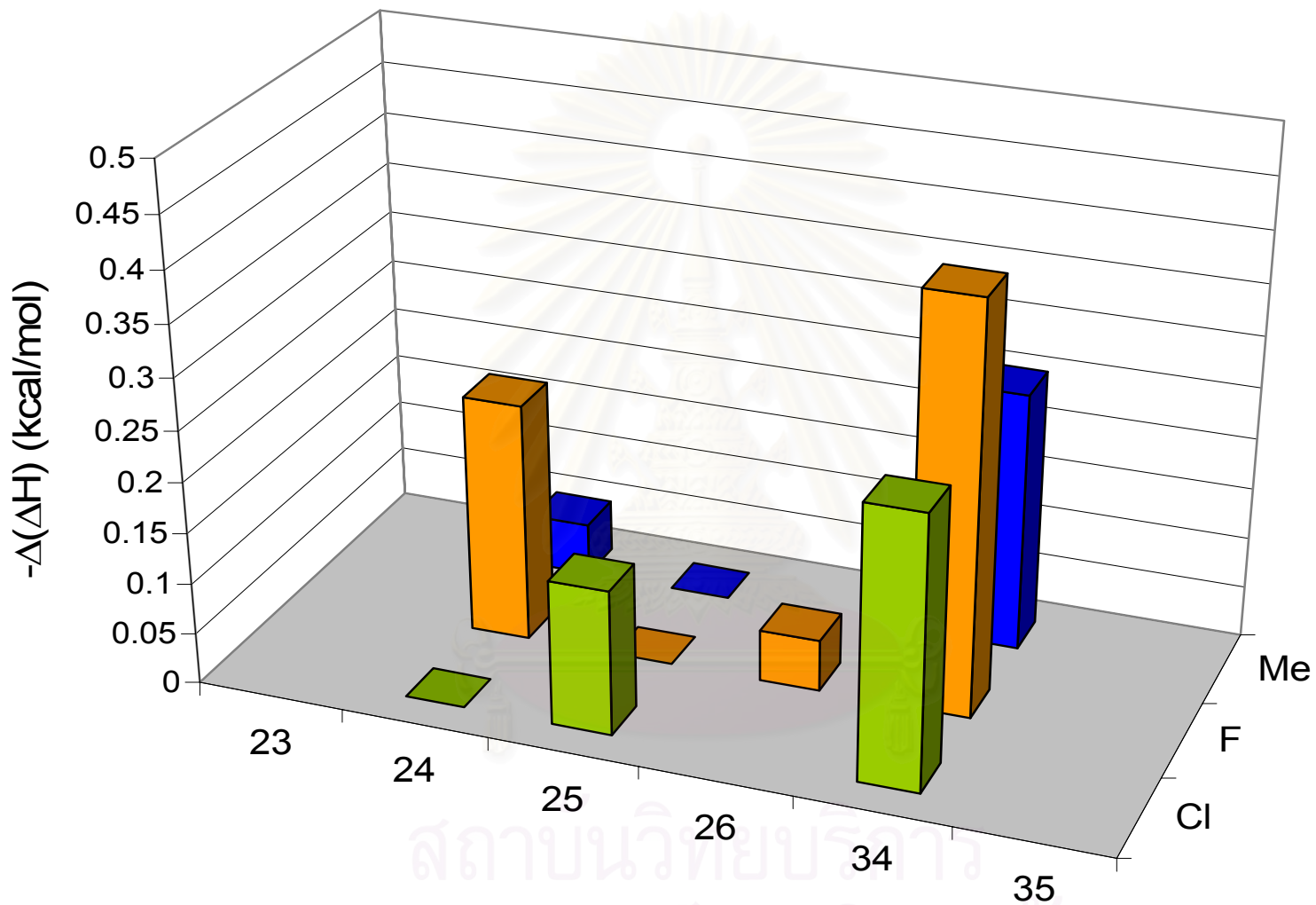
Figure 4.21   Difference in enthalpy values (-Δ(ΔH), kcal/mol) of the enantiomers of di-substituted styrene oxide derivatives on BSiAc phase obtained from *van't Hoff approach*.
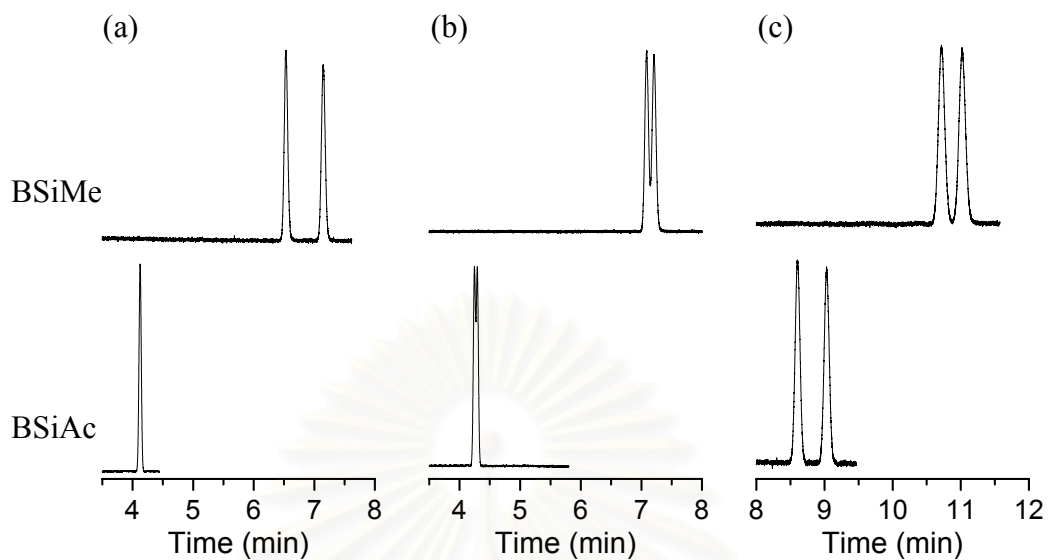
Figure 4.22   Chromatograms of three dichlorostyrene oxides (a) **24Cl**; (b) **25Cl**;
and (c) **34Cl** on (top) BSiMe and (bottom) BSiAc phases at 130 °C.
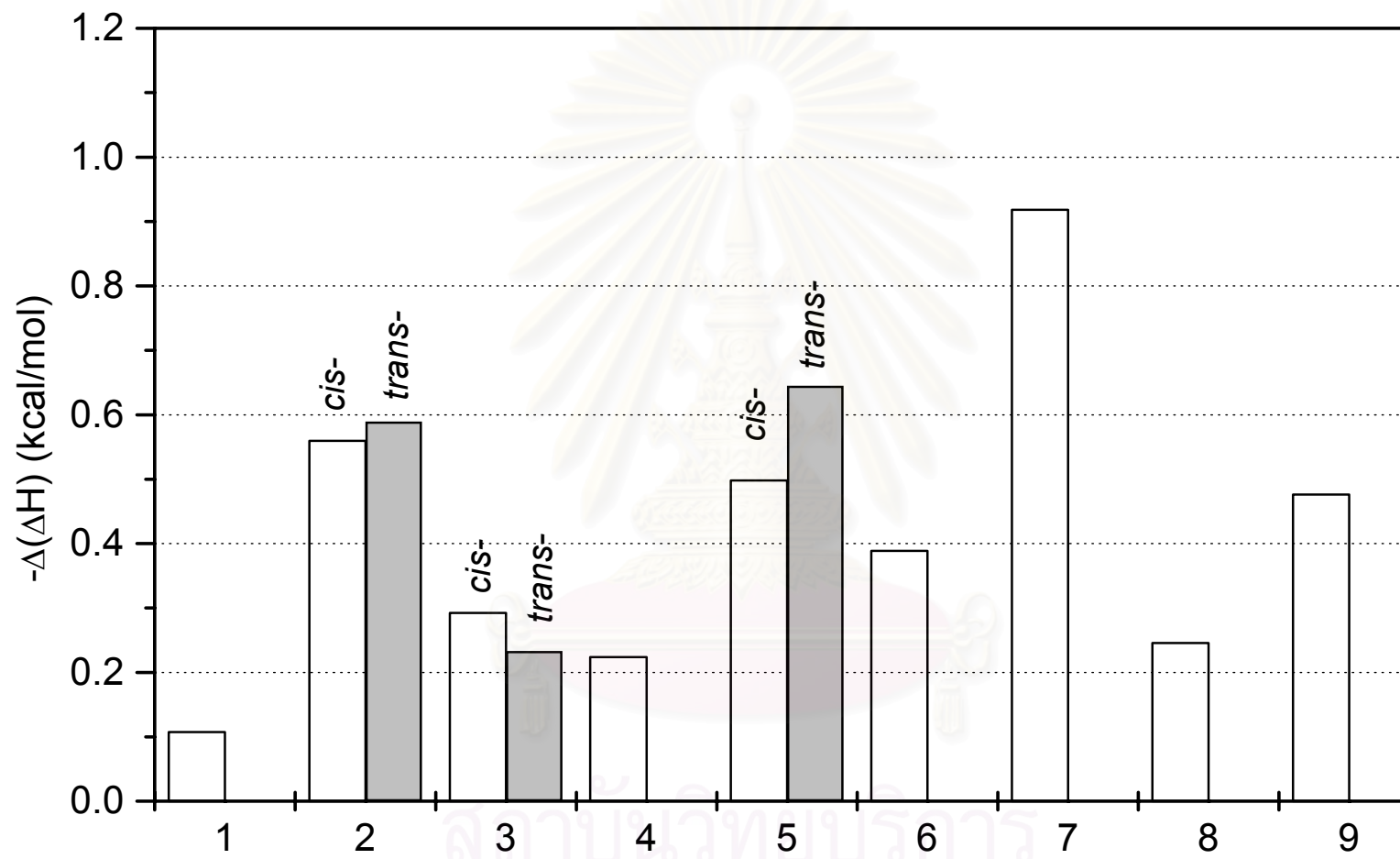
Figure 4.23   Difference in enthalpy values (-Δ(ΔH), kcal/mol) of the enantiomers of styrene oxide derivatives **1-9** on BSiAc phase obtained from *van't Hoff approach.*
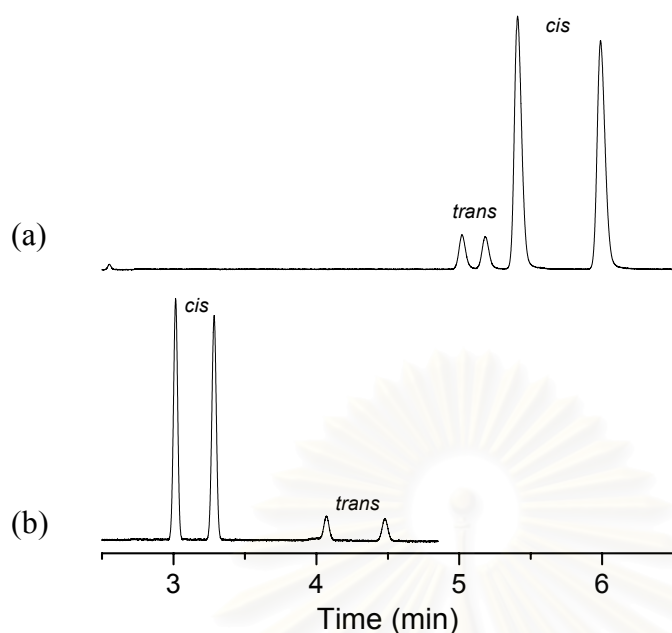
Figure 4.24   Chromatograms of phenylpropylene oxide (**2**) on (a) BSiMe and (b) BSiAc phases at 100 °C.

Enantiomer separation of analytes **1**, **2**, and **4** were previously reported using heptakis(2,6-di-*O*-methyl-3-*O*-trifluoroacetyl)-β-cyclodextrin, or TFA-CD, as chiral selector [10]. Using TFA-CD mixed in OV-1701 as stationary phase [8], it was found that the separation selectivities were mostly lower than those obtained from BSiMe or BSiAc columns under identical separation temperature. Moreover, the enantioresolution of **1** could not be detected even at lower temperature (85 °C). When TFA-CD chemically bonded to polydimethylsiloxane (known as Chirasil-Dex-TFA) was used as stationary phase, the enantioselectivity of these analytes was much higher compared to the diluted system. These results demonstrated the effect of polysiloxane polarity, which added to the strength of interaction, but not to the enantioselectivity. Therefore, smaller selectivity values were observed with the more polar OV-1701. Enantiomers of analytes **1**, **2**, and **4** could be separated with good selectivities on Chirasil-Dex-TFA, which were comparable or higher than those obtained from BSiMe or BSiAc columns.

The alkyl chain length attached to the epoxy group enhanced enantiorecognition to a great extent as previously reported by König and Gehrcke

[11]. The effect of alkyl chain length was depicted in Figure 4.25. Among all tested analytes, 1,2-epoxy-3-phenoxypropane (**7**) displayed the greatest enantiorecognition on BSiAc phase. Lengthening the side chain of analyte **7** by only one carbon (as in **8**) could drastically decrease the enantioselectivity. For epichlorohydrin (**9**), a small and the only aliphatic epoxide used in this study, the enantiomers could not be separated on BSiMe column and; moreover, they showed very weak interaction with BSiMe phase. On the contrary, they were more strongly retained at the same temperature and were perfectly resolved on BSiAc column at120 °C in less than 1.4 min (Figure 4.26).
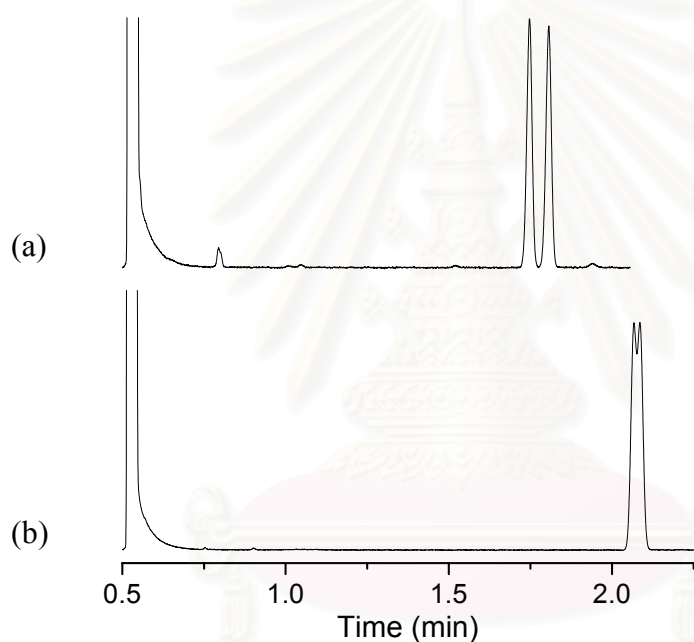
Figure 4.25   Chromatograms of (a) **7** and (b) **8** on BSiAc phase at 160 °C.
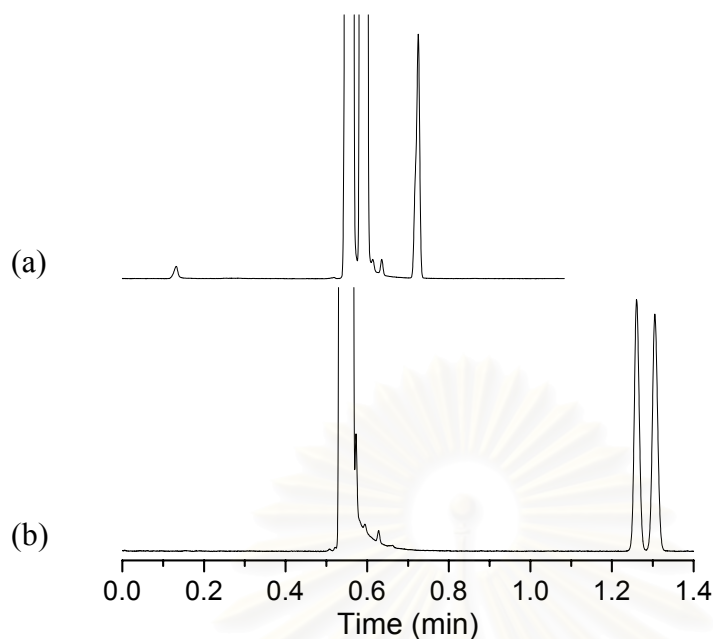
Figure 4.26   Chromatograms of epichlorohydrin (**9**) on (a) BSiMe and (b) BSiAc
phases at 120 °C.

4.5   Thermodynamic investigation by *Schurig approach*

In this method, enthalpy (-ΔH) and entropy (-ΔS) values are calculated
from the plot of ln R′ (retention increment) versus 1/T. In this study, R′ was obtained
from relative retention factors (k′) of each enantiomer with respect to *n*-alkane
standards (C8-C12). These small alkanes should have relatively weak interaction
towards both chiral columns and a polysiloxane column. The determination of
thermodynamic data by *Schurig approach* on both columns showed random data
points. In this study, the linearity (R^2 value) of ln R′ vs. 1/T plot was generally lower
than that of ln k′ vs. 1/T plot obtained by *van't Hoff method*, along with scattered data
points, as illustrated in Figure 4.27. These nonlinear plots possibly resulted from the
non-ideal behavior of *n*-alkane standards. The calculation of thermodynamic data for
several analytes using *Schurig approach* were, therefore, not possible.

Some thermodynamic parameters (-ΔH_2 and -Δ(ΔH) values) of mono-
substituted styrene epoxides separated on BSiMe column obtained by *van't Hoff
approach* and *Schurig approach* were compared in Figures 4.28-4.29. Full detail of
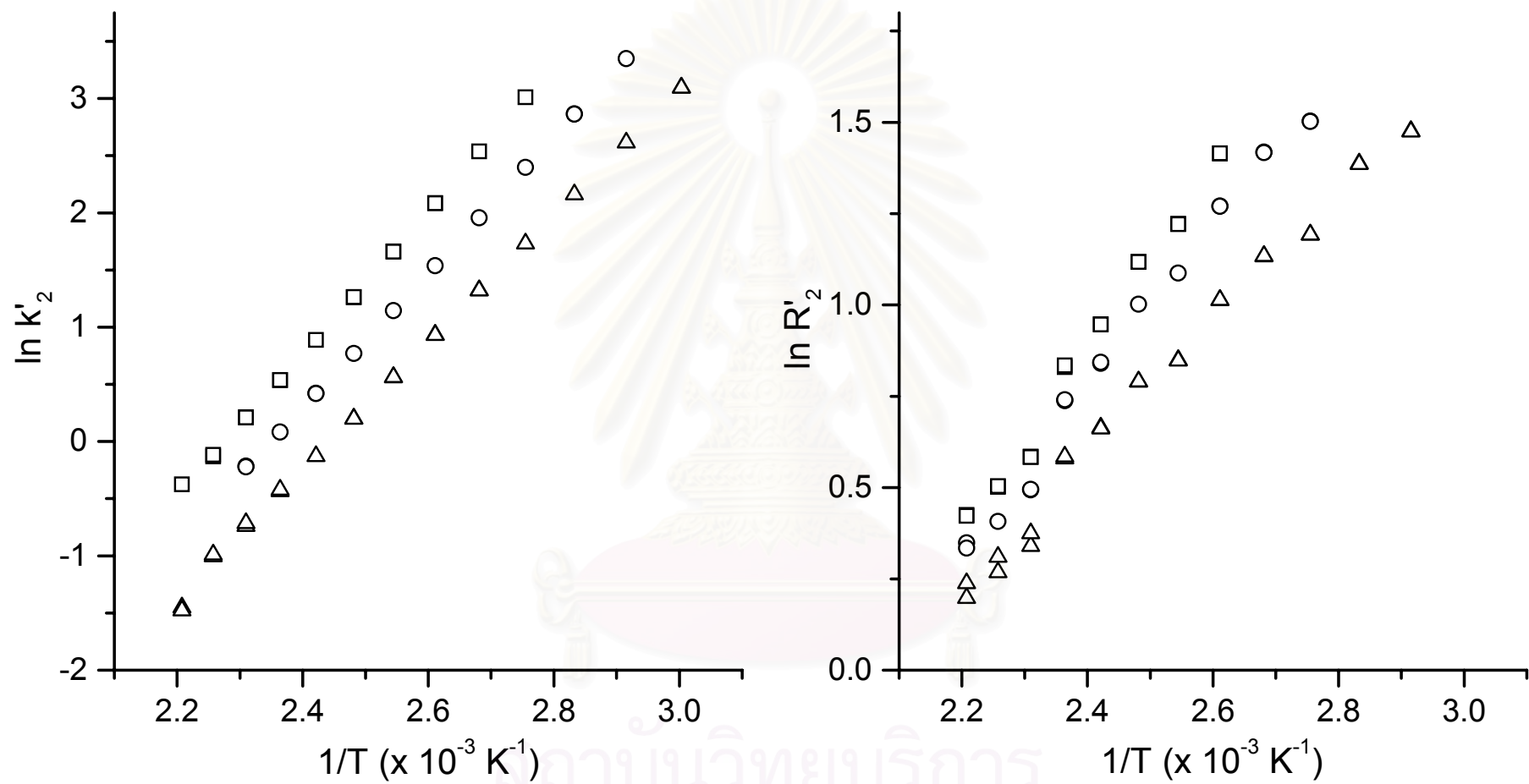
Figure 4.27   Comparison of ln k′ vs. 1/T plot by *van't Hoff approach* and ln R′ vs. 1/T plot by *Schurig approach* for more retained enantiomers of **2Br** (□), **2Cl** (○), and **2F** (△) on BSiMe phase.
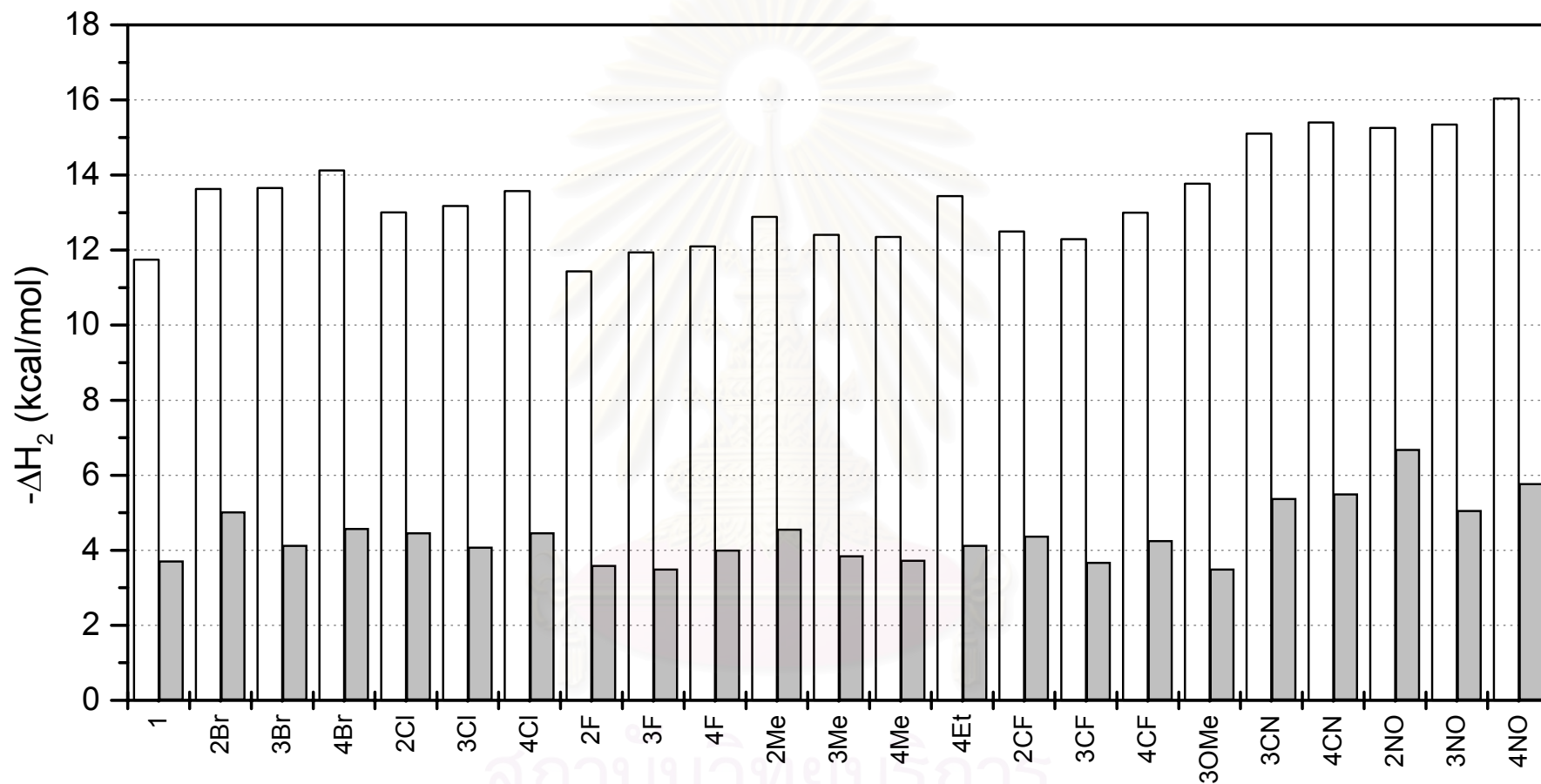
Figure 4.28   Comparison of enthalpy values of the more retained enantiomers of mono-substituted styrene oxides on BSiMe phase obtained from (white bar) *van't Hoff approach* and (gray bar) *Schurig approach*.
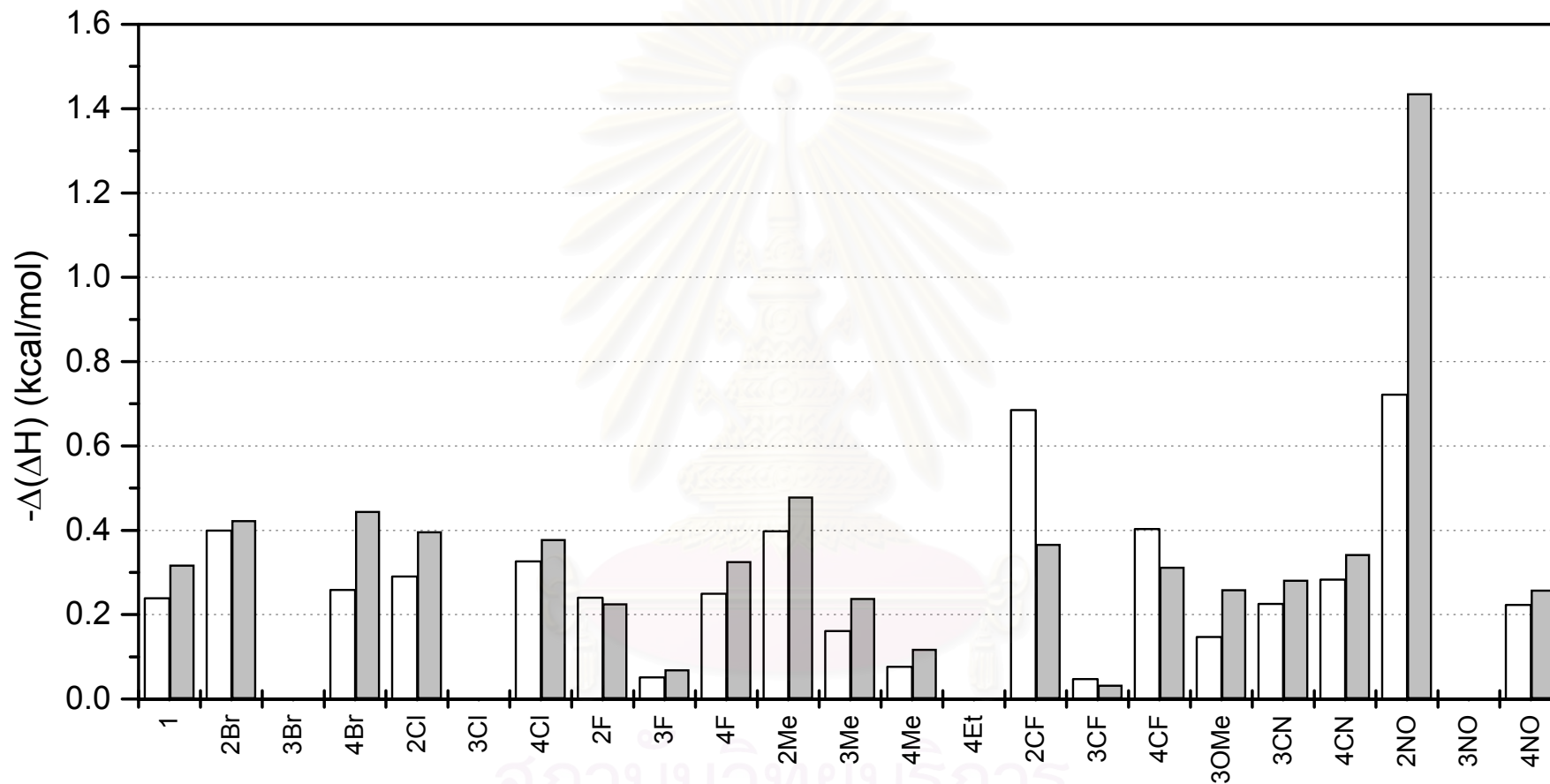
Figure 4.29   Comparison of enthalpy differences of the enantiomers of mono-substituted styrene oxides on BSiMe phase obtained from (white bar) *van't Hoff approach* through ln k′ vs.1/T plots and (gray bar) *Schurig approach* through ln R′ vs.1/T plots.

these data could be found in appendix C. In general, $-\Delta H_2$ values obtained by *Schurig approach* were lower than those obtained by *van't Hoff approach*, since only contributions from cyclodextrin selector were accounted for. The $-\Delta(\Delta H)$ values acquired by both *van't Hoff approach* and *Schurig approach* should be theoretically identical. Nevertheless, some discrepancies were detected, e.g. **2Me** vs. **2CF**, as detailed in Table 4.1. It can be seen that the values calculated by *van't Hoff approach* through either $\ln k'$ vs.$1/T$ plots or $\ln \alpha$ vs.$1/T$ plots are in better agreement than those calculated by *Schurig approach*. In addition, only the values determined by *Schurig approach* through $\ln (R'_2/R'_1)$ vs.$1/T$ plots are comparable with those done by *van't Hoff approach*. Although values from *Schurig approach* will not rely on CD concentration or type of polysiloxane used and should provide more dependable data, results from *van't Hoff approach* are in good agreement with chromatographic results than those from *Schurig approach*. Additionally, other advantages of *van't Hoff approach* are the simplicity of data treatment and that no analysis on a reference column is required.

Table 4.1   The $-\Delta(\Delta H)$ and $-\Delta(\Delta S)$ values of the enantiomers of **2Me** and **2CF** on BSiMe phase calculated by *van't Hoff approach* and *Schurig approach*.

analyte		*van't Hoff approach*		*Schurig approach*	
		$\ln k'$ vs.$1/T^a$	$\ln \alpha$ vs.$1/T^b$	$\ln R'$ vs.$1/T^c$	$\ln \dfrac{R'_2}{R'_1}$ vs.$1/T^d$
2Me	$-\Delta(\Delta H)$	0.39	0.38	0.47	0.41
	$-\Delta(\Delta S)$	0.85	0.64	1.00	0.85
2CF	$-\Delta(\Delta H)$	0.68	0.64	0.36	0.68
	$-\Delta(\Delta S)$	1.53	1.42	0.58	1.44

Note: [a] The $-\Delta(\Delta H)$ and $-\Delta(\Delta S)$ values were obtained from the difference in $-\Delta H$ and $-\Delta S$ values of each enantiomer. Each $-\Delta H$ and $-\Delta S$ value was obtained from $\ln k'$ vs.$1/T$ plots according to equation (7).

[b] The $-\Delta(\Delta H)$ and $-\Delta(\Delta S)$ values were obtained from $\ln \alpha$ vs.$1/T$ plots according to equation (4).

[c] The $-\Delta(\Delta H)$ and $-\Delta(\Delta S)$ values were obtained from the difference in $-\Delta H$ and $-\Delta S$ values of each enantiomer. Each $-\Delta H$ and $-\Delta S$ value was obtained from $\ln R'$ vs.$1/T$ plots according to equation (13).

[d] The $-\Delta(\Delta H)$ and $-\Delta(\Delta S)$ values were obtained from $\ln (R'_2/R'_1)$ vs.$1/T$ plots according to equation (11).

CHAPTER V

CONCLUSIONS AND SUGGESTIONS FOR FUTURE WORK

A number of styrene oxide derivatives with different number, type (e.g. bromo, chloro, fluoro, methyl, methoxy, cyano, and nitro), and position (*ortho*, *meta*, and *para*) of substitution could be successfully prepared. Separation of enantiomers of styrene oxide and its derivatives was studied by gas chromatography using chiral stationary phases containing modified β-cyclodextrins: heptakis(2,3-di-*O*-methyl-6-*O*-*tert*-butyldimethylsilyl)-β-cyclodextrin (or BSiMe) and heptakis(2,3-di-*O*-acetyl-6-*O*-*tert*-butyldimethylsilyl)-β-cyclodextrin (or BSiAc). Both selectors possess identical ring size and 6-*O*-*tert*-butyldimethylsilyl substituents, but have different substituents (*O*-methyl vs. *O*-acetyl) at C2 and C3 chiral carbons. All analytes could be enantioseparated with either BSiMe phase or BSiAc phase, or both of them. The information acquired systematically from the gas chromatographic experiments were used to calculate thermodynamic parameters for the association between chiral analytes and cyclodextrin derivatives in order to realize the effect of analyte and selector structures on enantiomer recognition.

From thermodynamic data obtained by *van't Hoff approach*, the $-\Delta H$ and $-\Delta S$ values of analytes on two chiral columns are greater than those on a nonchiral polysiloxane column, which indicates stronger interaction and more interaction sites between analytes and chiral phases. Comparing these values acquired from both chiral columns, it can be seen that both $-\Delta H_2$ and $-\Delta S_2$ values display similar trend, with a few exceptions. In addition, the values of all analytes on the same column are relatively comparable. This indicates that the main analyte contributions to the interaction arise from the primary functional groups: aromatic ring and epoxy group. The thermodynamic differences ($-\Delta(\Delta H)$ and $-\Delta(\Delta S)$ values), on the other hand, display different trend from $-\Delta H_2$ and $-\Delta S_2$ values. Analytes showing strong interaction do not necessarily exhibit high enantioseparation.

Apparently, in this study, retention and degree of separation of all chiral analytes depend on numerous factors: number, type, and position of substituent

on the aromatic ring or epoxy side chain as well as the type of substituent on cyclodextrin ring. On BSiMe column, substitution at *ortho-* or *para-*position of the aromatic ring seems to enhance the enantiorecognition, while substitution at *meta-*position reduces the enantiorecognition. Among all the analytes tested, 2-nitrostyrene oxide (**2NO**) and 2-trifluoromethylstyrene oxide (**2CF**) show highest degree of enantioseparation (largest $-\Delta(\Delta H)$ and $-\Delta(\Delta S)$ values).

On BSiAc column, the trend for both $-\Delta(\Delta H)$ and $-\Delta(\Delta S)$ values was quite reverse. Substitution at *meta-*position of the aromatic ring tends to promote the enantiorecognition. Better enantioseparation was also observed for styrene oxide derivatives with substitution on the epoxy side chain. A small, aliphatic epichlorohydrin (**9**), which could not be resolved on the BSiMe column, was very well separated. The analyte showing the best enantiorecognition on BSiAc phase is 1,2-epoxy-3-phenoxy propane (**7**).

Calculation of thermodynamic parameters via *Schurig approach* poses some difficulties as, sometimes, the values obtained from ln R′ vs.1/T plots and ln (R'_2/R'_1) vs.1/T plots do not agree. Moreover, the linearity of the plots was not good. Results from *van't Hoff approach* are in better agreement with chromatographic results than those from *Schurig approach*.

The great difference in enantioseparation of epoxides on BSiMe and BSiAc columns is essentially due to the difference in substitution at C2 and C3 chiral carbons of cyclodextrin molecule, which results in different shape and position favorable for interaction with particular analytes. Hopefully, with larger number of epoxide analytes containing various substitution patterns as well as molecular modeling experiments, more conclusive assumption about analyte-stationary phase interaction that leads to separation mechanism could be obtained.

REFERENCES

1. N. M. Maier, P. Franco, and W. Lindner. Separation of enantiomers: Needs, challenges, perspectives. J. Chromatogr. A 906 (2001): 3-33.

2. J. Szymurz-Oleksiak, J. Bojarski, and H. Y. Aboul-Enein. Recent application of stereoselective chromatography. Chirality 14 (2002): 417-435.

3. A. N. Collins, G. N. Sheldrake, and J. Crosby. Chirality in industrial II: Developments the manufacture and applications of optically active compounds. Chichester:Wiley, 1997, p. 226.

4. V. Schurig. Separation of enantiomers by gas chromatography. J. Chromatogr. A 906 (2001): 275-299.

5. V. Schurig. Chiral separation using gas chromatography. Trends Anal. Chem. 21 (2002): 647-661.

6. W. −Y. Li, H. L. Jin, and D. W. Armstrong. 2,6-Di-*O*-pentyl-3-*O*-trifluoroacetyl cyclodextrin liquid stationary phases for capillary gas chromatographic separation of enantiomers. J. Chromatogr. 509 (1990): 303-324.

7. D. W. Armstrong, W. Li, A. M. Stalcup, H. V. Secor, R. R. Izac, and J. I. Seeman. Capillary gas chromatographic separation of enantiomers with stable dipentyl-α-, β- and γ-cyclodextrin-derivatized stationary phases. Anal. Chim. Acta 234 (1990): 365-380.

8. V. Schurig, M. Jung, D. Schmalzing, M. Schleimer, J. Duvekot, J. C. Buyten, J. A. Peene, and P. Mussche. CGC enantiomer separation on diluted cyclodextrin derivatives coated on fused silica columns. J. High Resolut. Chromatogr. 13 (1990): 470-474.

9. T. Reiher and H. J. Hamann. Enantioselective separation of epoxides and alcohols with perpentylated α-cyclodextrin. J. High Resolut. Chromatogr. 15 (1992): 346-349.

10. M. Jung and V. Schurig. Chirasil-Dex-TFA: A new polysiloxane-bonded and immobilizable cyclodextrin stationary phase for enantiomer separation by GC. J. High Resolut. Chromatogr. 16 (1993): 289-298.

11. W. A. König and B. Gehrcke. Gas chromatographic enantiomer separation with modified cyclodextrins: Carboxylic acid esters and epoxides. J. High Resolut. Chromatogr. 16 (1993): 175-181.

12. N. Koen de Vries, B. Coussens, and R. J. Meier. The separation of enantiomers on modified cyclodextrin columns: Measurements and molecular modeling. J. High Resolut. Chromatogr. 15 (1992): 499-504.

13. W. A. König. Collection of enantiomer separation factors obtained by capillary gas chromatography on chiral stationary phases. J. High Resolut. Chromatogr. 16 (1993): 312-322.

14. K. Jaques, W. M. Buda, A. Venema, and P. Sandra. Enantioselective separations by capillary gas chromatography on derivatized cyclodextrins III. Separation of some racemic 2,2-dialkyl-4-alkoxycarbonyl-1,3-dioxane derivatives on 2,3-di-*O*-acetyl-6-*O*-tert*-butyldimethylsilyl-β-and γ-cyclodextrin. J. Chromatogr. A 666 (1994): 131-136.

15. M. Oehme, L. Muller, and H. Karlsson. High-resolution gas chromatographic test for characterisation of enantioselective separation of organochlorine compounds application to *tert*-butyldimetylsilyl β-cyclodextrin. J. Chromatogr. A 775 (1997): 275-285.

16. M. Y. Nie, L. M. Zhou, X. L. Liu, Q. H. Wang, and D. Q. Zhu. Separation of the enantiomers of 2-phenylcyclopropane carboxylate esters by capillary gas chromatogrphy on derivatized cyclodextrin stationary phases. Chromatographia 51 (2000): 450-454.

17. T. Beck, J. Nandzik, and A. Mosandl. Diluted modified cyclodextrins as chiral stationary phases in capillary gas chromatography-octakis(2,3-di-*O*-propionyl-6-*O-tert*-butyldimethylsilyl)-γ-cyclodextrin. J. Microcol. Sep. 12 (2000): 482-492.

18. T. Beck, J. M. Liepe, J. Nandzik, S. Rohn, and A. Mosandl. Comparison of different di-*tert*-butyldimethyl-silylated cyclodextrins as chiral stationary phases in capillary gas chromatography. J. High Resolut. Chromatogr. 23 (2000): 569-575.

19. H. G. Schmarr and A. Mosandl. Influence of derivatization on the chiral selectivity of cyclodextrins: Alkylated/acylated cyclodextrins and γ-/δ-lactones as an example. J. Microcol. Sep. 3 (1991): 395-402.

20. A. Dietrich, B. Maas, V. Karl, P. Kreis, D. Lehmann, B. Weber, and A. Mosandl. Stereoisomeric flavor compounds. Part LV: stereodifferentiation of some chiral volatiles on heptakis(2,3-*O*-acetyl-6-*O*-*tert*-butyldimethylsilyl)-β-cyclodextrin. J. High Resolut. Chromatogr. 15 (1992): 176-179.

21. A. Dietrich, B. Maas, W. Messer, G. Bruche, V. Karl, A. Kaunzinger, and A. Mosandl. Stereoisomeric flavor compounds. Part LVIII: The use of heptakis(2,3-di-*O*-methyl-6-*O*-*tert*-butyldimethylsilyl)-β-cyclodextrin as a chiral stationary phase in flavor analysis. J. High Resolut. Chromatogr. 15 (1992): 590-593.

22. F. Kobor and G. Schomburg. 6-*tert*-Butyldimethylsilyl-2,3-dimethyl-α-,β-, and γ-cyclodextrin, dissolved in polysiloxanes, as chiral selectors for gas chromatography: Influence of selector concentration and polysiloxane matrix polarity on enantioselectivity. J. High Resolut. Chromatogr. 16 (1993): 693-699.

23. B. Maas, A. Dietrich, and A. Mosandl. Comparison of different 6-*tert*-butyldimethyl-silylated cyclodextrins as chiral stationary phase in GC. J. Microcol. Sep. 8 (1996): 47-56.

24. B. E. Kim, K. P. Lee, K. –S. Park, S. H. Lee, and J. H. Park. Enantioselectivity of 6-*O*-alkyldimethylsilyl-2,3-di-*O*-methyl-β-cyclodextrins as chiral stationary phases in capillary GC. Chromatographia 46 (1997): 145-150.

25. U. Klobes, W. Vetter, B. Luckas, and G. Hottinger. Enantioseparation of the compounds of technical toxaphene (CTTs) on 35% heptakis(6-*O*-*tert*-butyldimethylsilyl-2,3-di-*O*-methyl)-β-cyclodextrin in OV-1701. Chromatographia 47 (1998): 565-569.

26. C. Bicchi, G. Cravotto, A. D'Amato, P. Rubiolo, A. Galli, and M. Galli. Cyclodextrin derivatives in gas chromatographic separation of racemates with different volatility. Part XV: 6-*O*-*t*-Butyldimethylsilyl versus 6-*O*-*t*-hexyldimethylsilyl-β and –γ derivatives. J. Microcol. Sep. 11 (1999): 487-500.

27. M. da C. K.V. Ramos, L. H.P. Teixeira, F. R. de A. Neto, E. J. Barreiro, C. R. Rodrigues, and C. A.M. Fraga. Chiral separation of γ-butyrolactone derivatives by

gas chromatography on 2,3-di-*O*-methyl-6-*O-tert*-butyldimethylsilyl-β-cyclodextrin. J. Chromatogr. A 985 (2003): 321-331.

28. Z. Juvancz. The role of cyclodextrins in chiral selective chromatography. Trends Anal. Chem. 21 (2002): 379-388.

29. S. Allemark and V. Schurig. Chromatography on chiral stationary phase. J. Mater. Chem. 7 (1997): 1955-1963.

30. V. Schurig. Enantiomer separation by gas chromatography on chiral stationary phases. J. Chromatogr. A 666 (1994): 111-129.

31. V. Schurig and H. -P. Nowotny. Gas chromatographic separation of enantiomers on cyclodextrin derivatives. Angew. Chem. Int. Ed. Engl. 29 (1990): 939-957.

32. R. Stuart Tipson and D. Horton. Advances in carbohydrate chemistry and biochemistry. Acedamic Press Inc., Califonia 1988. p. 207.

33. W. A. König. Enantioselective gas chromatography. Trends Anal. Chem. 12 (1993): 130-137.

34. A. Buvari-Barcza and L. Barcza. Influence of the guests, the type and degree of substitution on inclusion complex formation of substituted β-cyclodextrins. Talanta 49 (1999): 577-585.

35. K. Uekama, F. Hirayama, and T. Irie. Cyclodextrin drugs carrier systems. Chem. Rev. 98 (1998): 2045-2076.

36. J. Szejtli. Introduction and general overview of cyclodextrin chemistry. Chem. Rev. 98 (1998): 1743-1753.

37. M. Jung, D. Schmalzing, and V. Schurig. Theoretical approach to the gas chromatographic separation of enantiomers on dissolved cyclodextrin derivatives. J. Chromatogr. 552 (1991): 43-57.

38. V. Schurig and M. Juza. Approach to the thermodynamics of enantiomer separation by gas chromatography- Enantioselectivity between the chiral inhalation anesthetics enflurane, isoflurane and desflurane and a diluted γ-cyclodextrin derivative. J. Chromatogr. A 757 (1997): 119-135.

39. I. Špánik, J. Krupčik, and V. Schurig. Comparison of two methods for the gas chromatographic determination of thermodynamic parameters of enantioselectivity. J. Chromatogr. A 843 (1999): 123-128.

40.   K. Grob. Making and manipulating capillary columns for gas chromatography. Heidelberg: Hüthig, 1986.

41.   K. Grob, Jr., G. Grob, and K. Grob. Comprehensive standardized quality test for glass capillary columns. J. Chromatogr. 156 (1978): 1-20.

42.   G. Grob, K. Grob, and K. Grob, Jr. Testing capillary gas chromatographic columns. J. Chromatogr. 219 (1981): 13-20.

43.   R. T. Morrison and R. N. Boyd. Organic chemistry. Allyn and Bacon: USA, 1973. p. 552-573.

44.   F. A. Carey. Organic chemistry. McGraw-Hill: USA, 1996. p. 241-243, 652-660.

45.   A. Péter, G. Török, D. W. Armstrong, G. Tóth, and D. Tourwé. Effect of temperature on retention of enantiomers of β-methyl amino acids on a teicoplanin chiral stationary phase. J. Chromatogr. A 828 (1998): 177-190.

46.   B. Loukili, C. Dufresne, E. Jourdan, C. Grosset, A. Ravel, A. Villet, and E. Peyrin. Study of tryptophan enantiomer binding to a teicoplanin-based stationary phase using the perturbation technique investigation of the role of sodium perchlorate in solute retention and enantioselectivity. J. Chromatogr. A 986 (2003): 45-53.

47.   I. Slama, E. Jourdan, A. Villet, C. Grosset, A. Ravel, and E. Peyrin. Temperature and solute molecular size effects on the retention and enantioslectivity of a series of D, L dansyl amino acids on a vancomycin-based chiral stationary phase. Chromatographia 58 (7/8) (2003): 399-404.

48.   B. Mass, A. Dietrich, T. Beck, S. Börner, A. Mosandl. Di-*tert*-butyldimethyl-silylated cyclodextrins as chiral stationary phases-Thermodynamic investigations. J. Microcol. Sep. 7 (1995): 65-73.

APPENDICES

Appendix A

Glossary

Adjusted retention time (t'_R) is the absolute retention of the compound a compounds on a stationary phase. This value is calculated by subtracting the time of unretained compound (t_M) from the compound's retention time (t_R), according to

$$t'_R = t_R - t_M$$

Correlation coefficient (R^2) is a number between 0 and 1 which indicates the degree of linear relationship between two variables.

Distribution coefficient (K) is defined as ratio of the concentrations of the compound in the stationary phase (C_S) and in mobile phase (C_M). K is related to retention factor by the following equation.

$$K = k' \cdot \frac{V_M}{V_S} = k' \cdot \beta$$

$$= \frac{C_S}{C_M}$$

Number of theoretical plates (N) is used as a measure of column efficiency. It is defined as the square of the ratio of the retention of analyte divided by peak broadening.

$$N = 16 \left(\frac{t_R}{W_b} \right)^2 = 5.545 \left(\frac{t_R}{W_h} \right)^2$$

where W_b and W_h are peak width at base and at half height, respectively.

Phase ratio (β) is defined as the ratio of the volume of mobile phase (V_M) to the volume of stationary phase (V_S) in the column. β is a unitless value and can be calculated from column dimension: column diameter and, stationary phase film thickness by the following equation.

$$\beta = \frac{r_c}{2d_f}$$

where r_c and d_f is the capillary column radius and stationary phase film thickness, respectively.

Retention factor or capacity factor (k′) is defined as the ratio of analyte masses in the stationary phase and mobile phase. It is equivalent to the ratio of time of analyte molecules spend in stationary phase (t'_R) to the time that they spend in that mobile phase (t_M). The retention factor is calculated from.

$$k' = \frac{t_R - t_M}{t_M}$$

Separation factor or selectivity (α) is a measure of the quantity of peak separation. It is calculated from the ratio of retention factors of the two adjacent peaks, where $k_2 \geq k_1$

$$\alpha = \frac{k'_2}{k'_1}$$

Separation number is another term used for measuring of separation efficiency of a column, which is calculated using the equation below. SN can be explained as the numbers of peaks, which can be placed close together between the two peaks of homologous series differing by one carbon. The higher the number, the more efficient the column.

$$SN = \left(\frac{t_{R2} - t_{R1}}{W_{h1} + W_{h2}} \right) - 1$$

t_{R1}, t_{R2} = the retention times of the first and second peaks, respectively.

W_{h1}, W_{h2} = the peak width at half height of the first and second peaks, respectively.

Appendix B

NMR SPECTRA
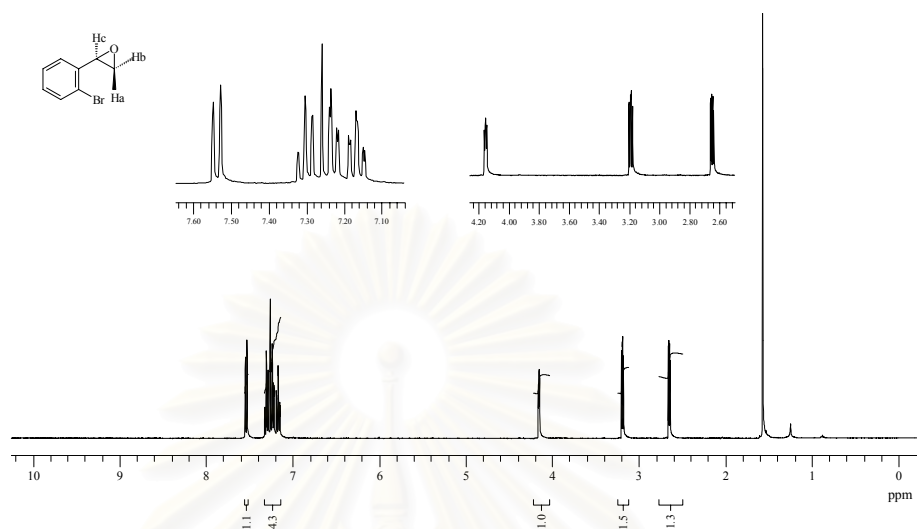
Figure B1   NMR spectrum of **2′-bromostyrene oxide (2Br)**; ^{1}H NMR (CDCl$_3$, 400 MHz): δ 2.65 (1H, dd, Ha of CH$_2$O, J = 2.5 Hz, 5.7 Hz), 3.19 (1H, dd, Hb of CH$_2$O, J = 4.1 Hz, 5.7 Hz), 4.18 (1H, t, Hc of CHAr), 7.10-7.60 (4H, m, ArH).
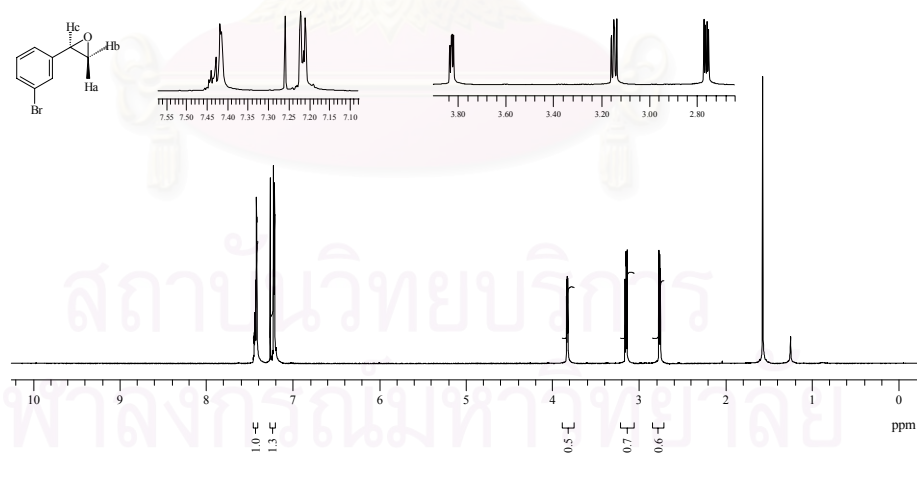
Figure B2   NMR spectrum of **3′-bromostyrene oxide (3Br)**; ^{1}H NMR (CDCl$_3$, 400 MHz): δ 2.78 (1H, dd, Ha of CH$_2$O, J = 2.5 Hz, 5.4 Hz), 3.18 (1H, dd, Hb of CH$_2$O, J = 4.0 Hz, 5.4 Hz), 3.82 (1H, dd, Hc of CHAr, J = 2.5 Hz, 4.0 Hz), 7.17-7.50 (4H, m, ArH).
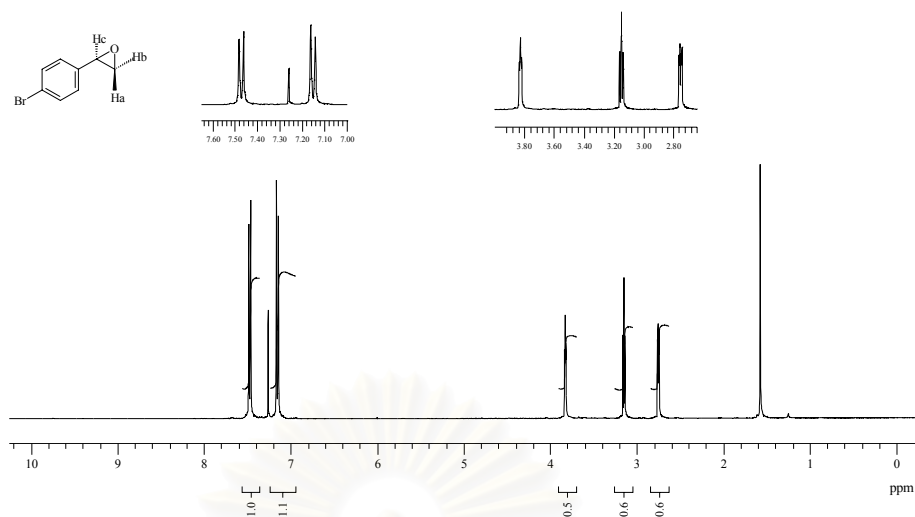
Figure B3　NMR spectrum of **4′-bromostyrene oxide (4Br)**; ^{1}H NMR (CDCl$_3$, 400 MHz): δ 2.78 (1H, dd, Ha of CH$_2$O, J = 2.5 Hz, 5.4 Hz), 3.18 (1H, dd, Hb of CH$_2$O, J = 4.1 Hz, 5.4 Hz), 3.82 (1H, t, Hc of CHAr), 7.10-7.58 (4H, m, ArH).
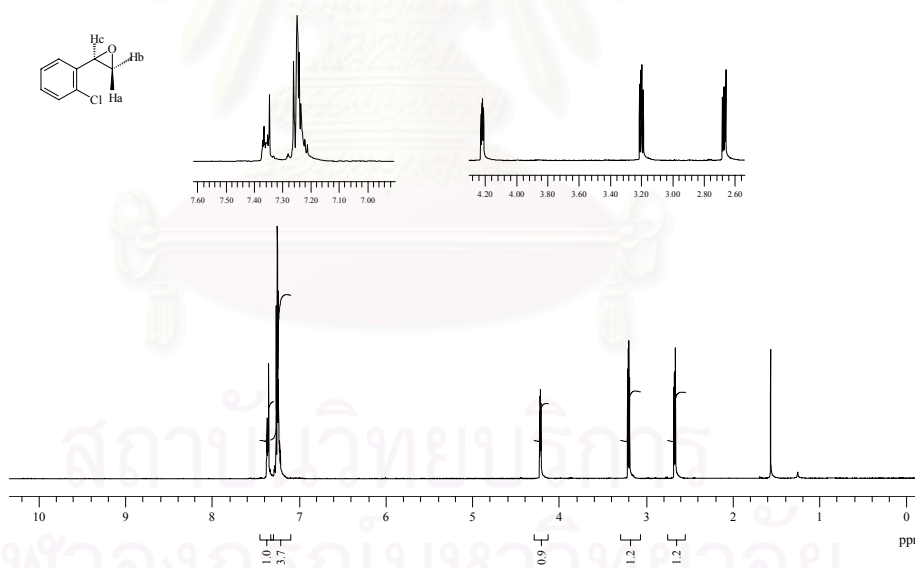
Figure B4　NMR spectrum of **2′-chlorostyrene oxide (2Cl)**; ^{1}H NMR (CDCl$_3$, 400 MHz): δ 2.65 (1H, dd, Ha of CH$_2$O, J = 2.5 Hz, 5.7 Hz), 3.20 (1H, dd, Hb of CH$_2$O, J = 4.1 Hz, 5.7 Hz), 4.20 (1H, dd, Hc of CHAr, J = 2.5 Hz, 4.1 Hz), 7.12-7.40 (4H, m, ArH).
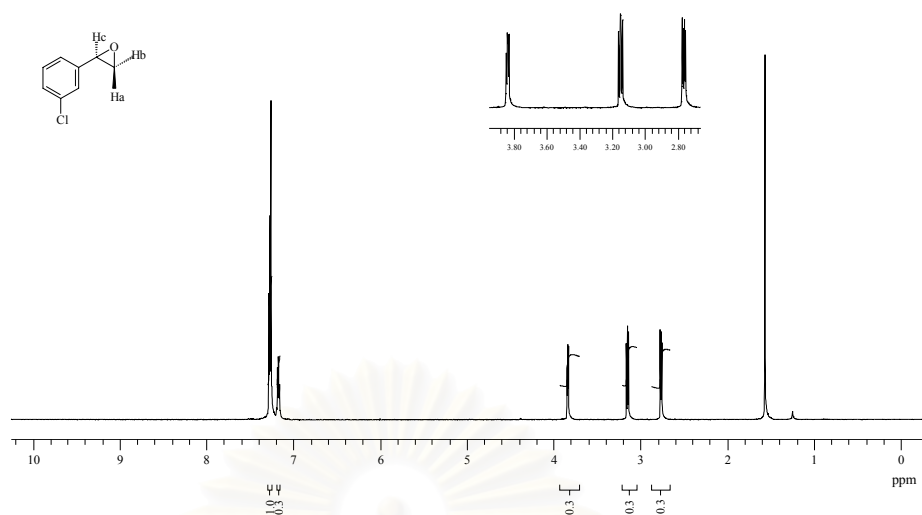
Figure B5   NMR spectrum of **3′-chlorostyrene oxide (3Cl)**; ^{1}H NMR (CDCl$_3$,

400 MHz): δ 2.78 (1H, dd, Ha of C$\underline{H}_2$O, J = 2.4 Hz, 5.4 Hz), 3.18 (1H,

dd, Hb of C$\underline{H}_2$O, J = 4.0 Hz, 5.4 Hz), 3.82 (1H, t, Hc of C$\underline{H}$Ar), 7.10-
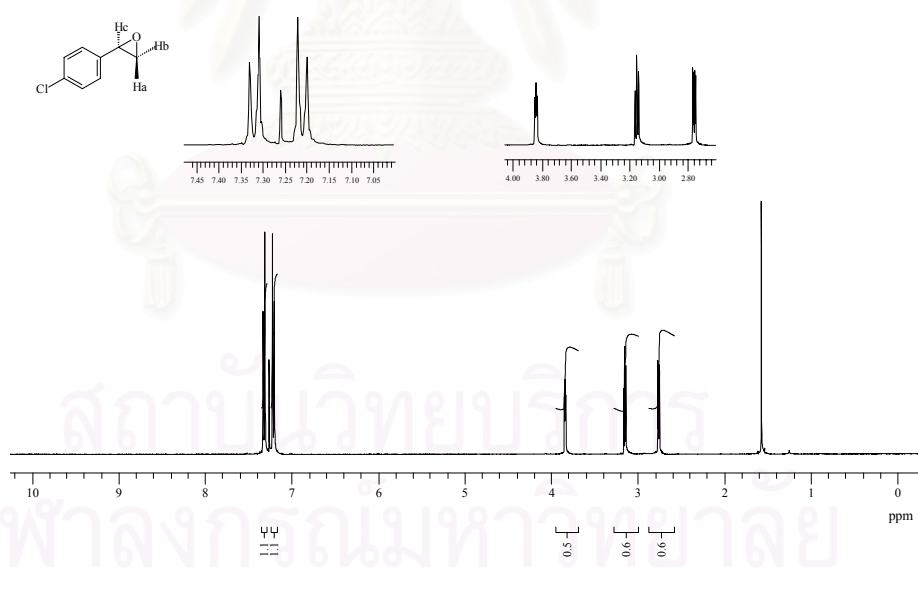
7.38 (4H, m, Ar$\underline{H}$).

Figure B6   NMR spectrum of **4′-chlorostyrene oxide (4Cl)**; ^{1}H NMR (CDCl$_3$,

400 MHz): δ 2.78 (1H, dd, Ha of C$\underline{H}_2$O, J = 2.5 Hz, 5.4 Hz), 3.18 (1H,

dd, Hb of C$\underline{H}_2$O, J = 4.0 Hz, 5.4 Hz), 3.82 (1H, t, Hc of C$\underline{H}$Ar), 7.10-

7.38 (4H, m, Ar$\underline{H}$)
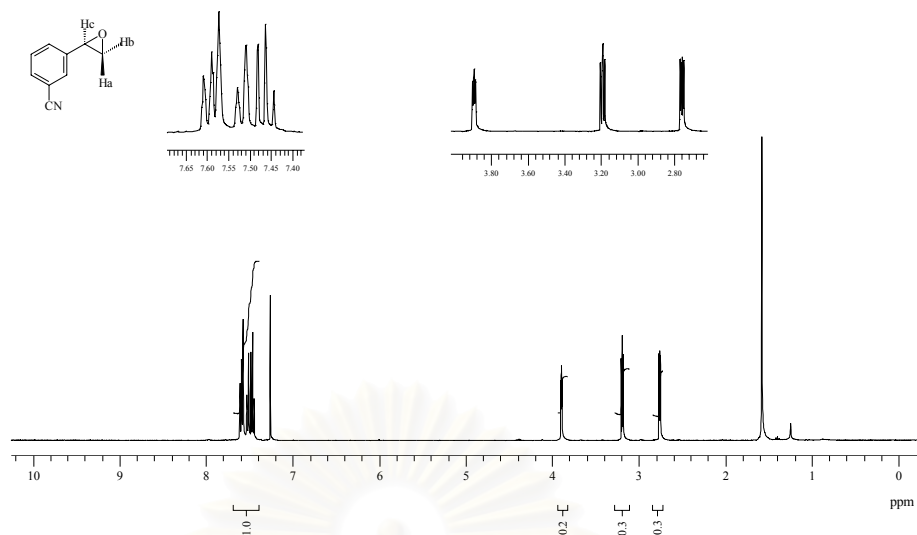
Figure B7   NMR spectrum of **3′-cyanostyrene oxide (3CN)**; ¹H NMR (CDCl₃,
              400 MHz): δ 2.78 (1H, dd, Ha of C$\underline{H}_2$O, J = 2.4 Hz, 5.3 Hz), 3.20 (1H,
              dd, Hb of C$\underline{H}_2$O, J = 4.0 Hz, 5.3 Hz), 3.85 (1H, dd, Hc of C$\underline{H}$Ar,
              J = 2.4 Hz, 4.0 Hz), 7.20-7.42 (4H, m, Ar$\underline{H}$).
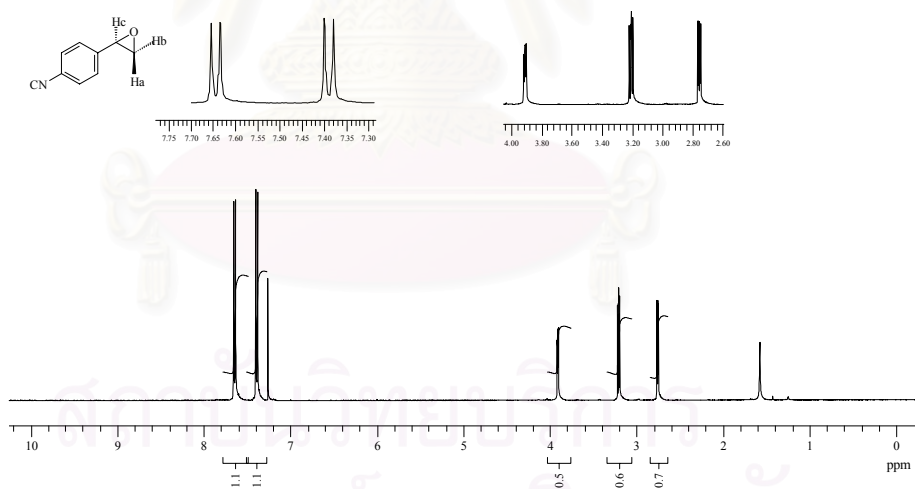
Figure B8   NMR spectrum of **4′-cyanostyrene oxide (4CN)**; ¹H NMR (CDCl₃,
              400 MHz): δ 2.78 (1H, dd, Ha of C$\underline{H}_2$O, J = 2.4 Hz, 5.5 Hz), 3.18 (1H,
              dd, Hb of C$\underline{H}_2$O, J = 4.0 Hz, 5.5 Hz), 3.82 (1H, dd, Hc of C$\underline{H}$Ar,
              J = 2.5 Hz, 4.0 Hz), 7.30-7.50 (4H, m, Ar$\underline{H}$).
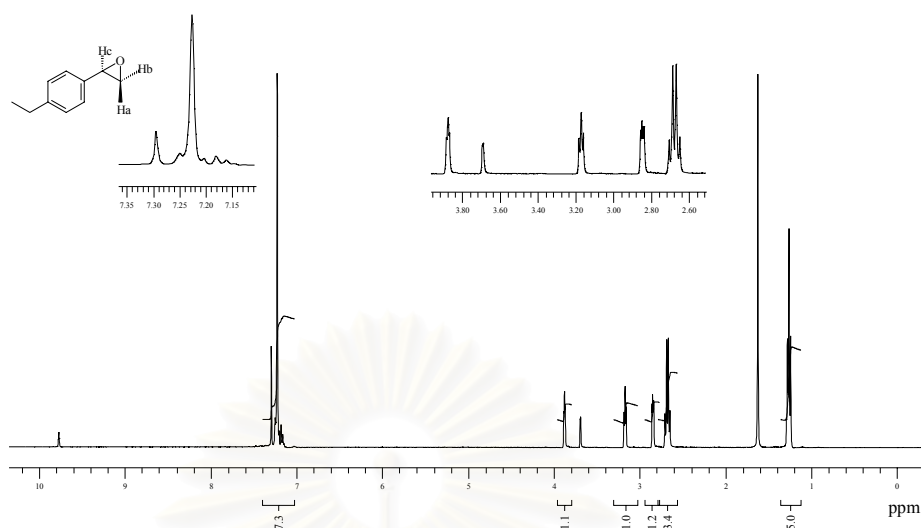
Figure B9   NMR spectrum of **4′-ethylstyrene oxide (4Et)**; ^{1}H NMR (CDCl$_3$, 400
MHz): δ 1.28 (3H, t, CH$_2$C$\underline{H}_3$), 2.70 (2H, q, C$\underline{H}_2$CH$_3$), 2.85 (1H, dd,
Ha of C$\underline{H}_2$O, J = 2.5 Hz, 5.3 Hz), 3.20 (1H, t, Hb of C$\underline{H}_2$O), 3.85 (1H,
t, Hc of C$\underline{H}$Ar), 7.15-7.45 (4H, m, Ar$\underline{H}$).
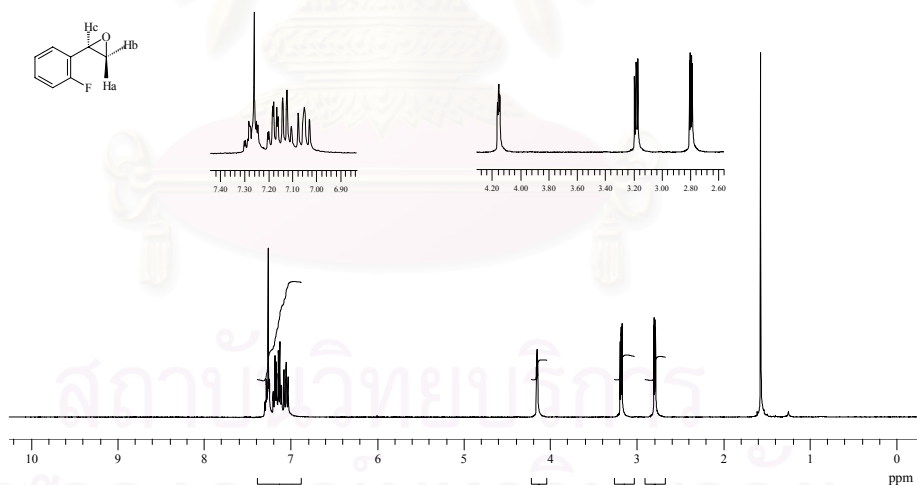
Figure B10   NMR spectrum of **2′-fluorostyrene oxide (2F)**; ^{1}H NMR (CDCl$_3$, 400
MHz): δ 2.80 (1H, dd, Ha of C$\underline{H}_2$O, J = 2.5 Hz, 5.5 Hz), 3.20 (1H, dd,
Hb of C$\underline{H}_2$O, J = 4.0 Hz, 5.5 Hz), 4.18 (1H, t, Hc of C$\underline{H}$Ar), 6.95-7.40
(4H, m, Ar$\underline{H}$).
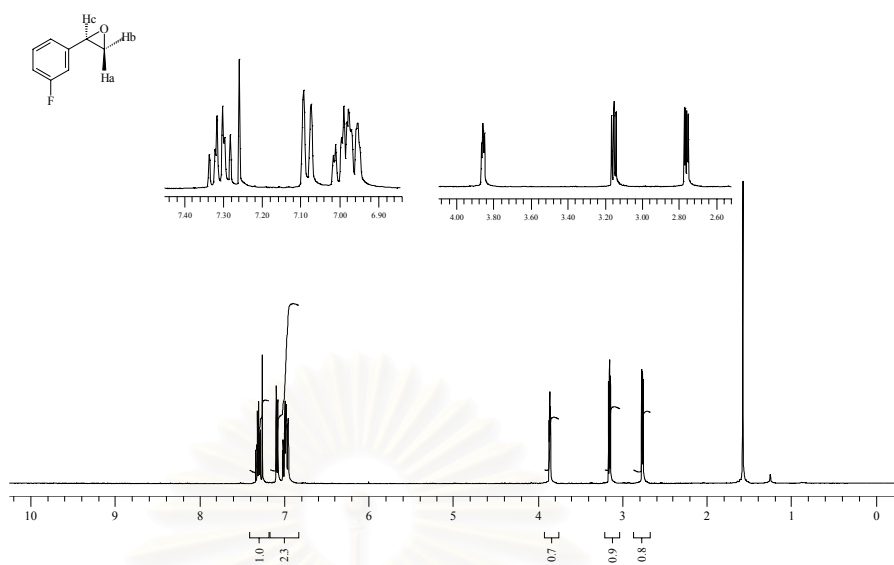
Figure B11   NMR spectrum of **3′-fluorostyrene oxide (3F)**; ¹H NMR (CDCl₃, 400
MHz): δ 2.78 (1H, dd, Ha of CH₂O, *J* = 2.5 Hz, 5.4 Hz), 3.18 (1H, dd,
Hb of CH₂O, *J* = 4.0 Hz, 5.4 Hz), 3.82 (1H, t, Hc of CHAr), 6.90-7.40
(4H, m, ArH).
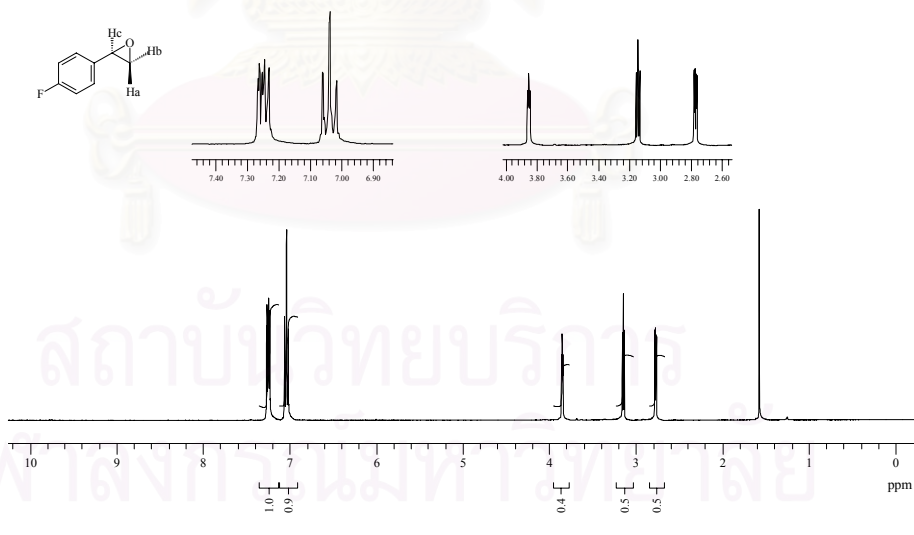
Figure B12   NMR spectrum of **4′-fluorostyrene oxide (4F)**; ¹H NMR (CDCl₃, 400
MHz): δ 2.78 (1H, dd, Ha of CH₂O, *J* = 2.5 Hz, 5.3 Hz), 3.18 (1H, dd,
Hb of CH₂O, *J* = 4.0 Hz, 5.3 Hz), 3.82 (1H, t, Hc of CHAr), 6.90-7.30
(4H, m, ArH).
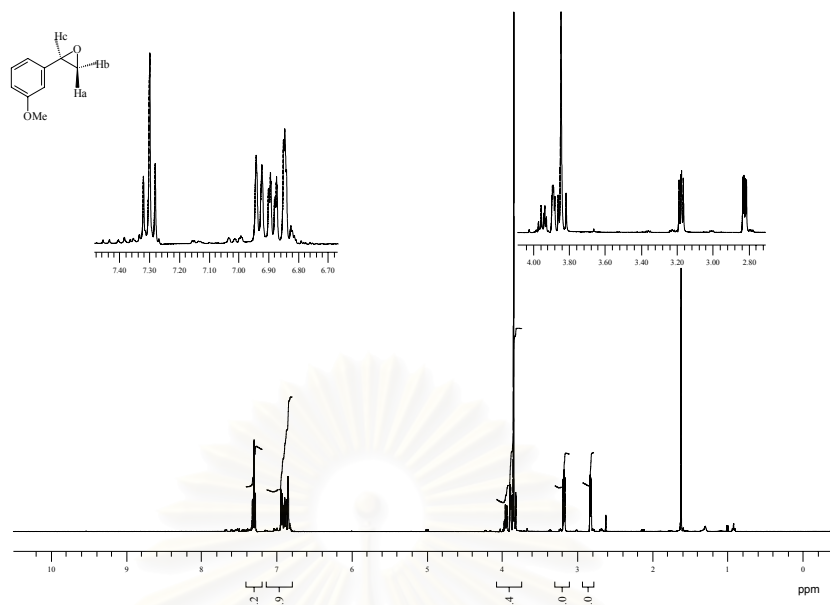
Figure B13   NMR spectrum of **3′-methoxystyrene oxide (3OMe)**; ^{1}H NMR
(CDCl$_3$, 400 MHz): δ 2.80 (1H, dd, Ha of C$\underline{H}_2$O, J = 2.6 Hz, 5.7 Hz),
3.20 (1H, dd, Hb of C$\underline{H}_2$O, J = 4.1 Hz, 5.5 Hz), 3.85 (3H, s, OC$\underline{H}_3$Ar),
3.90 (1H, t, Hc of C$\underline{H}$Ar), 6.80-7.38 (4H, m, Ar$\underline{H}$).
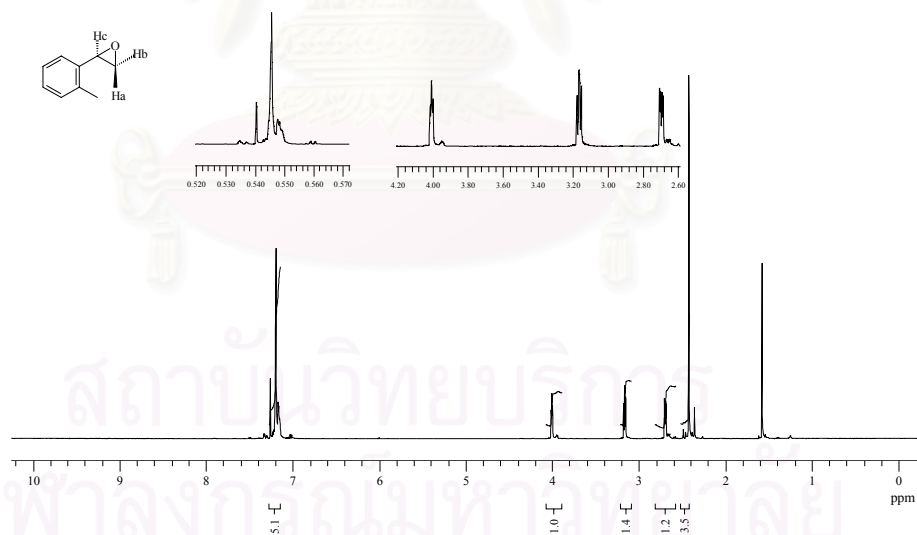
Figure B14   NMR spectrum of **2′-methylstyrene oxide (2Me)**; ^{1}H NMR (CDCl$_3$,
400 MHz): δ 2.40 (3H, s, ArC$\underline{H}_3$), 2.70 (1H, dd, Ha of C$\underline{H}_2$O, J = 2.6
Hz, 5.7 Hz), 3.18 (1H, dd, Hb of C$\underline{H}_2$O, J = 4.1 Hz, 5.6 Hz), 4.02 (1H,
t, Hc of C$\underline{H}$Ar), 7.10-7.30 (4H, m, Ar$\underline{H}$).
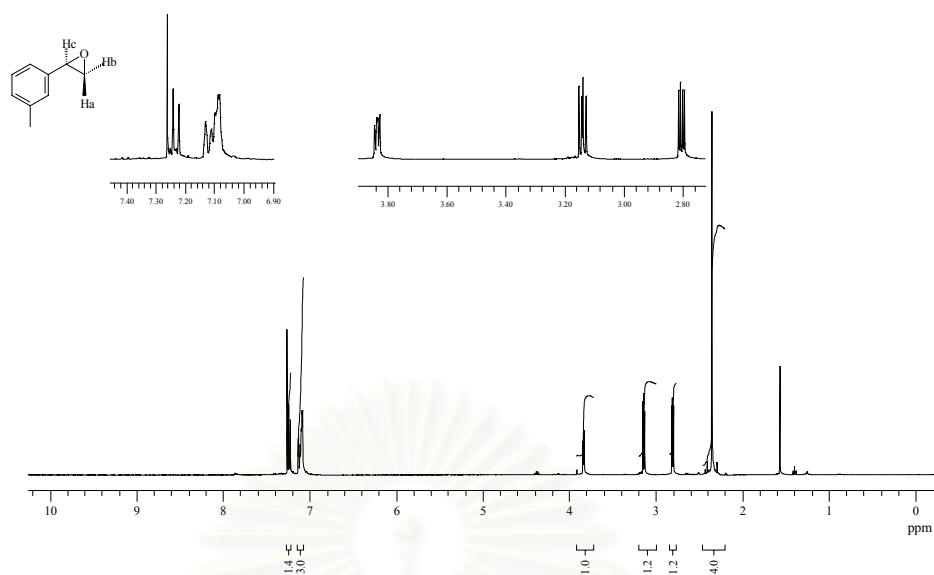
Figure B15   NMR spectrum of **3′-methylstyrene oxide (3Me)**; ^{1}H NMR (CDCl$_3$,
400 MHz): δ 2.38 (3H, s, ArC$\underline{H}_3$), 2.80 (1H, dd, Ha of C$\underline{H}_2$O, J =
2.5 Hz, 5.4 Hz), 3.15 (1H, dd, Hb of C$\underline{H}_2$O, J = 4.0 Hz, 5.4 Hz), 3.82
(1H, dd, Hc of C$\underline{H}$Ar, J = 2.6 Hz, 4.0 Hz), 7.00-7.30 (4H, m, Ar$\underline{H}$)
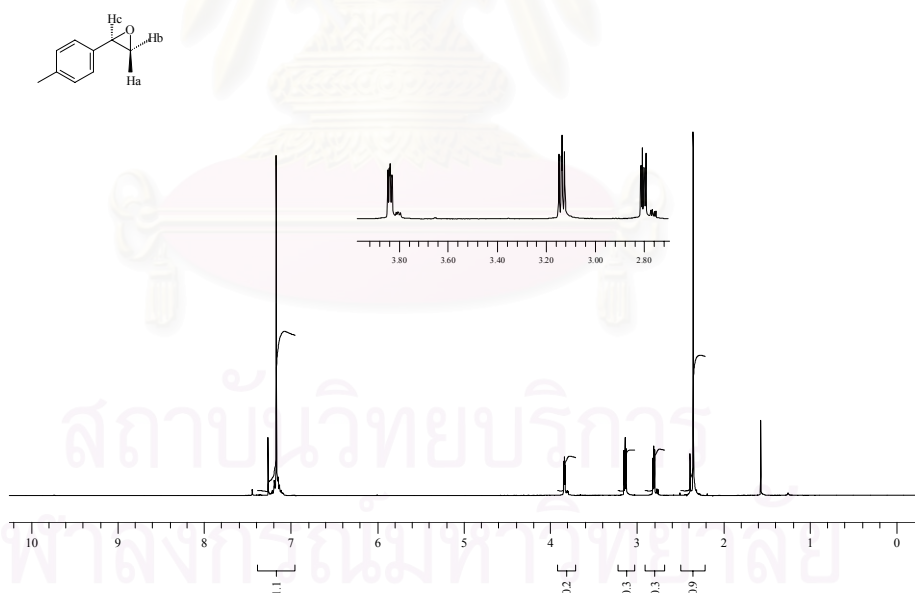
Figure B16   NMR spectrum of **4′-methylstyrene oxide (4Me)**; ^{1}H NMR (CDCl$_3$,
400 MHz): δ 2.30 (3H, s, ArC$\underline{H}_3$), 2.80 (1H, dd, Ha of C$\underline{H}_2$O, J = 2.6
Hz, 5.4 Hz), 3.15 (1H, dd, Hb of C$\underline{H}_2$O, J = 4.0 Hz, 5.4 Hz), 3.82 (1H,
dd, Hc of C$\underline{H}$Ar, J = 2.6 Hz, 4.0 Hz), 7.00-7.25 (4H, m, Ar$\underline{H}$).
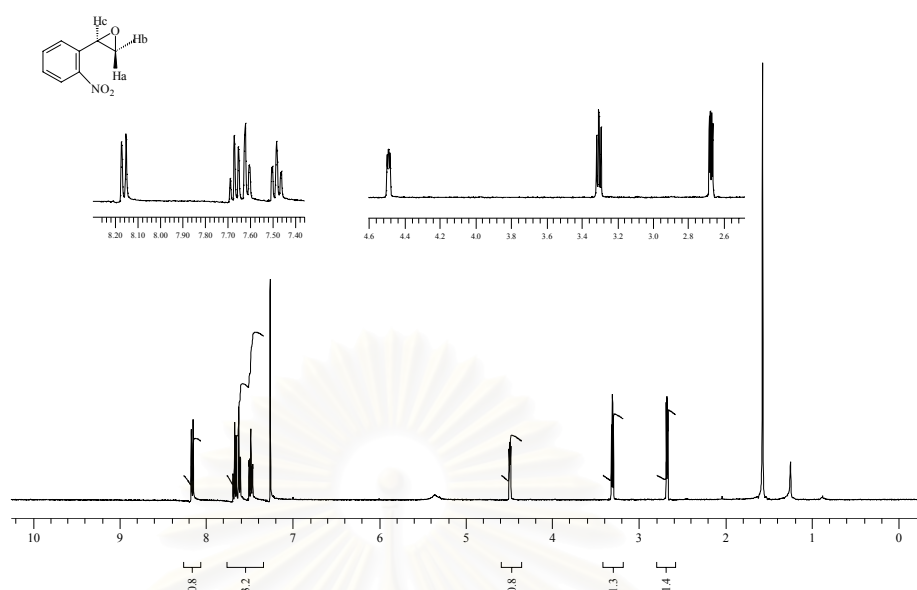
Figure B17   NMR spectrum of **2′-nitrostyrene oxide (2NO)**; ^{1}H NMR (CDCl$_3$,
400 MHz): δ 2.68 (1H, dd, Ha of C$\underline{H}_2$O, J = 2.6 Hz, 5.5 Hz), 3.30 (1H,
dd, Hb of C$\underline{H}_2$O, J = 4.4 Hz, 5.3 Hz), 4.50 (1H, dd, Hc of C$\underline{H}$Ar,
J = 2.8 Hz, 4.3 Hz), 7.40-8.20 (4H, m, Ar$\underline{H}$).
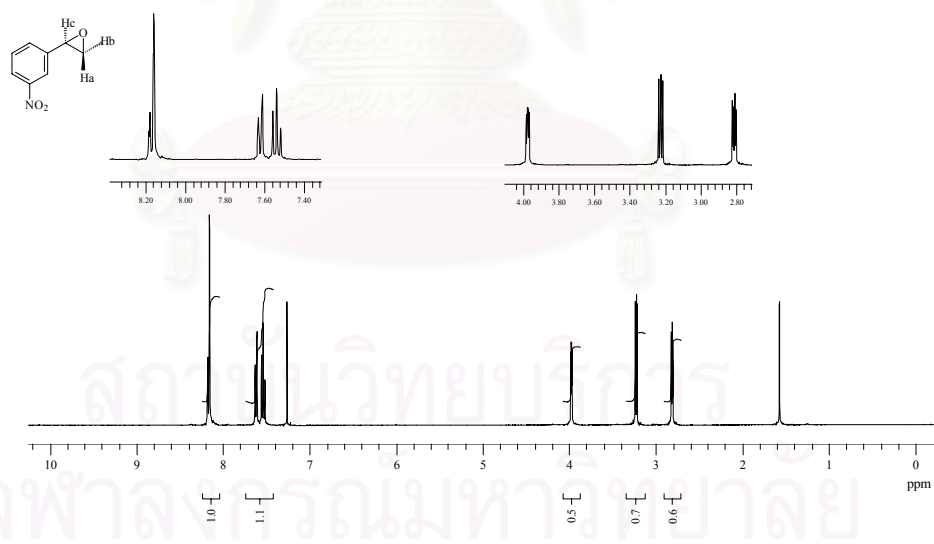
Figure B18   NMR spectrum of **3′-nitrostyrene oxide (3NO)**; ^{1}H NMR (CDCl$_3$,
400 MHz): δ 2.82 (1H, dd, Ha of C$\underline{H}_2$O, J = 2.4 Hz, 5.3 Hz), 3.22 (1H,
dd, Hb of C$\underline{H}_2$O, J = 4.0 Hz, 5.3 Hz), 3.98 (1H, dd, Hc of C$\underline{H}$Ar,
J = 2.5 Hz, 4.0 Hz), 7.50-8.20 (4H, m, Ar$\underline{H}$).
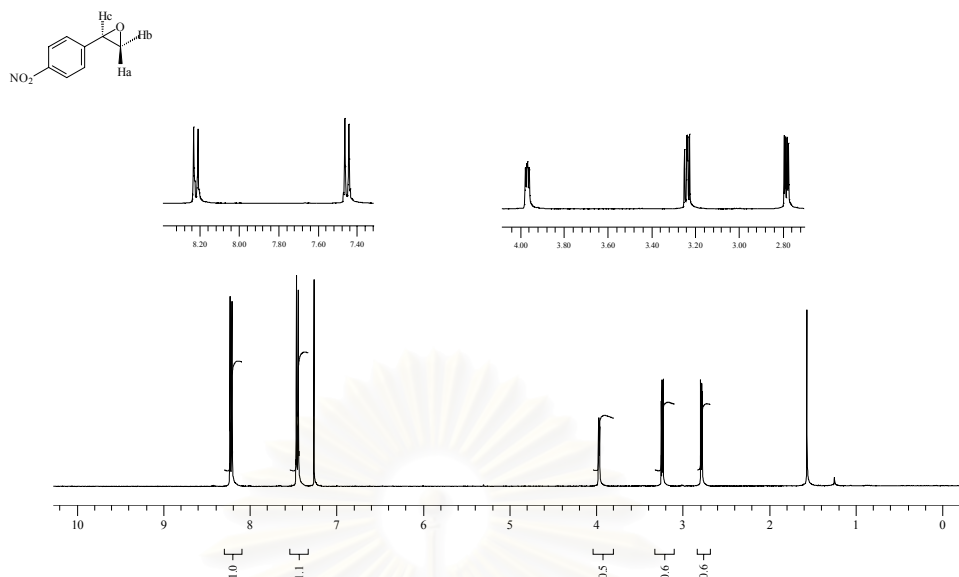
Figure B19   NMR spectrum of **4′-nitrostyrene oxide (4NO)**; ^{1}H NMR (CDCl$_3$,

400 MHz): δ 2.80 (1H, dd, Ha of C$\underline{H}_2$O, J = 2.4 Hz, 5.5 Hz), 3.22 (1H,

dd, Hb of C$\underline{H}_2$O, J = 4.1 Hz, 5.4 Hz), 3.98 (1H, dd, Hc of $\underline{C}$HAr,

J = 2.5 Hz, 4.0 Hz), 7.40-8.25 (4H, m, Ar$\underline{H}$).
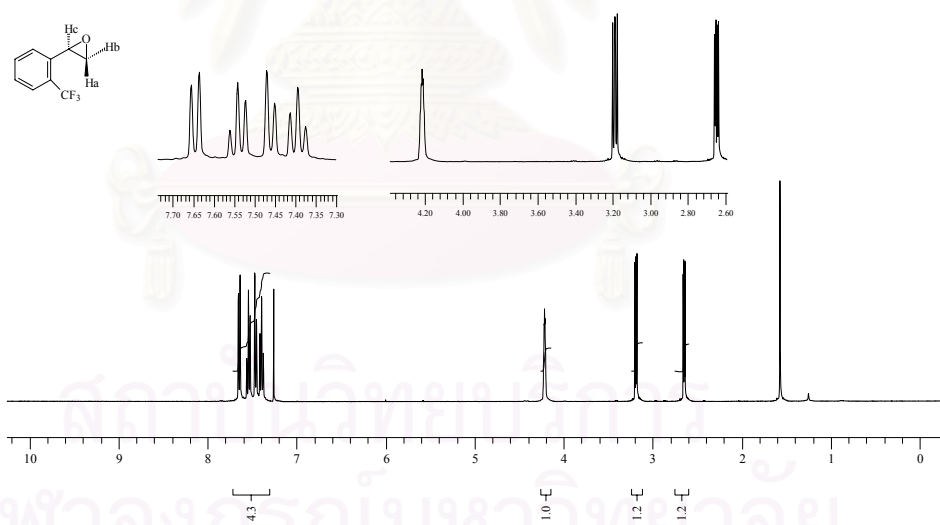
Figure B20   NMR spectrum of **2′-trifluoromethylstyrene oxide (2CF)**; ^{1}H NMR

(CDCl$_3$, 400 MHz): δ 2.65 (1H, dd, Ha of C$\underline{H}_2$O, J = 2.5 Hz, 5.7 Hz),

3.20 (1H, dd, Hb of C$\underline{H}_2$O, J = 4.2 Hz, 5.7 Hz), 4.22 (1H, t, Hc of

C$\underline{H}$Ar), 7.30-7.70 (4H, m, Ar$\underline{H}$).
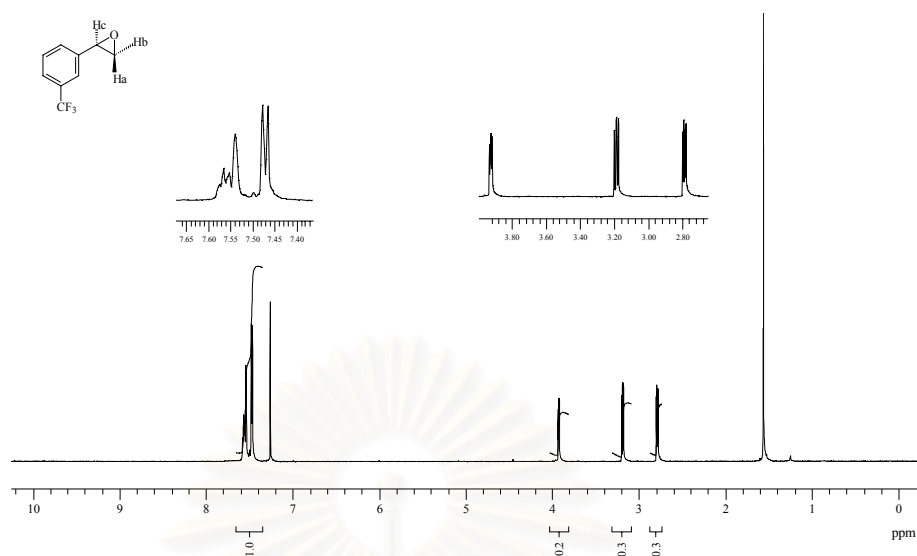
Figure B21   NMR spectrum of **3′-trifluoromethylstyrene oxide (3CF)**; ^{1}H NMR
(CDCl₃, 400 MHz): δ 2.80 (1H, dd, Ha of CH₂O, J = 2.5 Hz, 5.4 Hz),
3.2 (1H, dd, Hb of CH₂O, J = 4.0 Hz, 5.4 Hz), 3.98 (1H, dd, Hc of
CHAr, J = 2.5 Hz, 3.2 Hz), 7.40-7.65 (4H, m, ArH).
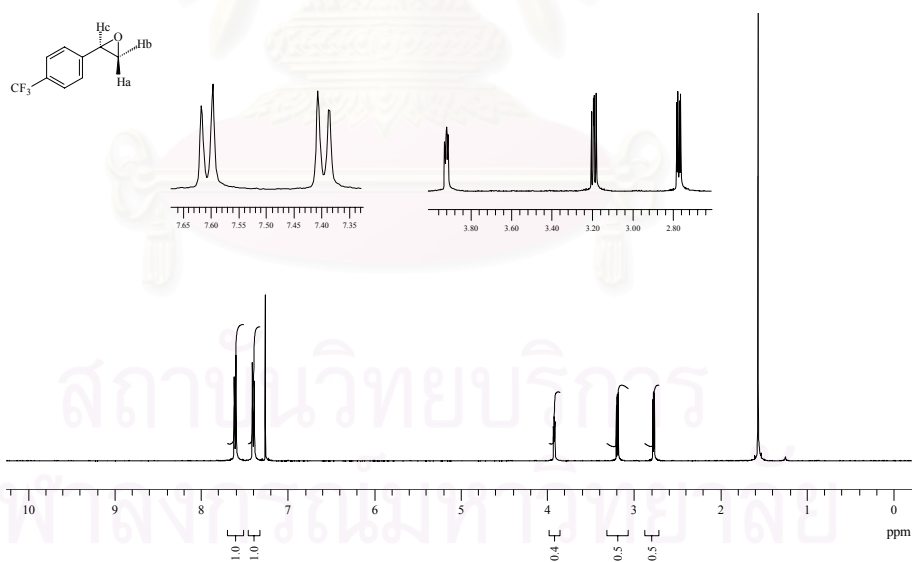
Figure B22   NMR spectrum of **4′-trifluoromethylstyrene oxide (4CF)**; ^{1}H NMR
(CDCl₃, 400 MHz): δ 2.78 (1H, dd, Ha of CH₂O, J = 2.5 Hz, 5.5 Hz),
3.20(1H, dd, Hb of CH₂O, J = 4.0 Hz, 5.4 Hz), 3.92 (1H, dd, Hc of
CHAr, J = 2.6 Hz, 3.9 Hz), 7.30-7.70 (4H, m, ArH).
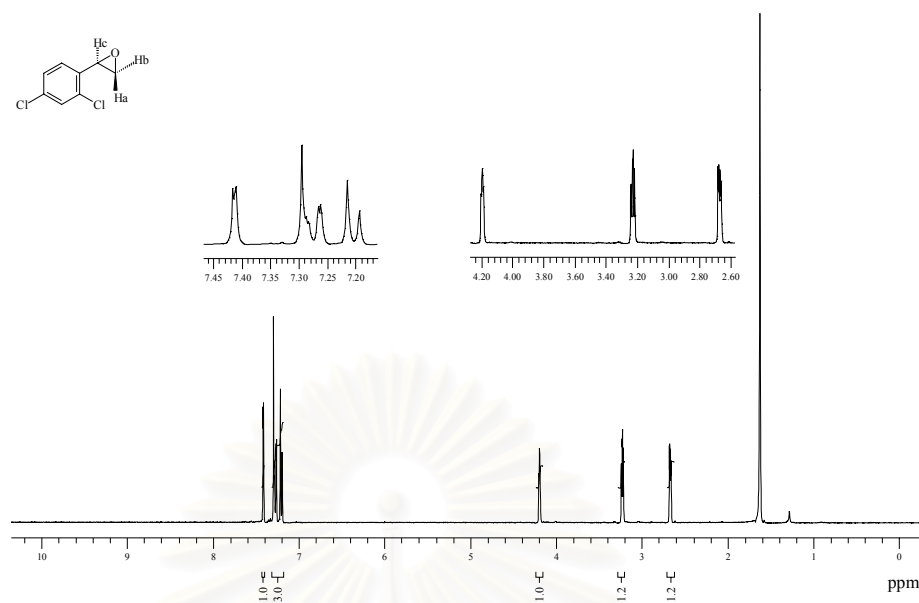
Figure B23   NMR spectrum of **2′, 4′-dichlorostyrene oxide (24Cl)**; ^{1}H NMR
(CDCl$_3$, 400 MHz): δ 2.65 (1H, dd, Ha of C$\underline{H}_2$O, J = 2.5 Hz, 5.6 Hz),
3.25 (1H, dd, Hb of C$\underline{H}_2$O, J = 4.1 Hz, 5.6 Hz), 4.20 (1H, t, Hc of
C$\underline{H}$Ar), 7.18-7.45 (3H, m, Ar$\underline{H}$).
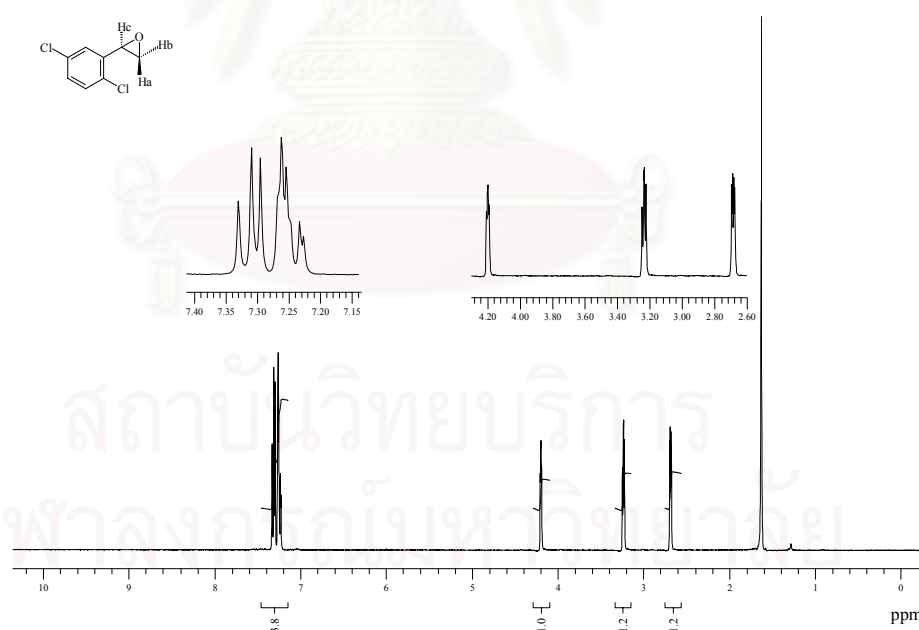
Figure B24   NMR spectrum of **2′, 5′-dichlorostyrene oxide (25Cl)**; ^{1}H NMR
(CDCl$_3$, 400 MHz): δ 2.65 (1H, dd, Ha of C$\underline{H}_2$O, J = 2.4 Hz, 5.6 Hz),
3.25 (1H, dd, Hb of C$\underline{H}_2$O, J = 4.1 Hz, 5.1 Hz), 4.20 (1H, dd, Hc of
C$\underline{H}$Ar, J = 2.6 Hz, 3.9 Hz), 7.20-7.40 (3H, m, Ar$\underline{H}$).
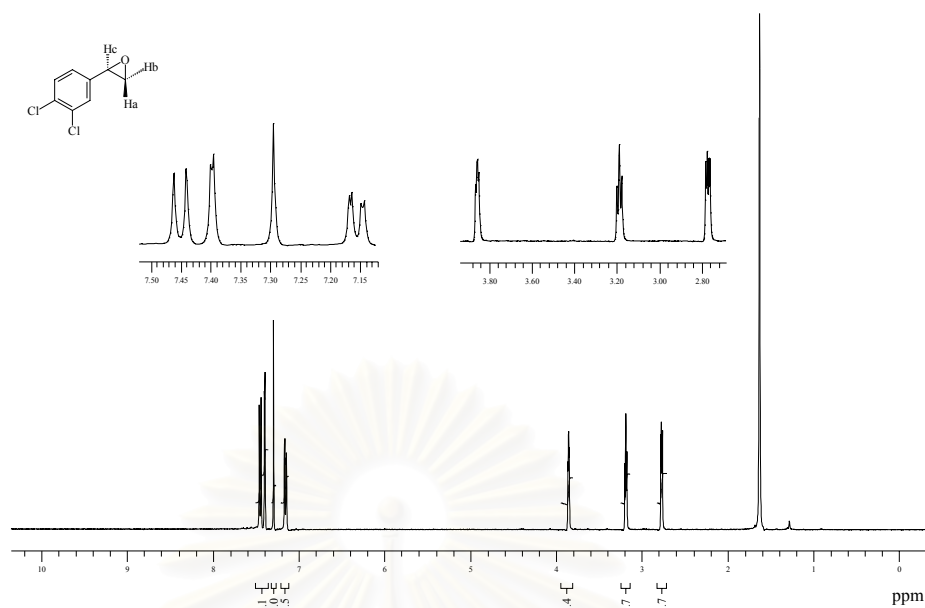
Figure B25   NMR spectrum of **3′, 4′-dichlorostyrene oxide (34Cl)**; ^{1}H NMR
(CDCl$_3$, 400 MHz): δ 2.80 (1H, dd, Ha of C$\underline{H}_2$O, J = 2.4 Hz, 5.4 Hz),
3.20 (1H, dd, Hb of C$\underline{H}_2$O, J = 4.0 Hz, 5.3 Hz), 3.85 (1H, dd, Hc of
C$\underline{H}$Ar, J = 2.5 Hz, 3.7 Hz), 7.15-7.45 (3H, m, Ar$\underline{H}$).
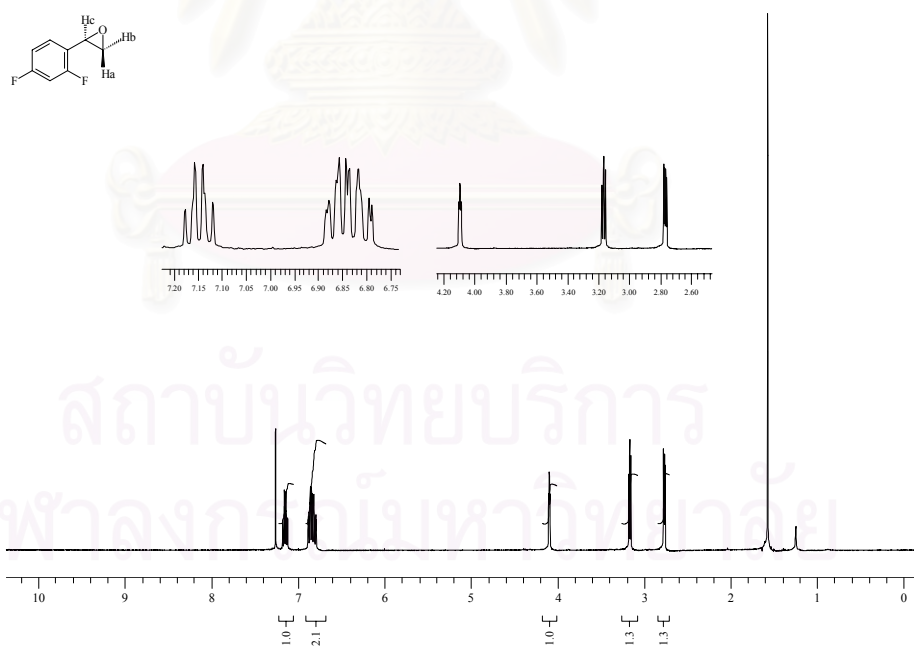
Figure B26   NMR spectrum of **2′, 4′-difluorostyrene oxide (24F)**; ^{1}H NMR
(CDCl$_3$, 400 MHz): δ 2.78 (1H, dd, Ha of C$\underline{H}_2$O, J = 2.5 Hz, 5.4 Hz),
3.18 (1H, dd, Hb of C$\underline{H}_2$O, J = 4.0 Hz, 5.4 Hz), 4.11 (1H, t, Hc of
C$\underline{H}$Ar), 6.70-7.20 (3H, m, Ar$\underline{H}$).
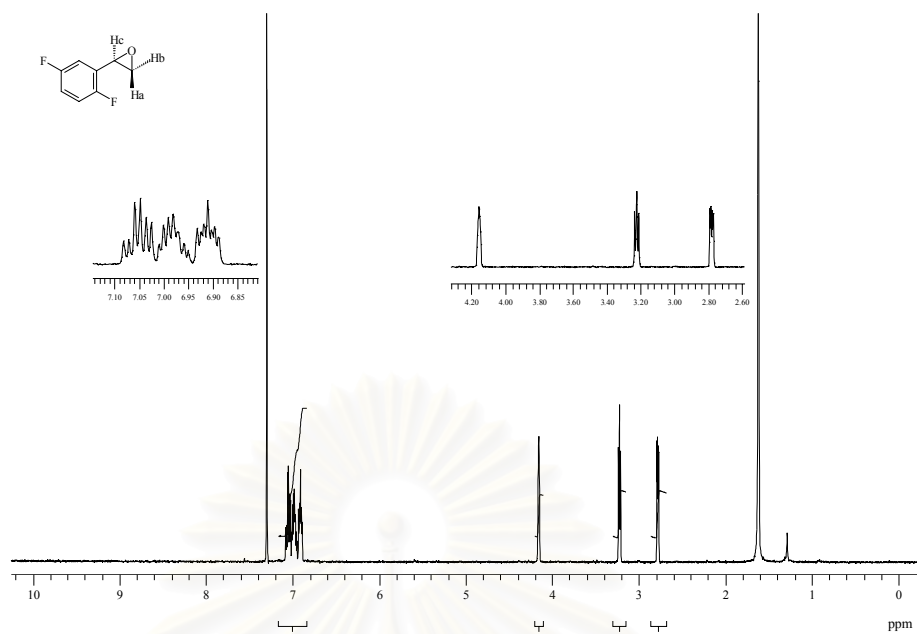
Figure B27   NMR spectrum of **2′, 5′-difluorostyrene oxide (25F)**; ^{1}H NMR
(CDCl$_3$, 400 MHz): δ 2.80 (1H, dd, Ha of C$\underline{H}_2$O, J = 2.4 Hz, 5.5 Hz),
3.22 (1H, dd, Hb of C$\underline{H}_2$O, J = 4.2 Hz, 5.4 Hz), 4.18 (1H, t, Hc of
C$\underline{H}$Ar), 6.90-7.10 (3H, m, Ar$\underline{H}$)
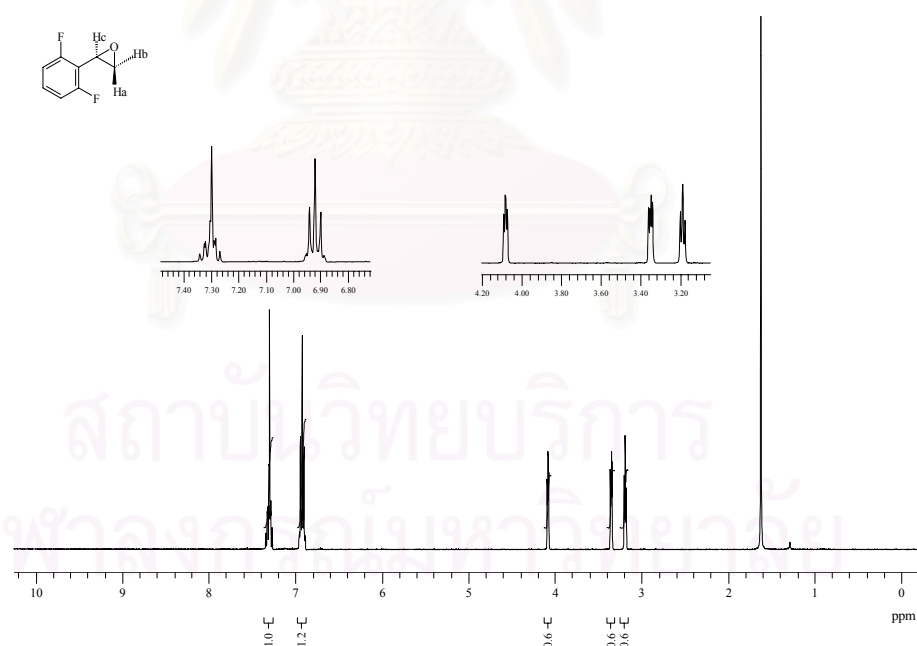
Figure B28   NMR spectrum of **2′, 6′-difluorostyrene oxide (26F)**; ^{1}H NMR
(CDCl$_3$, 400 MHz): δ 3.20 (1H, t, Hb of C$\underline{H}_2$O), 3.38 (1H, dd, Ha of
C$\underline{H}_2$O, J = 2.7 Hz, 5.3 Hz), 4.18 (1H, dd, Hc of C$\underline{H}$Ar, J = 2.9 Hz, 3.9
Hz), 6.88-7.40 (3H, m, Ar$\underline{H}$).
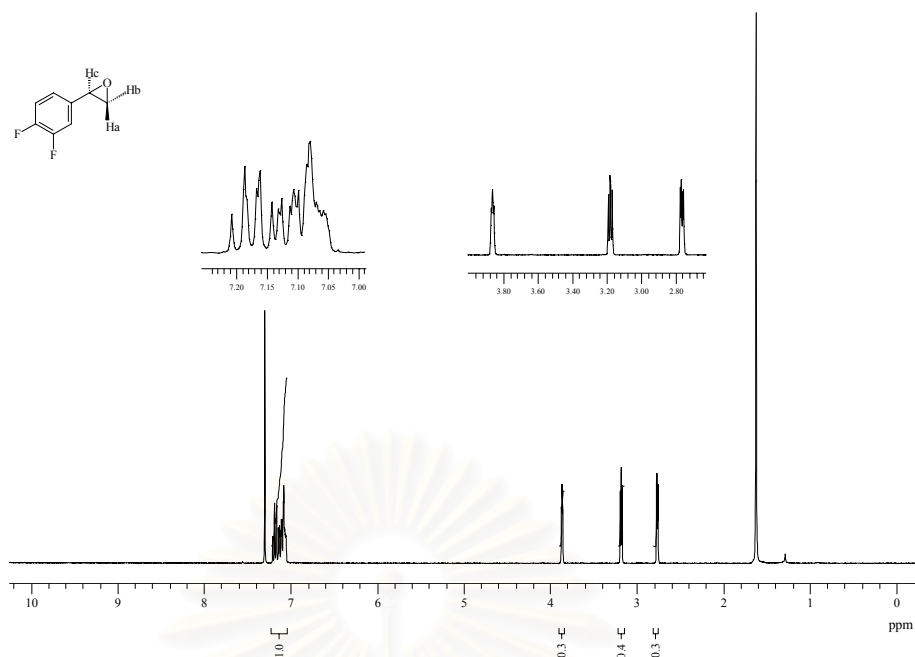
Figure B29   NMR spectrum of **3′, 4′-difluorostyrene oxide (34F)**; ^{1}H NMR
(CDCl₃, 400 MHz): δ 2.78 (1H, dd, Ha of CH₂O, J = 2.4 Hz, 5.3 Hz),
3.20 (1H, dd, Hb of CH₂O, J = 4.0 Hz, 5.3 Hz), 3.86 (1H, t, Hc of
CHAr), 7.02-7.22 (3H, m, ArH)
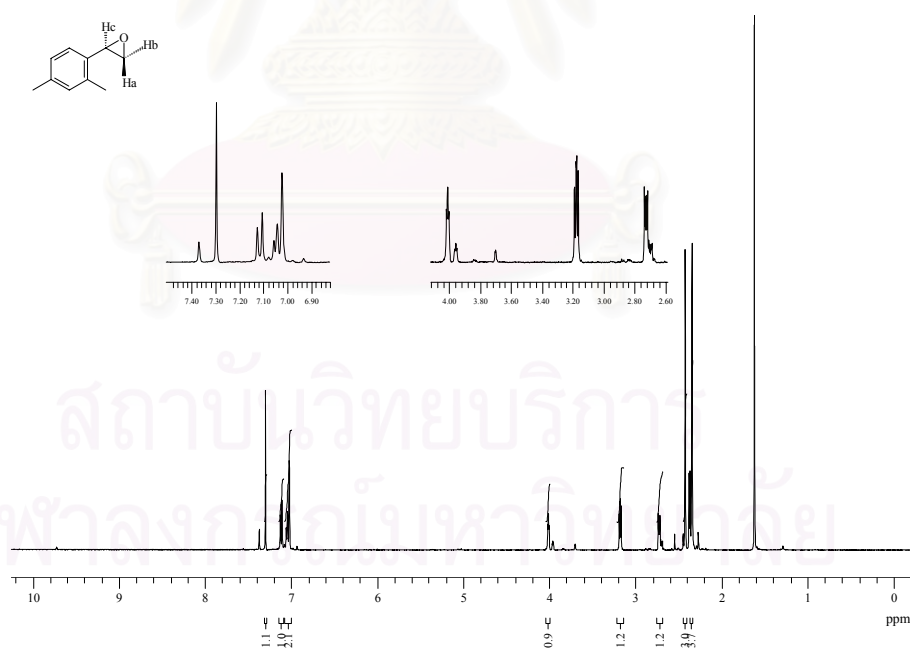
Figure B30   NMR spectrum of **2′, 4′-dimethylstyrene oxide (24Me)**; ^{1}H NMR
(CDCl₃, 400 MHz): δ 2.72 (1H, dd, Ha of CH₂O, J = 2.6 Hz, 5.6 Hz),
3.20 (1H, dd, Hb of CH₂O, J = 4.1 Hz, 5.6 Hz), 4.20 (1H, t, Hc of
CHAr), 7.00-7.20 (3H, m, ArH).
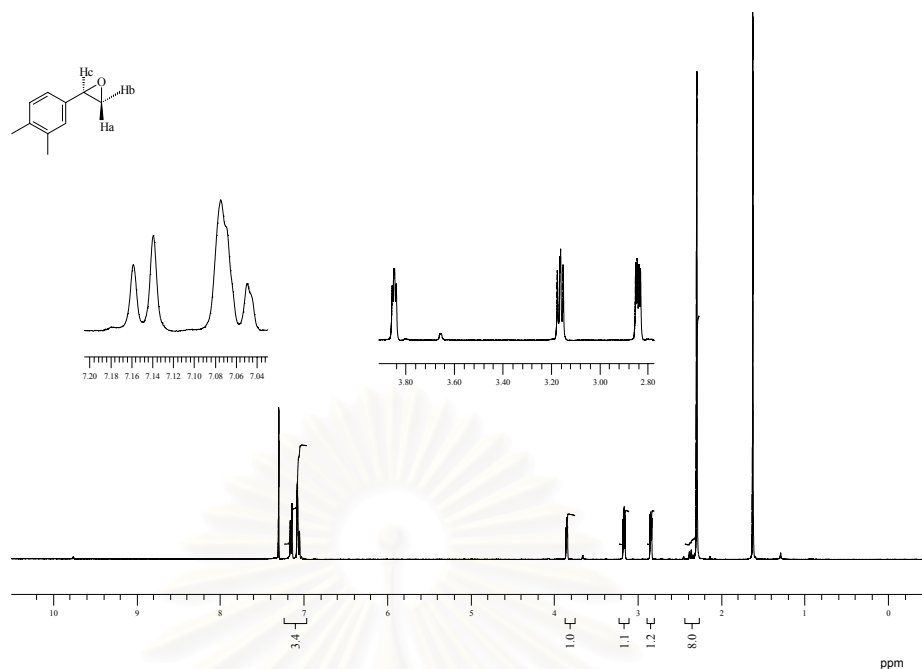
Figure B31   NMR spectrum of **3′, 4′-dimethylstyrene oxide (34Me)**; ^{1}H NMR
(CDCl$_3$, 400 MHz): δ 2.30 (3H x 2 , s, C$\underline{H}_3$Ar), 2.82 (1H, dd, Ha of
C$\underline{H}_2$O, J = 2.4 Hz, 5.4 Hz), 3.18 (1H, dd, Hb of C$\underline{H}_2$O, J = 4.0 Hz, 5.4
Hz), 3.84 (1H, dd, Hc of C$\underline{H}$Ar, J= 2.8 Hz, 3.7 Hz), 7.02-7.22 (3H, m,
Ar$\underline{H}$)
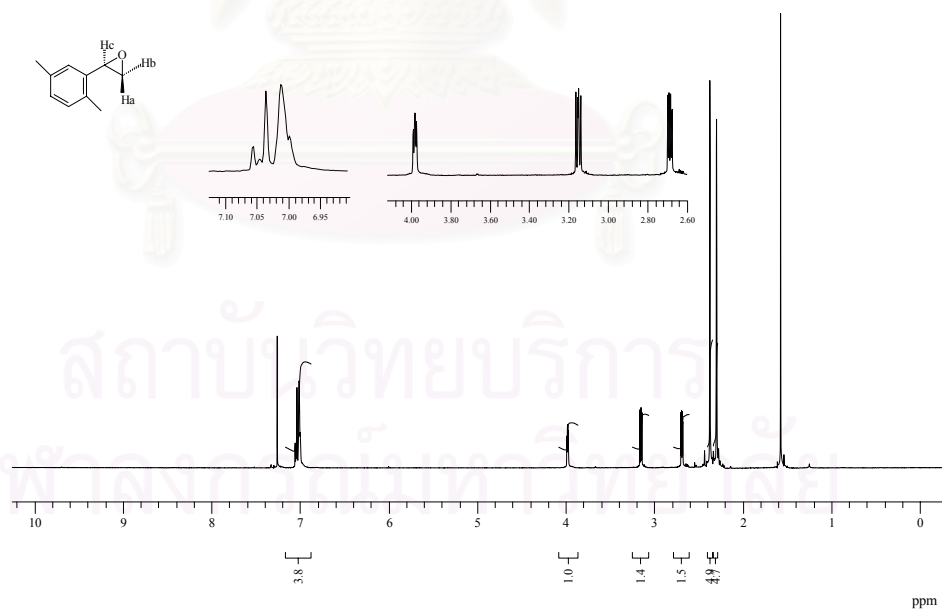
Figure B32   NMR spectrum of **2′, 5′-dimethylstyrene oxide (25Me)**; ^{1}H NMR
(CDCl$_3$, 400 MHz): δ 2.30 (3H, s, C$\underline{H}_3$Ar), 2.38 (3H, s, C$\underline{H}_3$Ar), 2.72
(1H, dd, Ha of C$\underline{H}_2$O, J = 2.6 Hz, 5.7 Hz), 3.18 (1H, dd, Hb of C$\underline{H}_2$O,
J = 4.1 Hz, 5.7 Hz), 3.98 (1H, t, Hc of C$\underline{H}$Ar), 7.02-7.22 (3H, m, Ar$\underline{H}$).
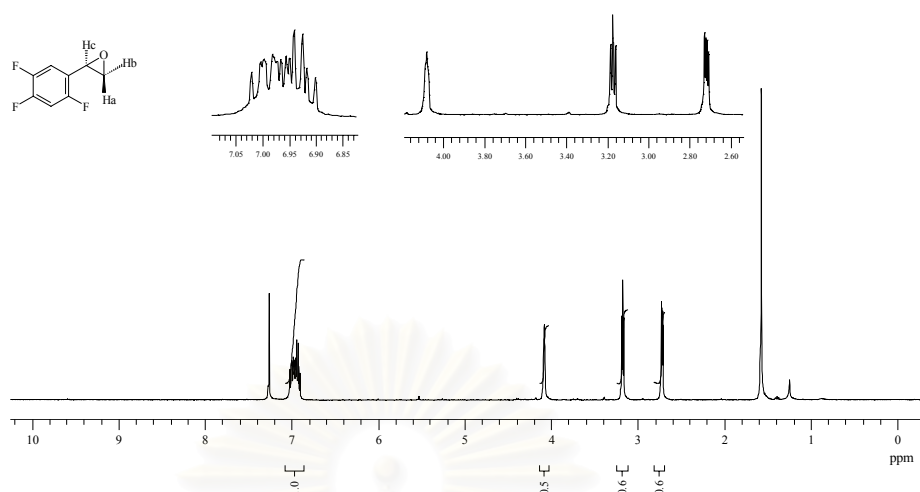
Figure B33   NMR spectrum of **trifluorostyrene oxide (TriF)**; ^{1}H NMR (CDCl$_3$,
400 MHz): δ 2.72(1H, dd, Ha of CH$_2$O, J = 2.5 Hz, 5.4 Hz), 3.20 (1H,
dd, Hb of CH$_2$O, J = 4.0 Hz, 5.4 Hz), 4.10 (1H, t, Hc of CHAr), 6.90-
7.10 (2H, m, ArH).
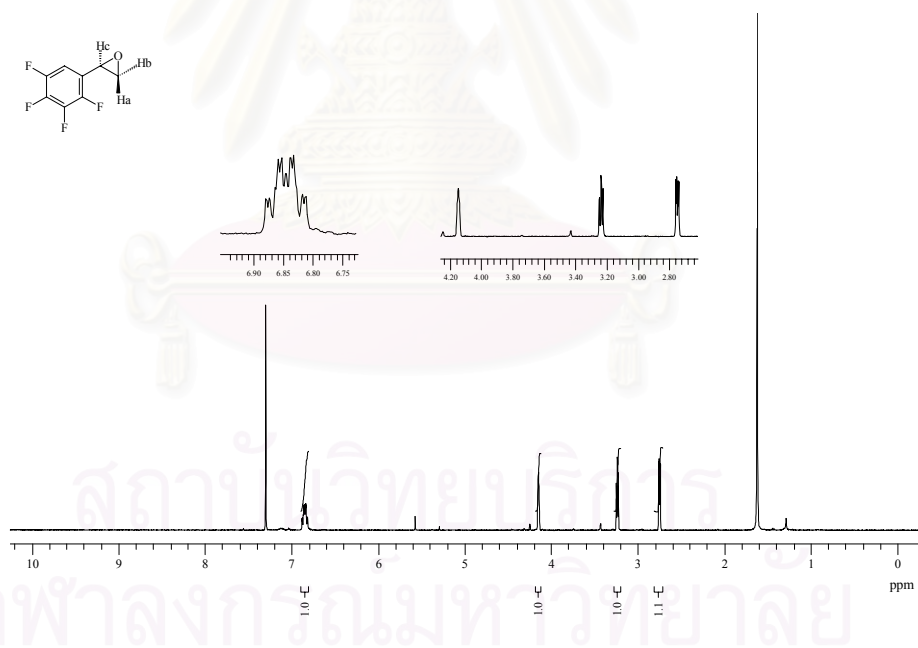
Figure B34   NMR spectrum of **tetrafluorostyrene oxide (TetraF)**; ^{1}H NMR
(CDCl$_3$, 400 MHz): δ 2.78 (1H, dd, Ha of CH$_2$O, J = 2.4 Hz, 5.4 Hz),
3.22 (1H, dd, Hb of CH$_2$O, J = 4.0 Hz, 5.4 Hz), 4.15 (1H, t, Hc of
CHAr), 6.70-7.00 (1H, m, ArH).
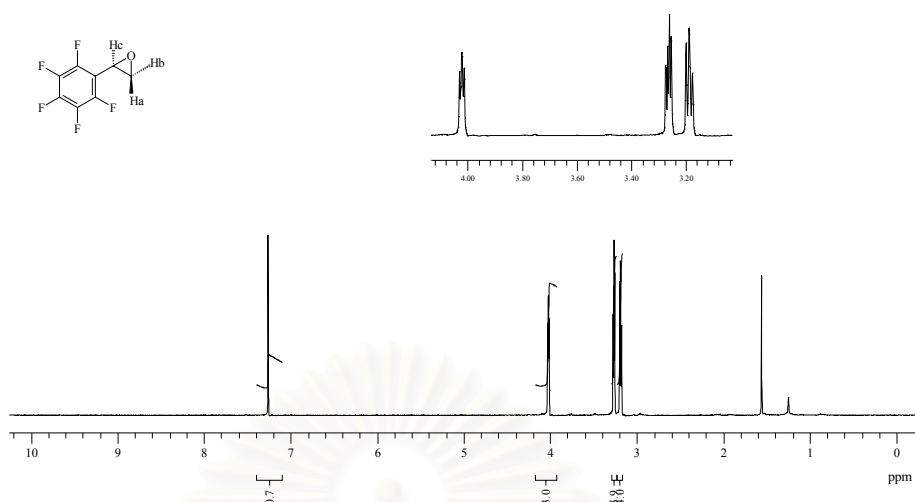
Figure B35   NMR spectrum of **pentafluorostyrene oxide (PentaF)**; ^{1}H NMR
(CDCl$_3$, 400 MHz): δ 3.18 (1H, dd, Hb of C<u>H</u>$_2$O, J = 4.2 Hz, 5.0 Hz),
3.28 (1H, dd, Ha of C<u>H</u>$_2$O, J = 2.6 Hz, 5.1 Hz), 4.05 (1H, t, Hc of
C<u>H</u>Ar)
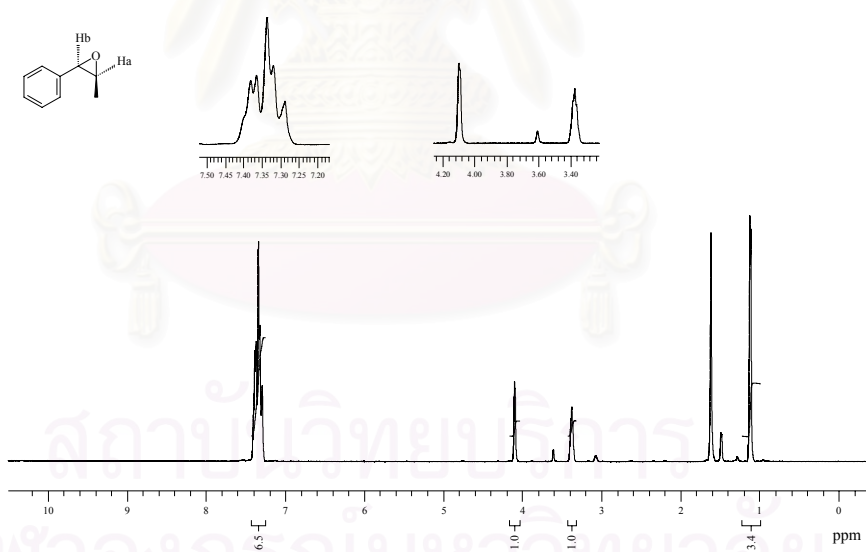
Figure B36   NMR spectrum of **phenylpropylene oxide (2)**; ^{1}H NMR (CDCl$_3$,
400 MHz): δ 1.15 (3H, d, OCHC<u>H</u>$_3$,), 3.12 (OC<u>H</u>CH$_3$, *trans-*) 3.40
(1H, m, OC<u>H</u>CH$_3$, *cis-*), 3.80 (C<u>H</u>Ar, *trans-*), 4.15 (1H, d, C<u>H</u>Ar, *cis-*,
J = 3.1 Hz), 7.30-7.50 (5H, m, Ar<u>H</u>).
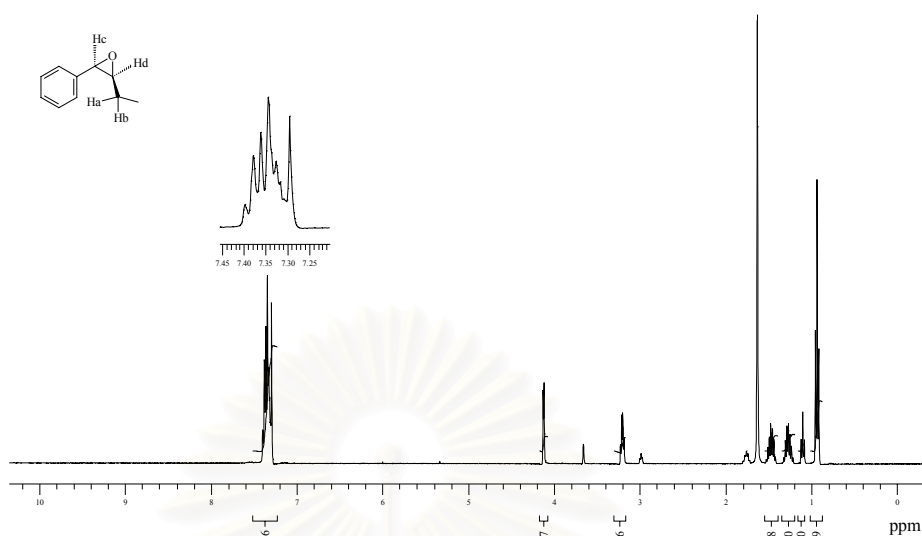
Figure B37   NMR spectrum of **phenylbutylene oxide (3)**; ¹H NMR (CDCl₃, 400
MHz): δ 0.95 (3H, t, OCHCH₂CH̲₃), 1.30 (1H, m, Ha of
OCHCH̲₂CH₃), 1.50 (1H, m, Hb of OCHCH̲₂CH₃), 3.00
(OCH̲CH2CH₃, *trans-*), 3.20 (1H, m, Hd of OCH̲CH₂CH₃, *cis-*), 3.82
(CH̲Ar, *trans-*), 4.15 (1H, d, Hc of CH̲Ar, *cis-, J* = 4.1 Hz), 7.20-7.42
(5H, m, ArH̲).
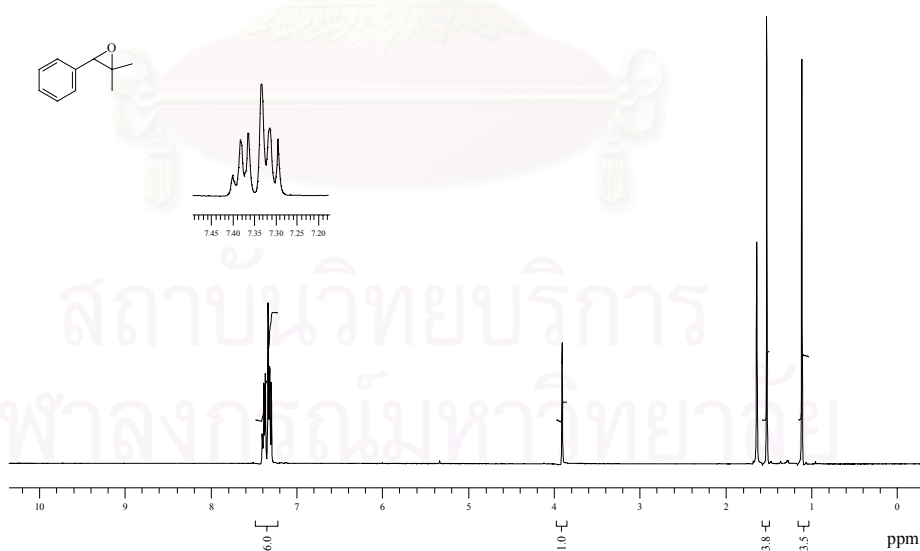
Figure B38   NMR spectrum of **phenylisopropylene oxide (4)**; ¹H NMR (CDCl₃,
400 MHz): δ 1.18 and 1.58 (6H, 2 x s, 2CCH̲₃), 3.90 (1H, s, CH̲Ar),
7.25-7.45 (5H, m, ArH̲).
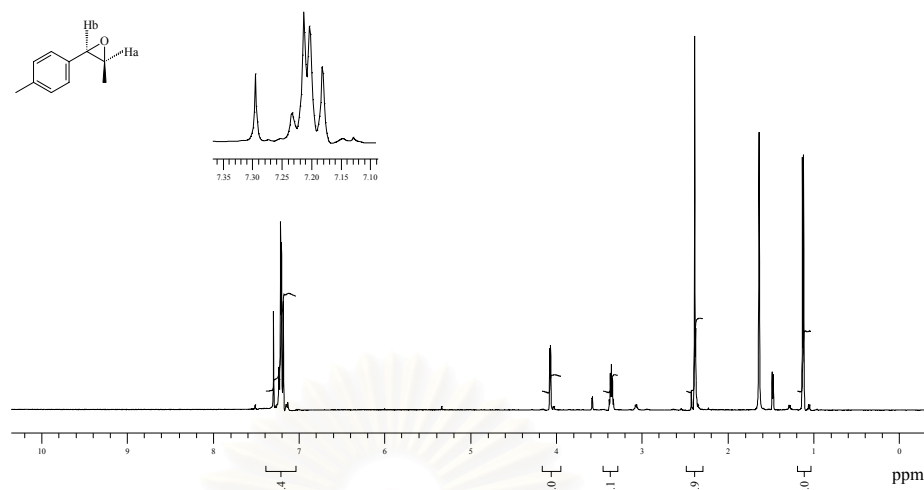
Figure B39   NMR spectrum of **4′-methylphenylpropylene oxide (5)**; [^1]H NMR
(CDCl₃, 400 MHz): δ 1.15 (3H, d, OCHC$\underline{H}_3$), 2.40 (3H, s, ArC$\underline{H}_3$),
3.12 (OC$\underline{H}$CH₃, *trans-*), 3.38 (1H, q, Ha of OC$\underline{H}$CH₃, *cis-*), 3.80
(OC$\underline{H}$Ar , *trans-*), 4.15 (1H, d, Hb of OC$\underline{H}$Ar, *cis-, J* = 4.1 Hz), 7.18-
7.30 (4H, m, Ar$\underline{H}$).

Appendix C

Thermodynamic Studies
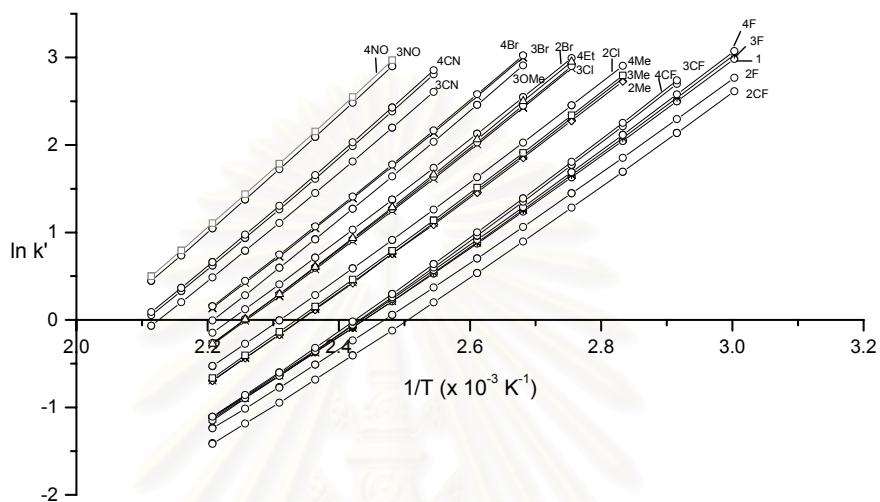
Figure C1   Plots of ln (capacity factor) versus reciprocal of temperature of styrene oxide
and its derivatives on OV-1701 column (part I).
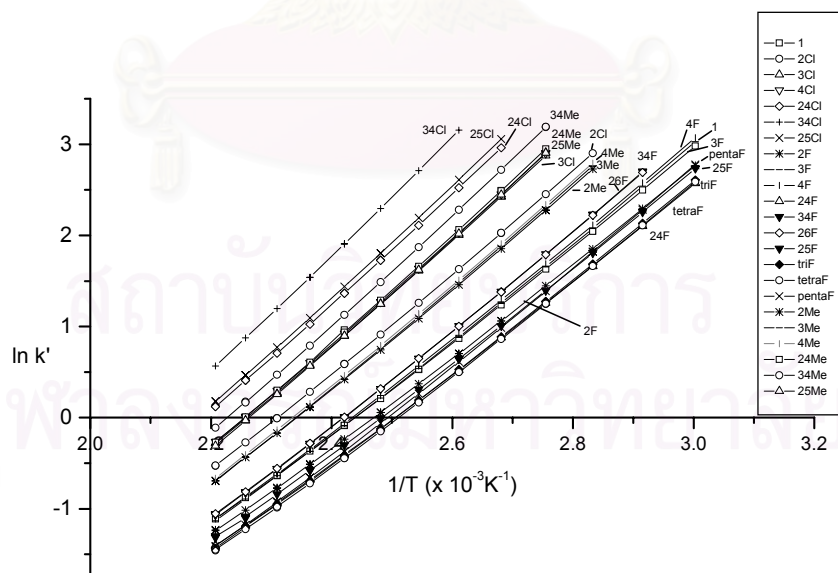
Figure C2   Plots of ln (capacity factor) versus reciprocal of temperature of styrene
oxide and its derivatives on OV-1701 column (part II).

Figure C3   Plots of ln (capacity factor) versus reciprocal of temperature of styrene
             oxide and its derivatives on OV-1701 column (part III).

Table C1   Equations and correlation coefficients of all analytes obtained from ln k′
            vs. 1/T plots on OV-1701 column.

analytes	Equation: ln k′ = m (1/T) + c		R^2
	m	c	
1	5106.95	-12.422	0.9993
2Br	5677.90	-12.690	0.9995
3Br	5986.60	-13.084	0.9996
4Br	5986.84	-13.063	0.9996
2Cl	5486.46	-12.675	0.9996
3Cl	5764.83	-13.037	0.9996
4Cl	5779.05	-13.051	0.9997
3CN	6395.73	-13.491	0.9997
4CN	6421.16	-13.509	0.9997
4Et	5889.53	-13.304	0.9996
2F	4995.02	-12.299	0.9992
3F	5178.50	-12.593	0.9992
4F	5205.47	-12.634	0.9992
3OMe	6155.24	-13.617	0.9998
2Me	5417.39	-12.667	0.9994
3Me	5472.65	-12.791	0.9994
4Me	5478.27	-12.774	0.9994
2NO	6213.50	-13.225	0.9998
3NO	6681.51	-13.696	0.9998
4NO	6714.52	-13.711	0.9998
2CF	5060.95	-12.642	0.9993
3CF	5423.94	-13.168	0.9994
4CF	5426.17	-13.136	0.9994
24Cl	5992.72	-13.127	0.9998

compound		Equation: ln k′ = m (1/T) + c		R^2
		m	c	
25Cl		6076.64	-13.257	0.9998
34Cl		6409.57	-13.599	0.9998
24F		4998.08	-12.492	0.9994
25F		5086.97	-12.600	0.9993
26F		5287.54	-12.773	0.9994
34F		5307.20	-12.825	0.9994
24Me		5875.36	-13.267	0.9997
25Me		5867.72	-13.291	0.9997
34Me		6026.82	-13.445	0.9997
triF		5071.42	-12.677	0.9994
tetraF		5078.72	-12.721	0.9993
pentaF		5221.05	-12.975	0.9991
2	*cis-*	5186.96	-12.521	0.9995
	trans-	5340.68	-12.772	0.9995
3	*cis-*	5548.24	-12.991	0.9995
	trans-	5750.99	-13.286	0.9995
4		5381.71	-12.899	0.9994
5	*cis-*	5655.96	-13.131	0.9995
	trans-	5815.76	-13.371	0.9995
6		5459.37	-12.784	0.9996
7		6204.55	-13.819	0.9996
8		6300.12	-13.691	0.9996
9		3914.97	-11.512	0.9997

Figure C4   Plots of ln (capacity factor) versus reciprocal of temperature of styrene oxide and its derivatives on BSiMe column (part I).

Figure C5   Plots of ln (capacity factor) versus reciprocal of temperature of styrene oxide and its derivatives on BSiMe column (part II).
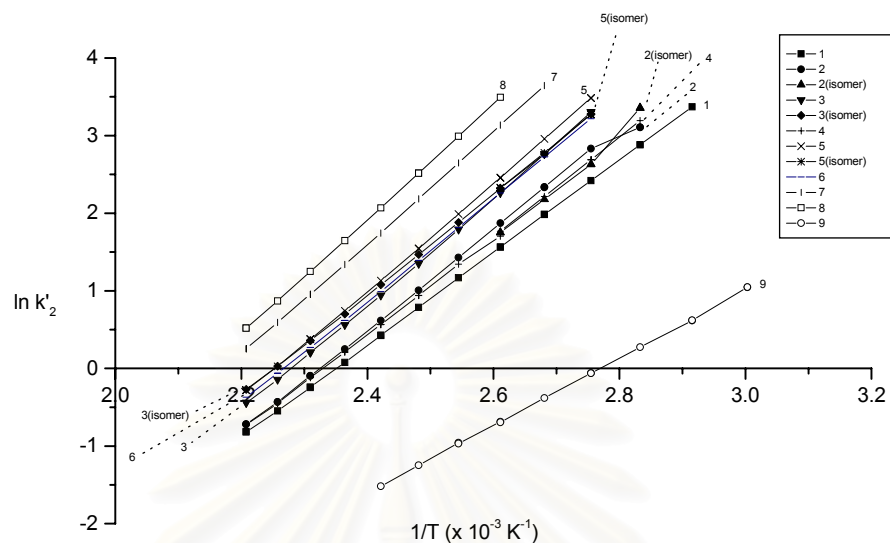
Figure C6   Plots of ln (capacity factor) versus reciprocal of temperature of styrene oxide and its derivatives on BSiMe column (part III).
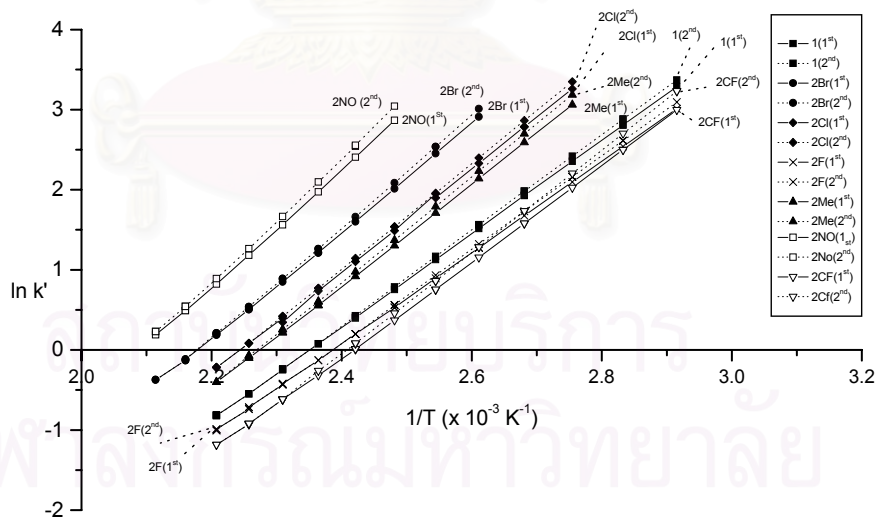
Figure C7   Plots of ln (capacity factor) versus reciprocal of temperature of styrene oxide and its derivatives on BSiMe column (part IV).

Table C2   Equations and correlation coefficients of all analytes obtained from ln k′
            vs. 1/T plots on BSiMe column.

| enantiomer | less retained enantiomer Equation: ln k′ = m (1/T) + c | | R^2 | more retained enantiomer Equation: ln k′ = m (1/T) + c | | R^2 |
	m	c		m	c	
1	5788.08	-13.596	0.9999	5908.23	-13.863	0.9998
2Br	6657.81	-14.502	0.9995	6858.81	-14.928	0.9995
3Br	6872.08	-14.683	0.9997	-		
4Br	6974.96	-14.785	0.9998	7105.01	-15.060	0.9998
2Cl	6399.43	-14.376	0.9996	6545.51	-14.692	0.9999
3Cl	6629.15	-14.607	0.9999	-		
4Cl	6665.15	-14.577	0.9999	6829.44	-14.934	0.9999
3CN	7486.97	-15.503	0.9997	7600.25	-15.737	0.9998
4CN	7608.75	-15.646	0.9998	7751.14	-15.940	0.9999
4Et	6763.15	-14.890	0.9998	-		
2F	5634.77	-13.432	0.9998	5755.62	-13.704	0.9997
3F	5981.33	-14.049	0.9999	6007.06	-14.109	0.9998
4F	5960.30	-13.917	0.9999	6085.91	-14.194	0.9998
3OMe	6852.83	-14.892	0.9999	6926.88	-15.061	0.9999
2Me	6284.26	-14.274	0.9996	6484.19	-14.702	0.9996
3Me	6162.98	-14.021	0.9998	6243.98	-14.202	0.9997
4Me	6176.95	-14.001	0.9997	6215.25	-14.088	0.9996
2NO	7315.27	-15.311	0.9995	7678.36	-16.043	0.9994
3NO	7721.86	-15.616	0.9997	-		
4NO	7960.24	-15.929	0.9998	8072.48	-16.153	0.9998
2CF	5942.34	-14.349	0.9997	6287.02	-15.120	0.9998
3CF	6163.11	-14.549	0.9999	6186.78	-14.606	0.9998

| enantiomer		less retained enantiomer			more retained enantiomer		
		Equation: $\ln k' = m\,(1/T) + c$		R^2	Equation: $\ln k' = m\,(1/T) + c$		R^2
		m	c		m	c	
4CF		6338.13	-14.750	0.9999	6541.08	-15.182	0.9999
24Cl		7000.54	-14.932	0.9997	7237.02	-15.420	0.9998
25Cl		7315.31	-15.611	0.9998	7393.62	-15.788	0.9998
34Cl		7390.00	-15.367	0.9999	7486.04	-15.576	0.9999
24F		5711.27	-13.741	0.9999	5866.38	-14.089	0.9999
25F		5909.23	-14.122	0.9999	6020.78	-14.377	0.9998
26F		5861.80	-13.813	0.9999	6013.64	-14.151	0.9999
34F		6103.22	-14.238	0.9999	6135.96	-14.314	0.9999
24Me		7082.57	-15.591	0.9998	-		
25Me		6746.06	-14.951	0.9998	6976.33	-15.437	0.9997
34Me		6875.82	-15.001	0.9998	-		
triF		5884.20	-14.180	0.9999	5889.03	-14.191	0.9999
tetraF		5611.89	-13.670	0.9999	5621.31	-13.692	0.9999
pentaF		5713.77	-13.872	0.9999	5844.75	-14.164	0.9998
2	*cis-*	6292.57	- 14.647	0.9998	6546.03	-15.212	0.9997
	trans-	6080.35	- 14.158	1.0000	6111.15	-14.205	1.0000
3	*cis-*	6588.02	-15.033	0.9994	6853.70	-15.624	0.9994
	trans-	6342.08	-14.286	0.9992	6481.64	-14.605	0.9998
4		6150.57	-14.346	0.9997	6283.40	-14.634	0.9997
5	*cis-*	6648.75	-14.987	0.9998	6902.30	-15.558	0.9997
	trans-	6618.12	-14.986	0.9996	6582.54	-14.863	0.9998
6		6518.21	-14.779	0.9999	6576.74	-14.913	0.9999
7		7135.87	-15.519	0.9999	7182.73	-15.627	0.9998
8		7190.50	-15.349	0.9997	7279.80	-15.543	0.9997
9		4358.52	-12.066	0.9998	-		
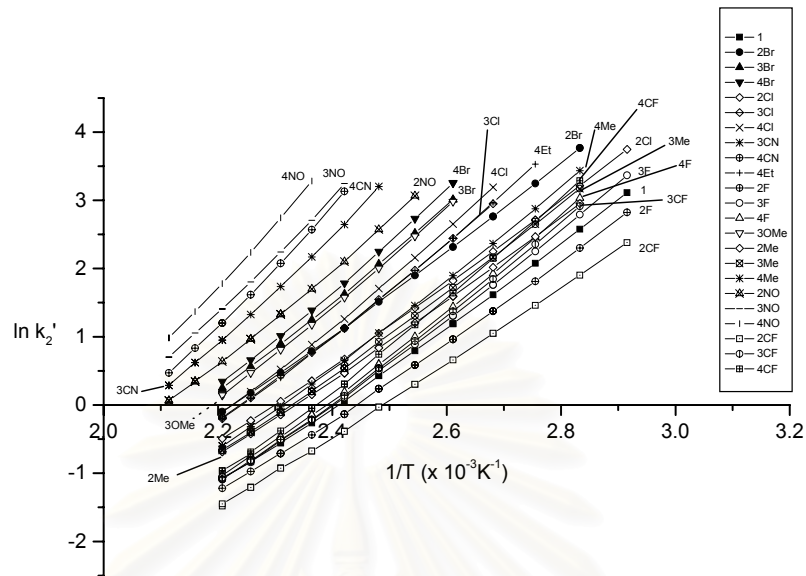
Figure C8   Plots of ln (capacity factor) versus reciprocal of temperature of styrene
oxide and its derivatives on BSiAc column (part I).
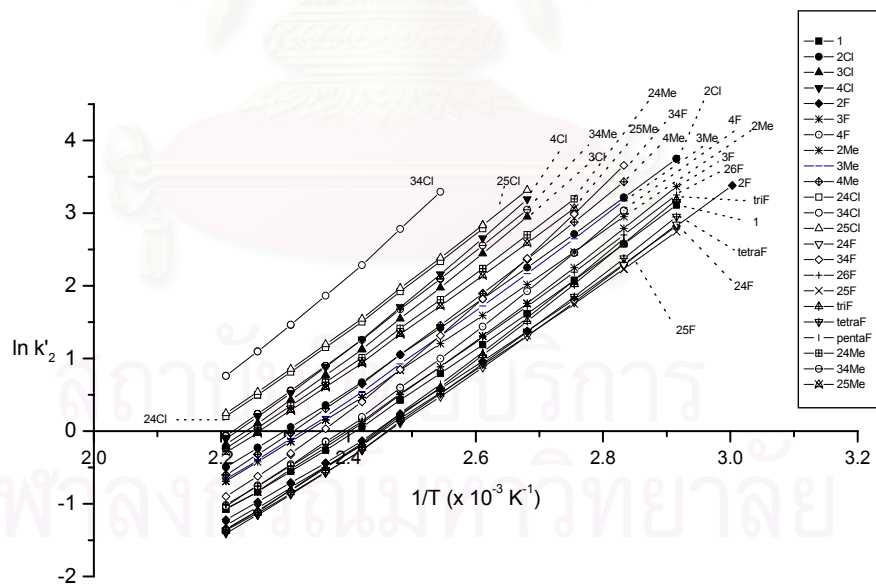
Figure C9   Plots of ln (capacity factor) versus reciprocal of temperature of styrene
oxide and its derivatives on BSiAc column (part II).
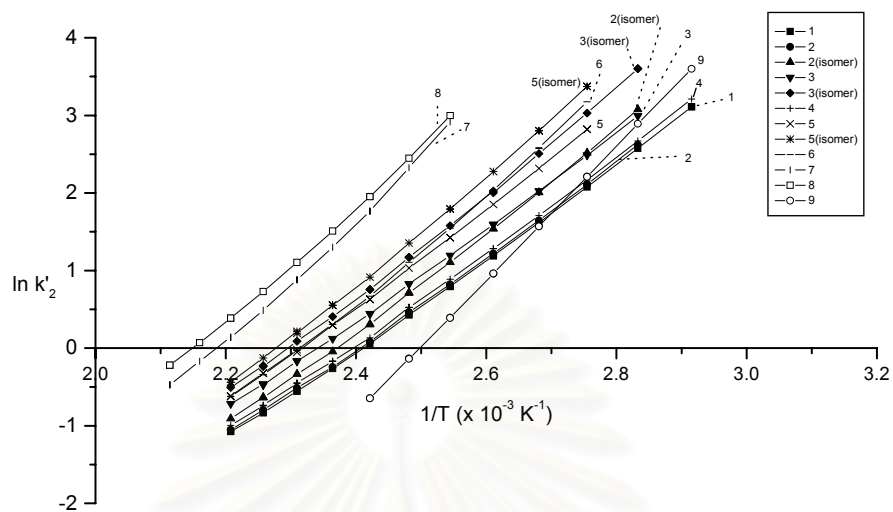
Figure C10   Plots of ln (capacity factor) versus reciprocal of temperature of styrene
oxide and its derivatives on BSiAc column (part III).
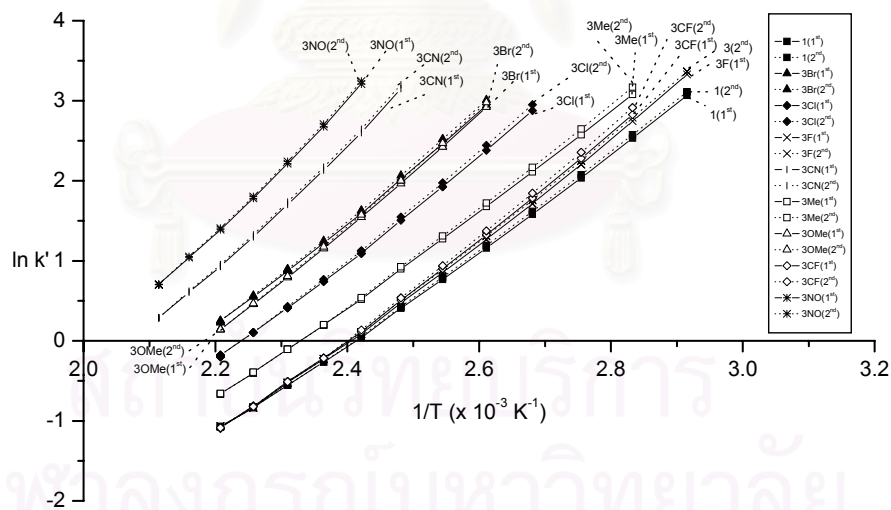
Figure C11   Plots of ln (capacity factor) versus reciprocal of temperature of styrene
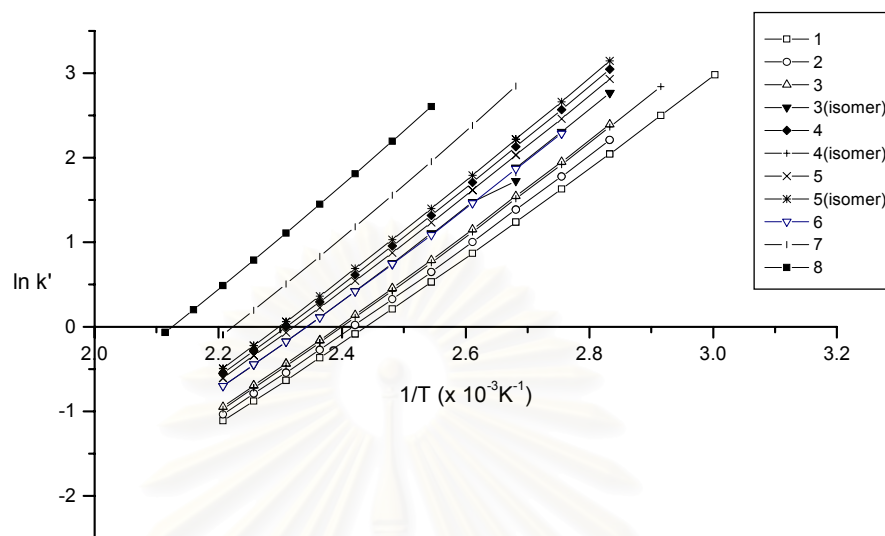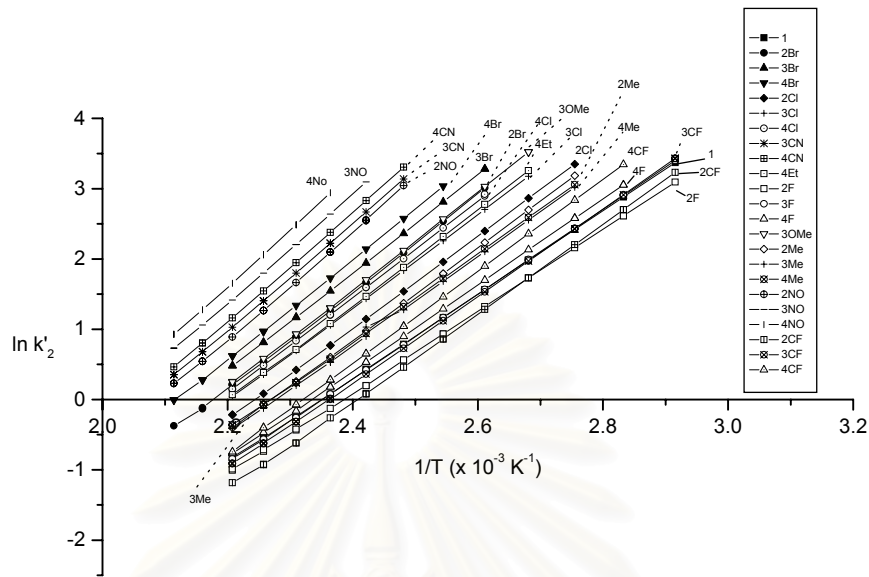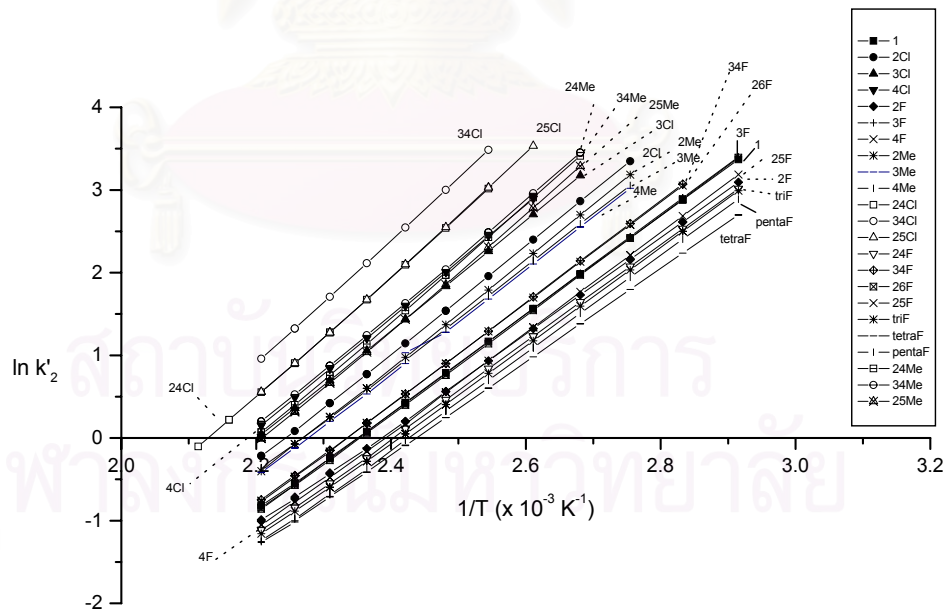oxide and its derivatives on BSiAc column (part IV).

Table C3　　Equations and correlation coefficients of all analytes obtained from ln k′ vs. 1/T plots on BSiAc column.

enantiomer	less retained enantiomer			more retained enantiomer		
	Equation: ln k′ = m (1/T) + c		R^2	Equation: ln k′ = m (1/T) + c		R^2
	m	c		m	c	
1	5878.73	-14.141	0.9984	5932.73	-14.259	0.9988
2Br	6171.38	-13.777	0.9994	6186.81	-13.814	0.9993
3Br	6689.87	-14.565	0.9990	6845.05	-14.903	0.9990
4Br	7129.38	-15.451	0.9985	7222.29	-15.655	0.9987
2Cl	5988.99	-13.781	0.9992	5998.16	-13.803	0.9992
3Cl	6473.01	-14.529	0.9988	6630.67	-14.879	0.9989
4Cl	6923.82	-15.458	0.9984	6978.59	-15.579	0.9986
3CN	7748.39	-16.150	0.9979	7875.04	-16.411	0.9982
4CN	8435.14	-17.413	0.9982	8621.13	-17.801	0.9983
4Et	6753.61	-15.181	0.9987	6814.18	-15.323	0.9983
2F	5751.07	-14.005	0.9989	5789.83	-14.098	0.9986
3F	6210.16	-14.887	0.9980	6284.62	-15.051	0.9984
4F	6410.46	-15.266	0.9983	6484.47	-15.441	0.9977
3OMe	6879.48	-15.082	0.9991	7014.97	-15.381	0.9991
2Me	5796.34	-13.528	0.9995	5829.82	-13.607	0.9994
3Me	5994.10	-13.951	0.9993	6143.72	-14.293	0.9991
4Me	6273.23	-14.513	0.9990	6458.04	-14.934	0.9989
2NO	6836.43	-14.445	0.9984	6959.78	-14.711	0.9983
3NO	8127.01	-16.523	0.9982	8234.02	-16.744	0.9984
4NO	9034.68	-18.163	0.9989	9202.92	-18.506	0.9989
2CF	5392.16	-13.403	0.9997	5464.29	-13.574	0.9994
3CF	6254.41	-14.971	0.9986	6406.26	-15.316	0.9985

enantiomer		less retained enantiomer			more retained enantiomer		
		Equation: ln k′ = m (1/T) + c		R^2	Equation: ln k′ = m (1/T) + c		R^2
		m	c		m	c	
4CF		6789.91	-16.063	0.9982	6834.94	-16.165	0.9981
24Cl		6413.97	-13.989	0.9993	-		
25Cl		6433.81	-13.995	0.9994	6505.53	-14.161	0.9992
34Cl		7376.00	-15.578	0.9987	7510.56	-15.860	0.9987
24F		5836.87	-14.340	0.9988	5954.96	-14.618	0.9981
25F		5711.87	-13.973	0.9991	-		
26F		6004.18	-14.351	0.9989	6029.72	-14.411	0.9987
34F		7096.81	-16.696	0.9974	7299.50	-17.170	0.9961
24Me		6257.64	-14.097	0.9994	6283.58	-14.158	0.9993
25Me		6155.24	-13.924	0.9995	-		
34Me		6453.19	-14.361	0.9988	6581.28	-14.637	0.9992
triF		6296.69	-15.362	0.9981	6421.12	-15.655	0.9974
tetraF		6137.98	-15.053	0.9985	6156.92	-15.098	0.9983
pentaF		6419.31	-15.633	0.9979	-		
2	cis-	5595.62	-13.451	0.9993	5877.06	-14.096	0.9987
	trans-	6076.74	-14.383	0.9989	6373.16	-15.063	0.9983
3	cis-	5799.81	-13.572	0.9994	5946.96	-13.911	0.9992
	trans-	6455.04	-14.830	0.9989	6572.31	-15.099	0.9986
4		5830.89	-13.934	0.9990	5943.37	-14.194	0.9988
5	cis-	6027.52	-13.956	0.9994	6278.08	-14.525	0.9992
	trans-	6624.16	-15.116	0.9989	6948.67	-15.845	0.9986
6		6736.34	-15.587	0.9973	6931.90	-16.032	0.9969
7		7765.77	-17.079	0.9978	8227.83	-18.092	0.9969
8		7320.25	-15.763	0.9979	7443.81	-16.033	0.9975
9		8365.17	-20.933	0.9998	8604.65	-21.492	0.9999

Table C4.   Thermodynamic parameters of all epoxides calculated from van't Hoff
plots of ln k′ versus 1/T on OV-1701 column.

compound	$-\Delta H$ (kcal/mol)	$-\Delta S$ (cal/mol.K)	compound	$-\Delta H$ (kcal/mol)	$-\Delta S$ (cal/mol.K)
1	10.15	35.66	**3NO**	13.28	38.19
2Br	11.28	36.19	**4NO**	13.34	38.22
3Br	11.89	36.97	**2CF**	10.06	36.09
4Br	11.89	36.93	**3CF**	10.77	37.14
2Cl	10.90	36.16	**4CF**	10.78	37.08
3Cl	11.45	36.88	**24Cl**	11.91	37.06
4Cl	11.48	36.91	**25Cl**	12.08	37.32
3CN	12.71	37.78	**34Cl**	12.74	37.99
4CN	12.76	37.82	**24F**	9.93	35.80
4Et	11.70	37.41	**25F**	10.11	36.01
2F	9.93	35.41	**26F**	10.51	36.37
3F	10.29	35.99	**34F**	10.55	36.46
4F	10.34	36.08	**24Me**	11.68	37.34
3OMe	12.23	38.03	**25Me**	11.66	37.38
2Me	10.76	36.15	**34Me**	11.98	37.69
3Me	10.88	36.39	**TriF**	10.08	36.17
4Me	10.89	36.36	**TetraF**	10.09	36.25
2NO	12.35	37.25	**PentaF**	10.38	36.76

compound	$-\Delta H$ (kcal/mol)	$-\Delta S$ (cal/mol.K)	compound	$-\Delta H$ (kcal/mol)	$-\Delta S$ (cal/mol.K)
2	10.31	35.85	**5**	11.55	37.54
2	10.61	36.35	**6**	10.84	36.37
3	11.02	36.78	**7**	12.32	38.45
3	11.42	37.37	**8**	12.52	38.18
4	10.69	36.60	**9**	7.78	33.85
5	11.23	37.06			

Table C5.   Thermodynamic parameters of all epoxides calculated from van't Hoff plots of ln k′ versus 1/T on BSiMe column.

compound	enthalpy term (kcal/mol)			entropy term (cal/mol.K)		
	$-\Delta H_1$	$-\Delta H_2$	$-\Delta(\Delta H)$	$-\Delta S_1$	$-\Delta S_2$	$-\Delta(\Delta S)$
1	11.50	11.74	0.24	37.99	38.52	0.53
2Br	13.23	13.63	0.40	39.79	40.64	0.85
3Br	13.66	-	0.00	40.15	-	0.00
4Br	13.86	14.12	0.26	40.35	40.90	0.55
2Cl	12.72	13.01	0.29	39.54	40.17	0.63
3Cl	13.17	-	0.00	39.99	-	0.00
4Cl	13.25	13.57	0.32	39.94	40.65	0.71
3CN	14.88	15.10	0.22	41.78	42.24	0.46
4CN	15.12	15.40	0.28	42.07	42.65	0.58
4Et	13.44	-	0.00	40.56	-	0.00
2F	11.20	11.44	0.24	37.66	38.20	0.54
3F	11.89	11.94	0.05	38.89	39.01	0.12
4F	11.84	12.09	0.15	38.63	39.18	0.55
3OMe	13.62	13.77	0.15	40.56	40.90	0.33
2Me	12.49	12.89	0.40	39.34	40.19	0.85
3Me	12.25	12.41	0.16	38.83	39.19	0.36
4Me	12.27	12.35	0.08	38.80	38.97	0.17
2NO	14.54	15.26	0.72	41.40	42.85	1.45

compound	enthalpy term (kcal/mol)			entropy term (cal/mol.K)		
	$-\Delta H_1$	$-\Delta H_2$	$-\Delta(\Delta H)$	$-\Delta S_1$	$-\Delta S_2$	$-\Delta(\Delta S)$
3NO	15.34	-	0.00	42.01	-	0.00
4NO	15.82	16.04	0.22	42.63	43.07	0.44
2CF	11.82	12.50	0.68	39.49	41.02	1.53
3CF	12.25	12.30	0.05	39.88	40.00	0.11
4CF	12.60	13.00	0.40	40.28	41.14	0.86
24Cl	13.91	14.38	0.47	40.65	41.62	0.97
25Cl	14.54	14.69	0.15	42.00	42.35	0.35
34Cl	14.68	14.87	0.19	41.51	41.92	0.41
24F	11.35	11.66	0.31	38.28	38.97	0.69
25F	11.74	11.96	0.22	39.03	39.54	0.51
26F	11.65	11.95	0.30	38.42	39.09	0.67
34F	12.13	12.19	0.06	39.27	39.42	0.15
24Me	14.07	-	0.00	41.95	-	0.00
25Me	13.40	13.86	0.46	40.68	41.64	0.96
34Me	13.66	-	0.00	40.78	-	0.00
TriF	11.69	11.70	0.01	39.15	39.17	0.02
TetraF	11.15	11.17	0.02	38.14	38.18	0.04
PentaF	11.35	11.61	0.26	38.54	39.12	0.58
2 *(cis)-*	12.50	13.00	0.50	40.07	41.20	1.12
2 *(trans-)*	12.08	12.14	0.06	39.10	39.20	0.09

compound	enthalpy term (kcal/mol)			entropy term (cal/mol.K)		
	$-\Delta H_1$	$-\Delta H_2$	$-\Delta(\Delta H)$	$-\Delta S_1$	$-\Delta S_2$	$-\Delta(\Delta S)$
3 *(cis)-*	13.09	13.62	0.53	40.84	42.02	1.17
3 *(trans-)*	12.60	12.88	0.03	39.36	40.05	0.69
4	12.22	12.48	0.26	39.48	40.05	0.57
5 *(cis)-*	13.21	13.71	0.50	40.45	41.89	1.13
5 *(trans-)*	13.15	13.08	0.07	40.75	40.50	0.24
6	12.95	13.07	0.12	40.34	40.61	0.27
7	14.18	14.27	0.09	41.81	42.02	0.21
8	14.29	14.67	0.18	41.47	41.85	0.38
9	8.66	-	0.00	34.95	-	0.00
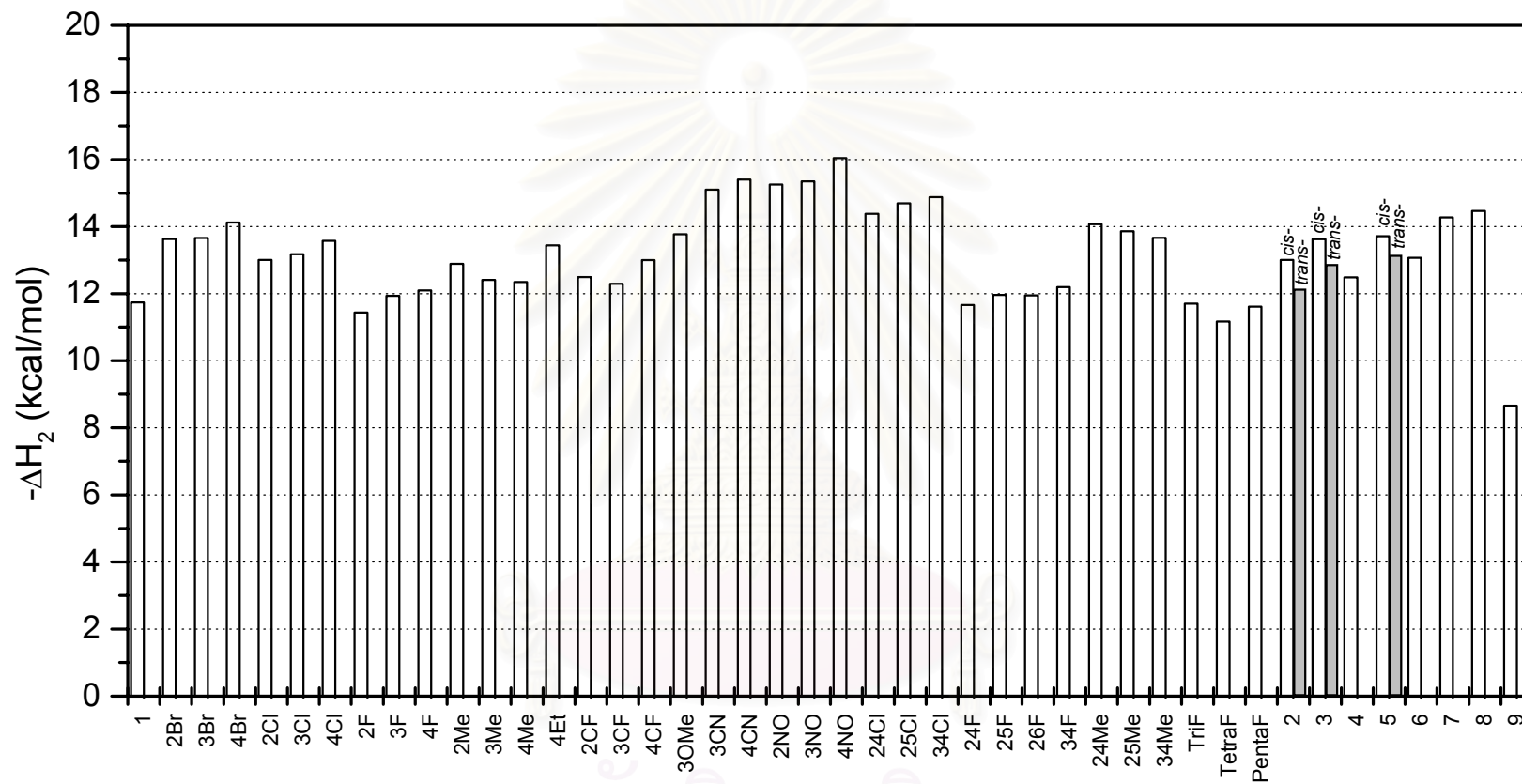
Figure C12   Enthalpy values ($-\Delta H_2$, kcal/mol) of the more retained enantiomers of styrene oxide derivatives on BSiMe phase

obtained from *van't Hoff approach* ($\bar{x} = 13.13$; SD = 1.37).
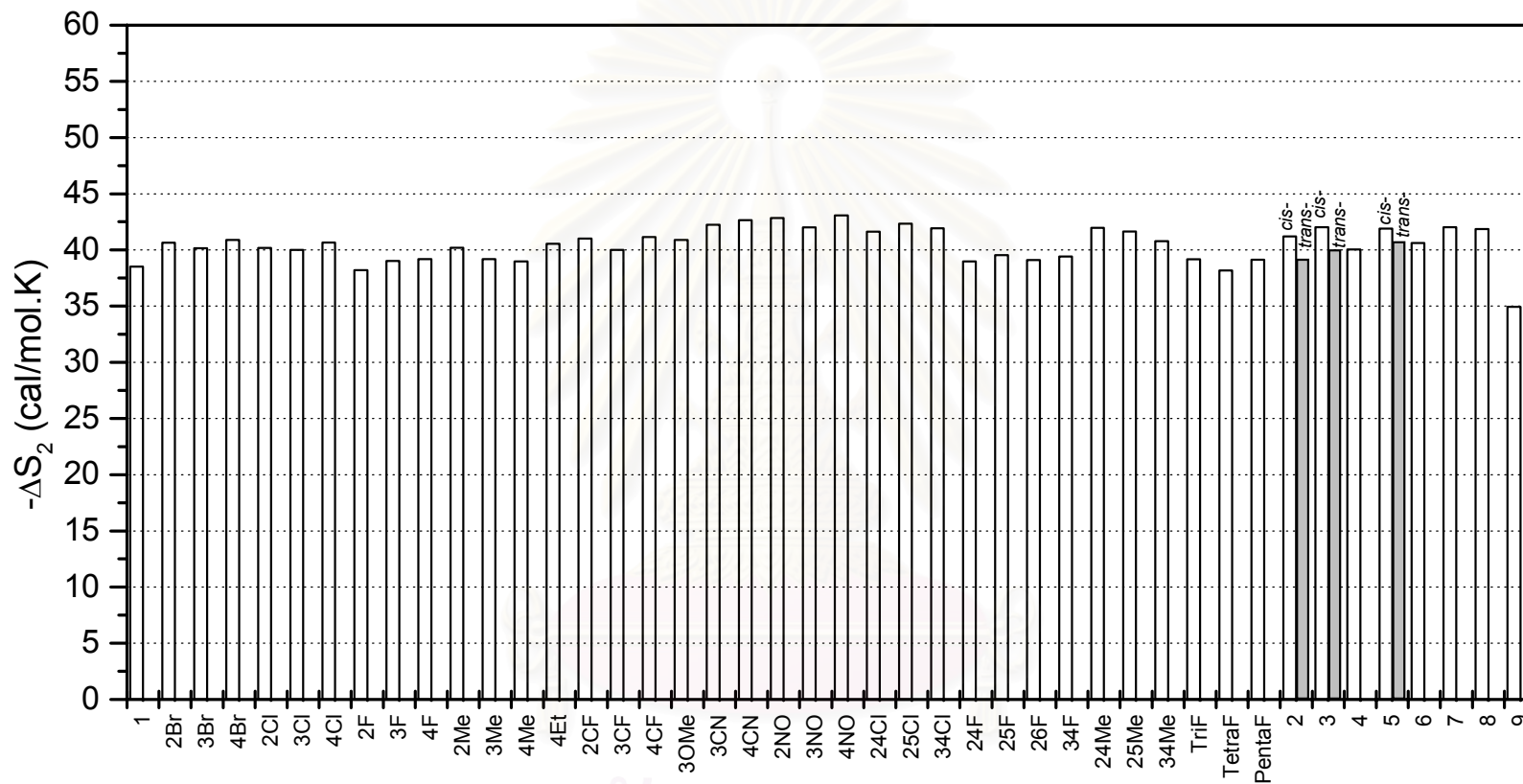
Figure C13   Entropy values (-ΔS_2, cal/mol·K) of the more retained enantiomers of styrene oxide derivatives on BSiMe phase obtained from *van't Hoff approach* ($\bar{x}$ = 40.43; SD = 1.53).
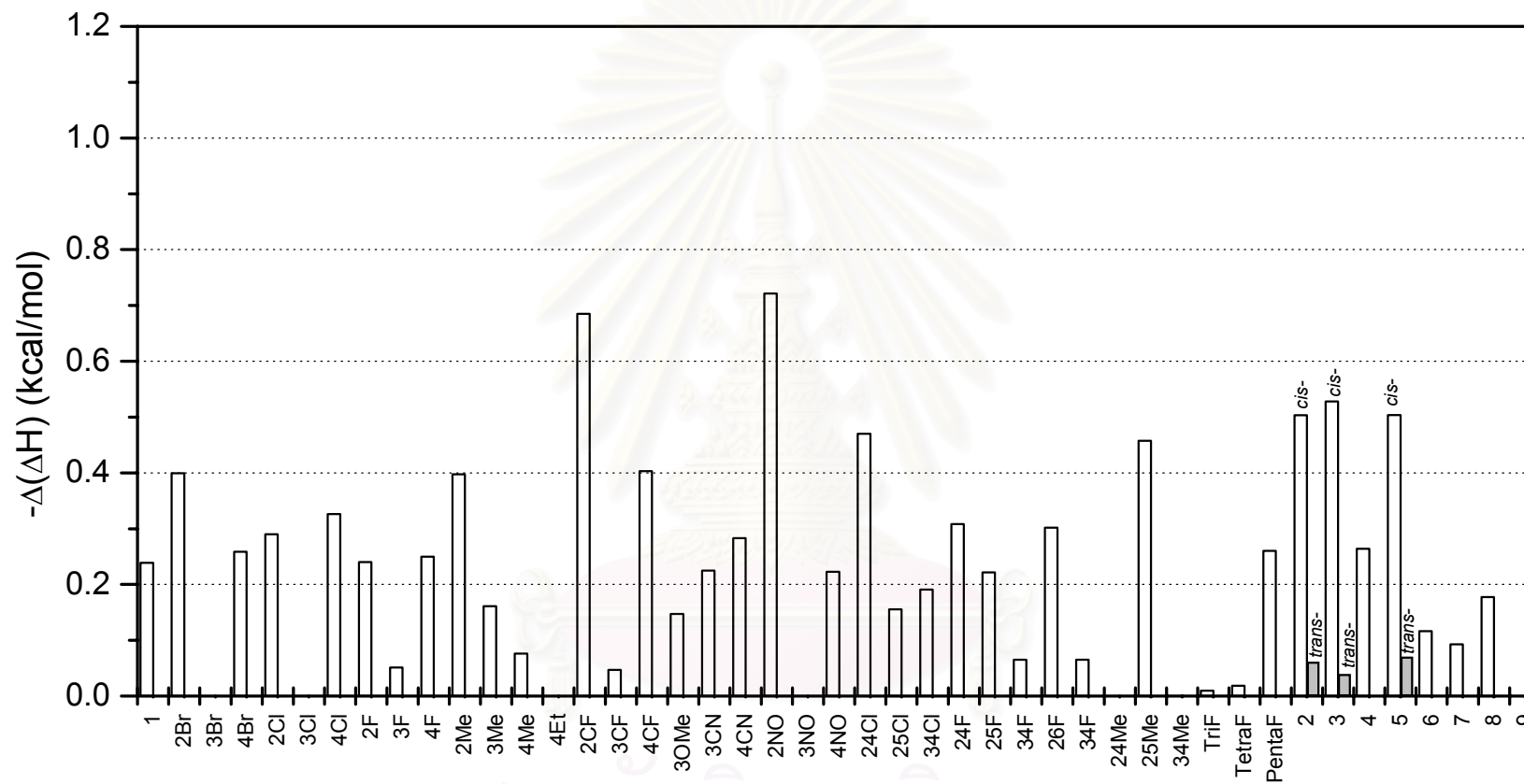
Figure C14   Difference in enthalpy values (-Δ(ΔH), kcal/mol) of the enantiomers of styrene oxide derivatives on BSiMe phase obtained from *van't Hoff approach*.

Figure C15   Difference in entropy values (-Δ(ΔS), cal/mol·K) of the enantiomers of styrene oxide derivatives on BSiMe phase obtained from *van't Hoff approach*.

Table C6.   Thermodynamic parameters of all epoxides calculated from van't Hoff
            plots of ln k′ versus 1/T on BSiAc column.

compound	enthalpy term (kcal/mol)			entropy term (cal/mol.K)		
	$-\Delta H_1$	$-\Delta H_2$	$-\Delta(\Delta H)$	$-\Delta S_1$	$-\Delta S_2$	$-\Delta(\Delta S)$
1	11.68	11.79	0.11	39.08	39.31	0.23
2Br	12.26	12.29	0.03	38.35	38.42	0.07
3Br	13.29	13.60	0.31	39.92	40.59	0.67
4Br	14.17	14.35	0.18	41.67	42.08	0.41
2Cl	11.90	11.92	0.02	38.36	38.40	0.04
3Cl	12.86	13.17	0.31	39.84	40.54	0.70
4Cl	13.76	13.87	0.11	41.69	41.93	0.24
3CN	15.40	15.65	0.25	43.06	43.58	0.52
4CN	16.76	17.13	0.37	45.57	46.34	0.77
4Et	13.42	13.54	0.12	41.14	41.42	0.28
2F	11.43	11.51	0.08	38.80	38.99	0.19
3F	12.34	12.49	0.15	40.55	40.88	0.33
4F	12.74	12.88	0.14	41.31	41.65	0.34
3OMe	13.67	13.94	0.26	40.94	41.53	0.59
2Me	11.52	11.58	0.06	37.85	38.01	0.16
3Me	11.91	12.21	0.30	38.69	39.37	0.68
4Me	12.46	12.83	0.37	39.81	40.65	0.84
2NO	13.58	13.83	0.25	39.68	40.21	0.53

compound	enthalpy term (Kcal/mol)			entropy term (cal/mol.K)		
	$-\Delta H_1$	$-\Delta H_2$	$-\Delta(\Delta H)$	$-\Delta S_1$	$-\Delta S_2$	$-\Delta(\Delta S)$
3NO	16.15	16.36	0.21	43.81	44.25	0.44
4NO	17.95	18.28	0.33	47.07	47.75	0.68
2CF	10.71	10.86	0.14	37.61	37.95	0.34
3CF	12.43	12.73	0.30	40.72	41.41	0.69
4CF	13.49	13.58	0.09	42.89	43.09	0.20
24Cl	12.74	-	0.00	38.77	-	0.00
25Cl	12.78	12.93	0.14	38.78	39.11	0.33
34Cl	14.65	14.92	0.27	41.93	42.49	0.56
24F	11.60	11.83	0.23	39.47	40.02	0.55
25F	11.35	-	0.00	38.74	-	0.00
26F	11.93	11.98	0.05	39.49	39.61	0.12
34F	14.10	14.50	0.40	44.15	45.09	0.94
24Me	12.43	12.48	0.05	38.98	39.10	0.12
25Me	12.23	-	0.00	38.64	-	0.00
34Me	12.82	13.07	0.25	39.51	40.06	0.55
TriF	12.51	12.76	0.25	41.50	42.08	0.58
TetraF	12.20	12.23	0.03	40.88	40.97	0.09
PentaF	12.75	-	0.00	42.04	-	0.00
2 *(cis)-*	11.12	11.68	0.56	37.70	38.98	1.28
2 *(trans-)*	12.07	12.66	0.59	39.55	40.90	1.35

compound	enthalpy term (kcal/mol)			entropy term (cal/mol.K)		
	$-\Delta H_1$	$-\Delta H_2$	$-\Delta(\Delta H)$	$-\Delta S_1$	$-\Delta S_2$	$-\Delta(\Delta S)$
3 *(cis)-*	11.52	11.82	0.30	37.94	38.61	0.67
3 *(trans-)*	12.82	13.06	0.23	40.44	40.97	0.54
4	11.59	11.81	0.22	38.66	39.18	0.52
5 *(cis)-*	11.98	12.47	0.49	38.71	39.84	1.13
5 *(trans-)*	13.16	13.80	0.64	41.01	42.46	1.45
6	13.39	13.78	0.39	41.95	42.83	0.88
7	15.43	16.35	0.92	44.91	46.92	2.01
8	14.54	14.79	0.25	42.30	42.83	0.53
9	16.62	17.09	0.47	52.57	53.68	1.11
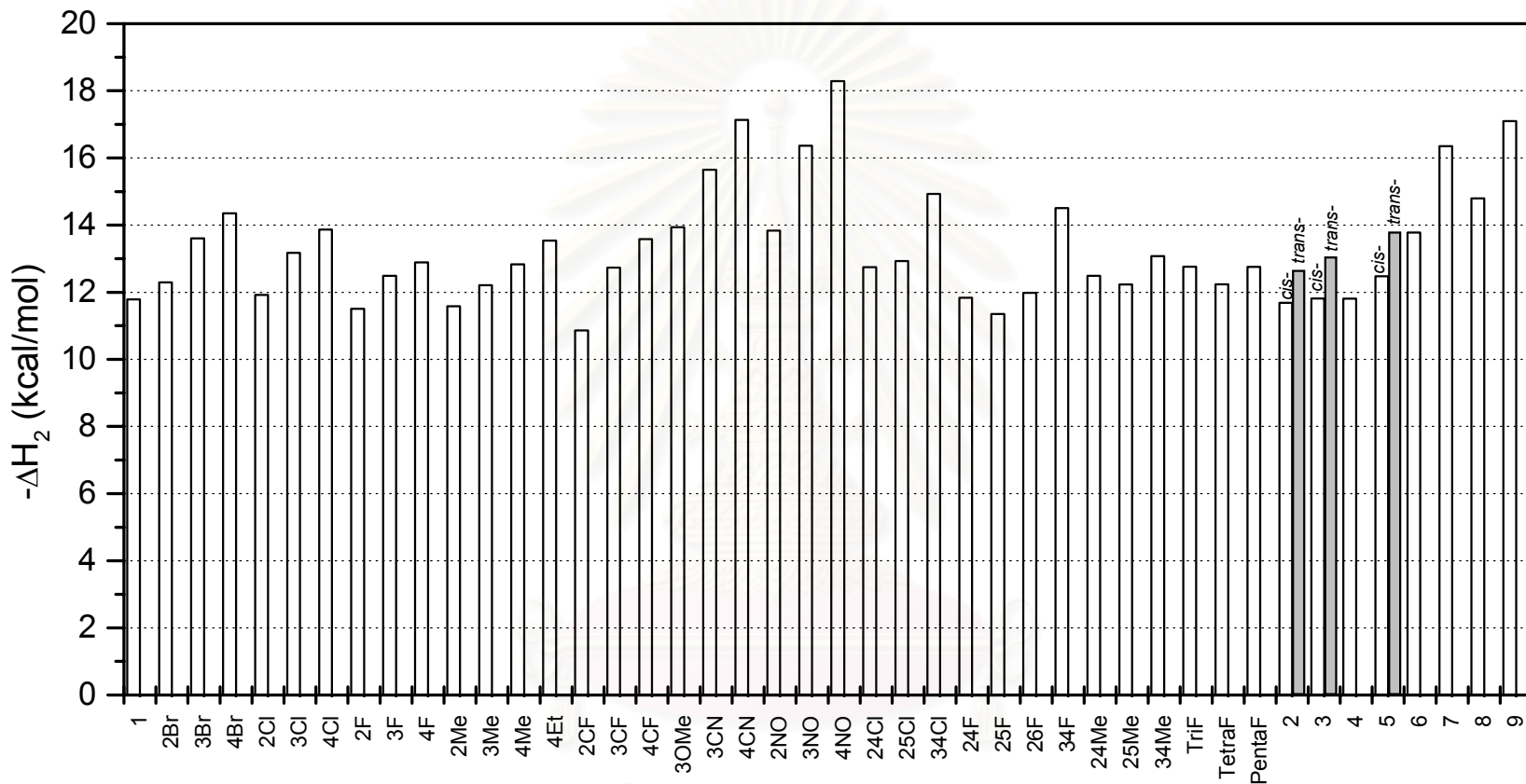
Figure C16   Enthalpy values (-ΔH_2, kcal/mol) of the more retained enantiomers of styrene oxide derivatives on BSiAc phase
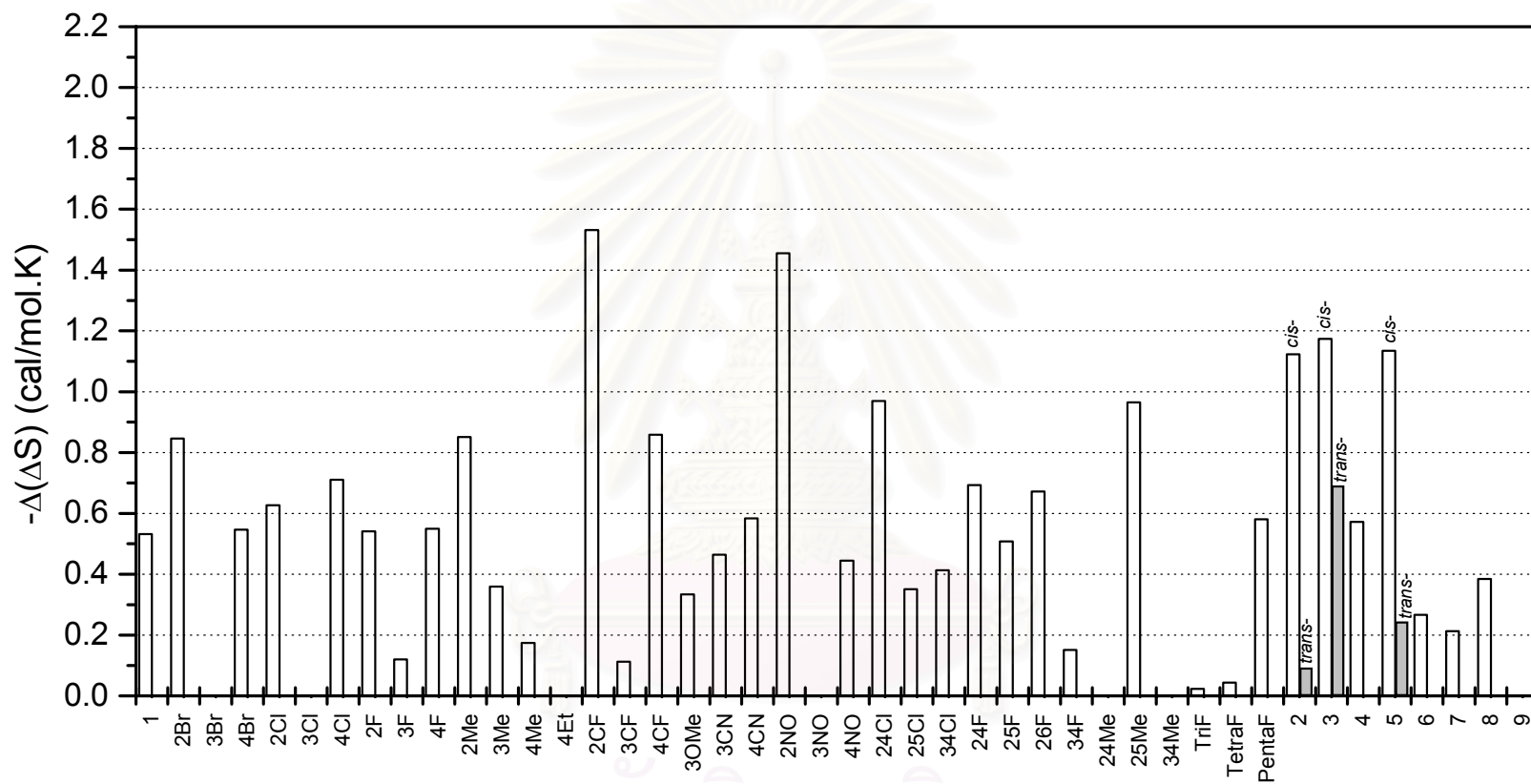obtained from *van't Hoff approach* ($\bar{x}$ = 13.31; SD = 1.66).
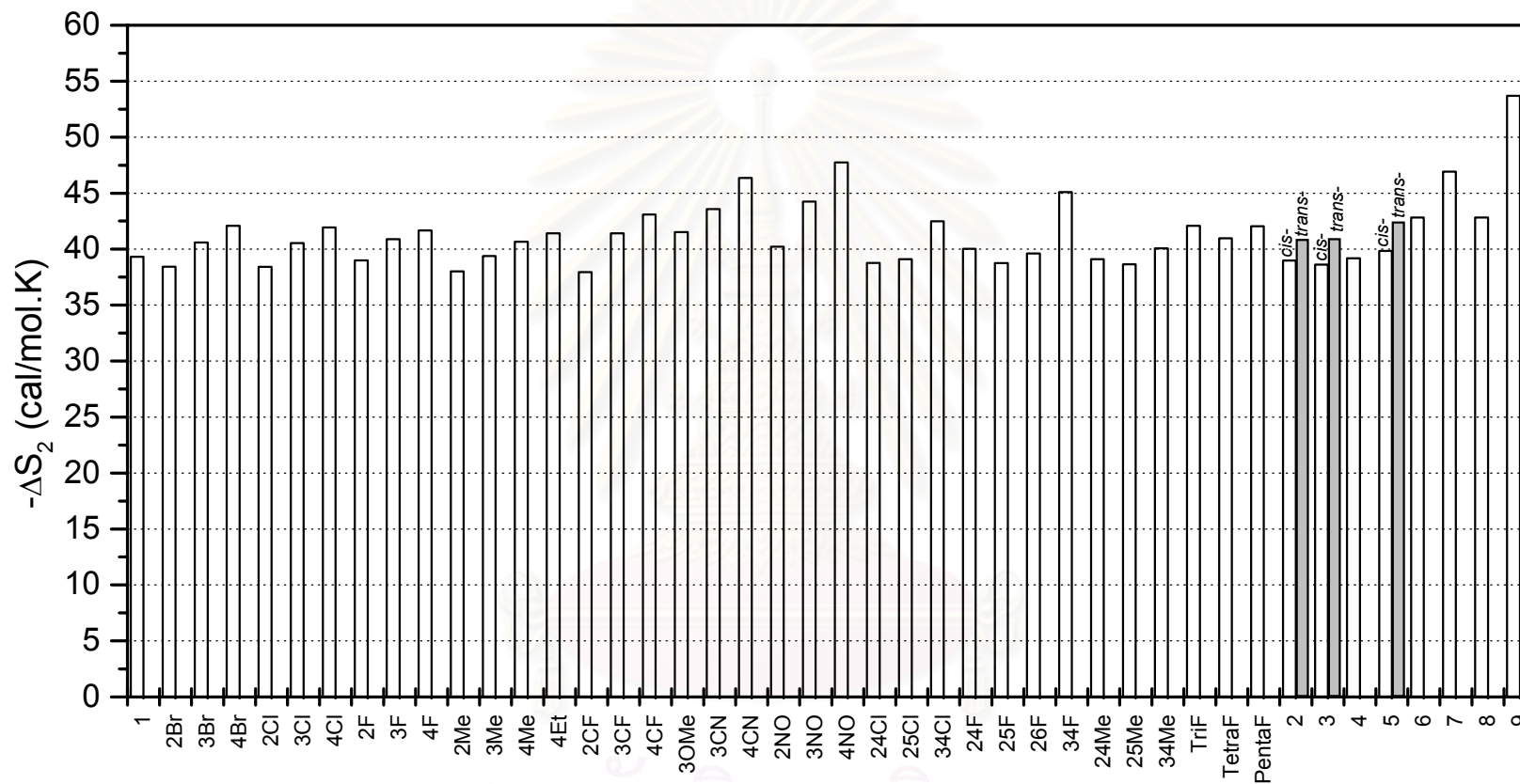
Figure C17   Entropy values (-ΔS_2, cal/mol·K) of the more retained enantiomers of styrene oxide derivatives on BSiAc phase

obtained from *van't Hoff approach* ($\bar{x}$ = 41.32; SD = 2.96).
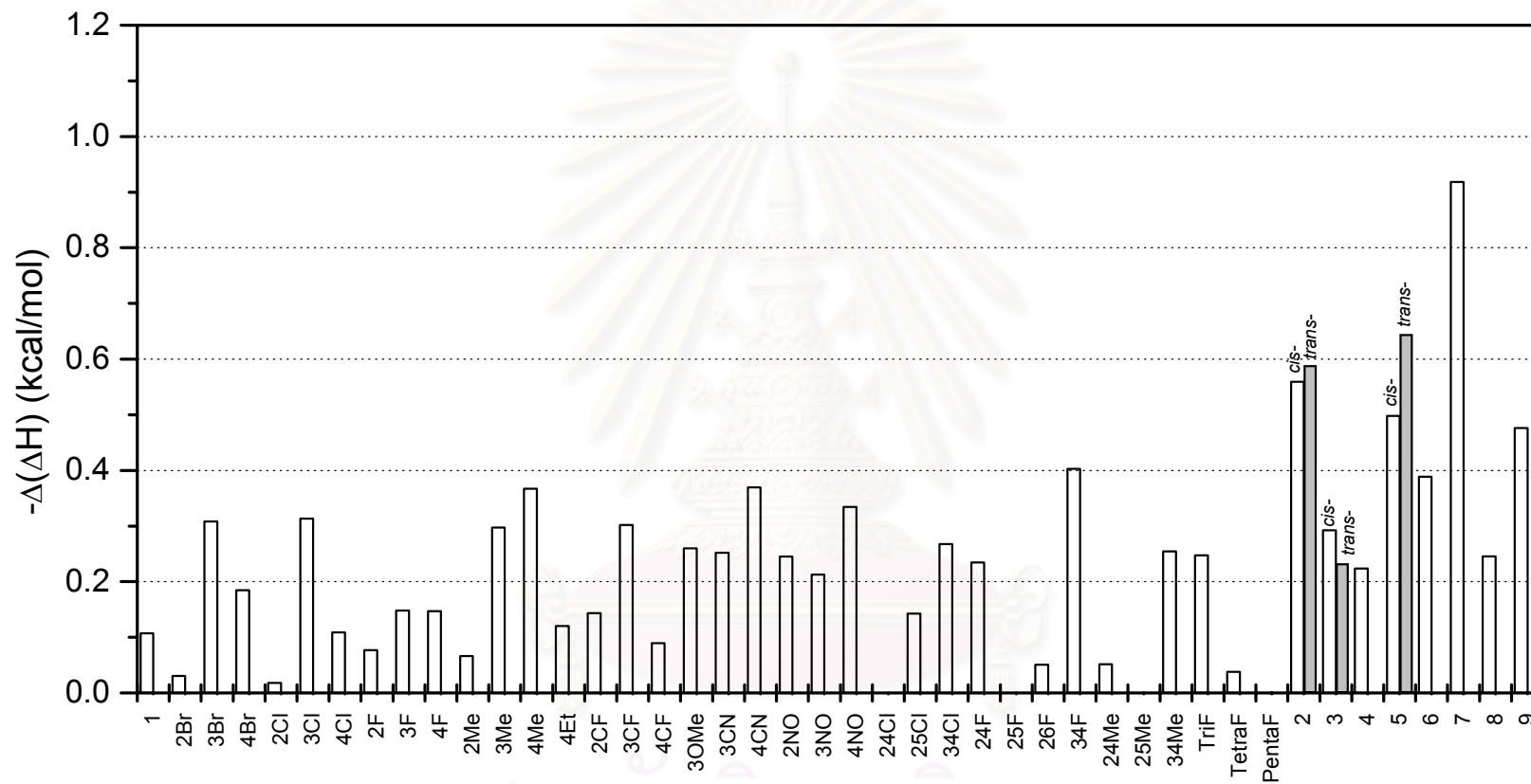
Figure C18   Difference in enthalpy values (-Δ(ΔH), kcal/mol) of the enantiomers of styrene oxide derivatives on BSiAc phase obtained from *van't Hoff approach*.
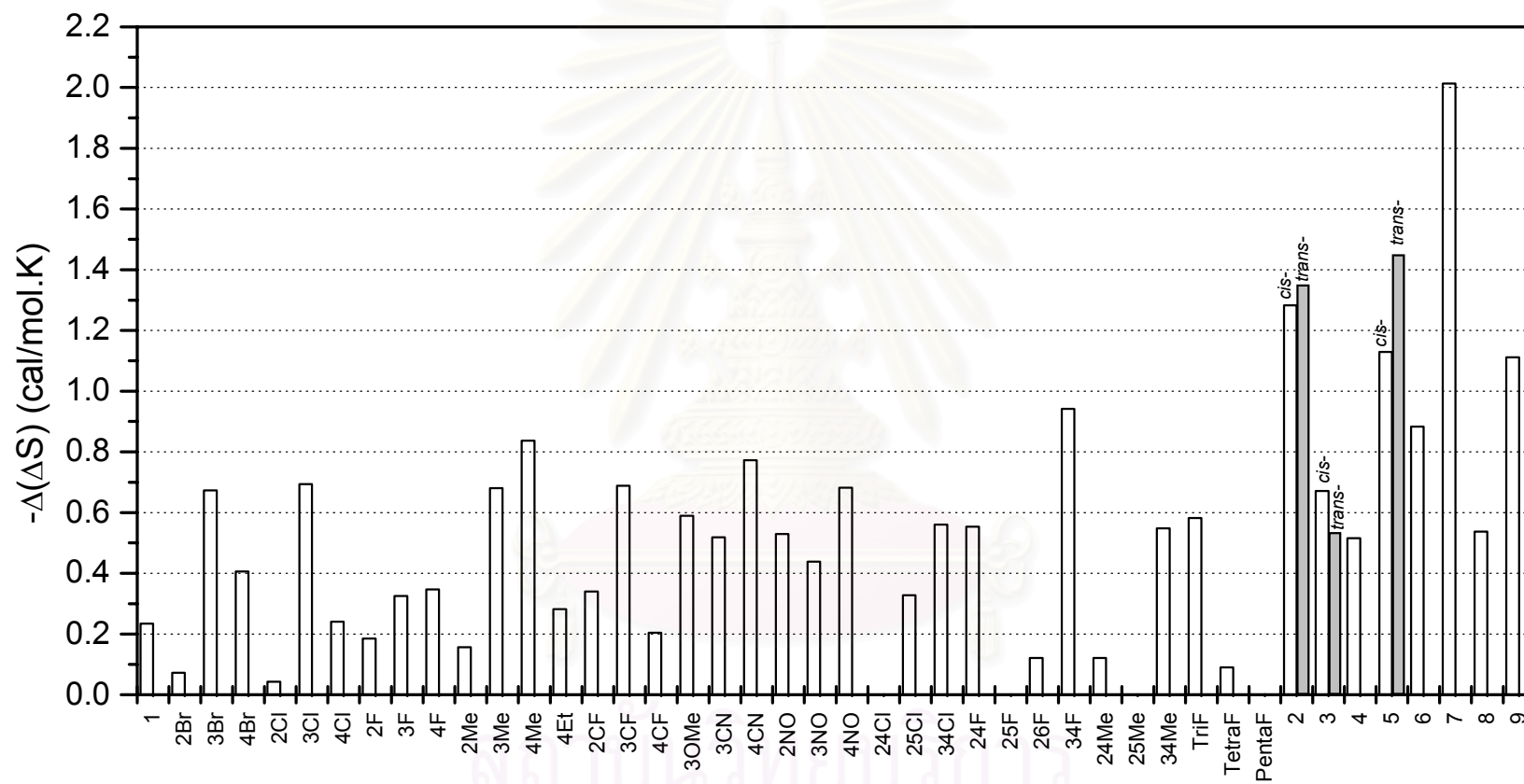
Figure C19   Difference in entropy values (-Δ(ΔS), cal/mol·K) of the enantiomers of styrene oxide derivatives on BSiAc phase obtained from *van't Hoff approach*.
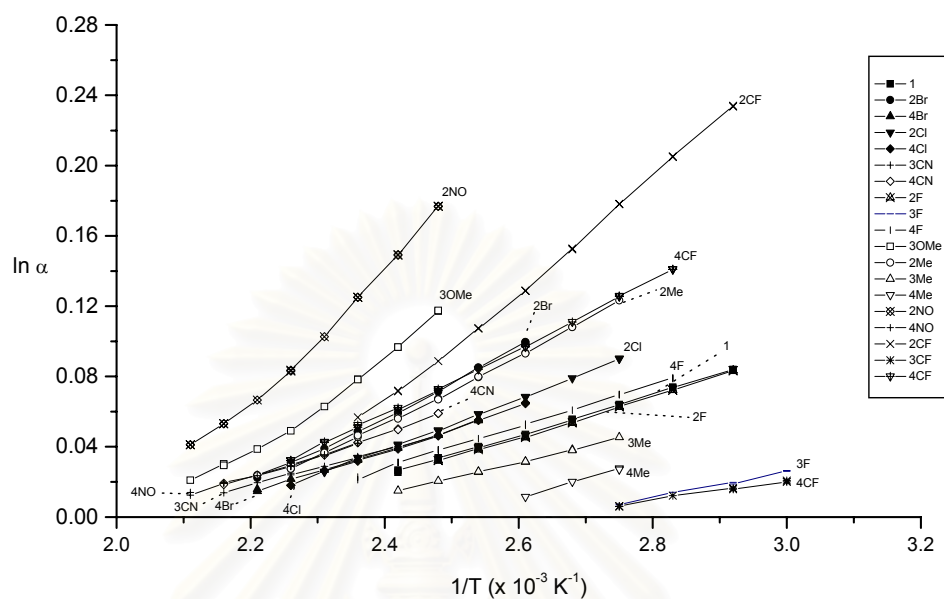
Figure C20   Plots of ln (separation factor) versus reciprocal of temperature of styrene oxide and its derivatives on BSiMe column (part I).
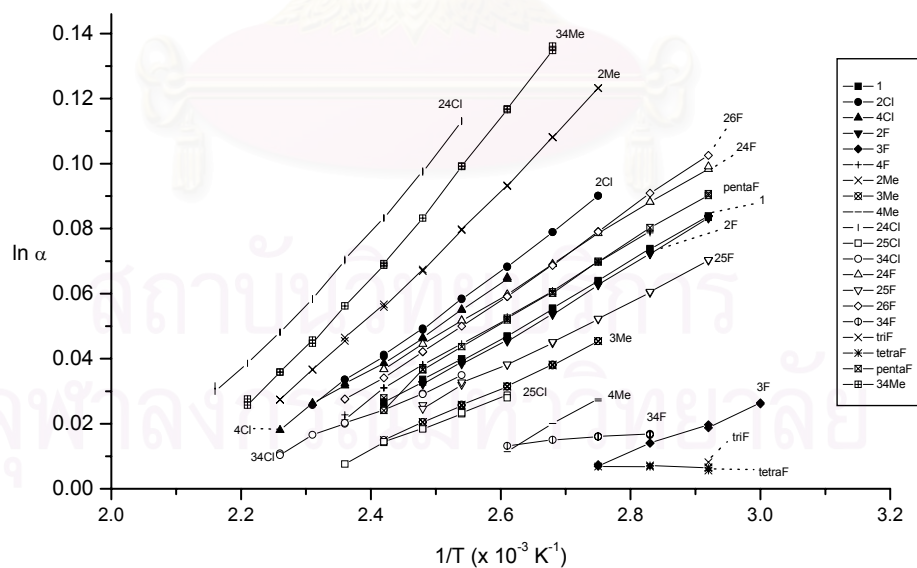
Figure C21   Plots of ln (separation factor) versus reciprocal of temperature of styrene oxide and its derivatives on BSiMe column (part II).

134
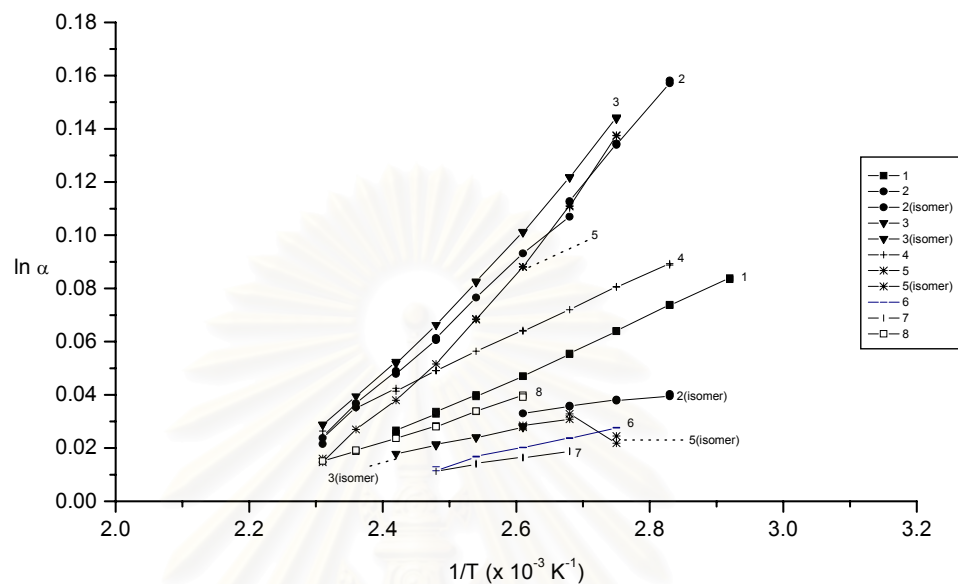
Figure C22   Plots of ln (separation factor) versus reciprocal of temperature of styrene
oxide and its derivatives on BSiMe column (part III).
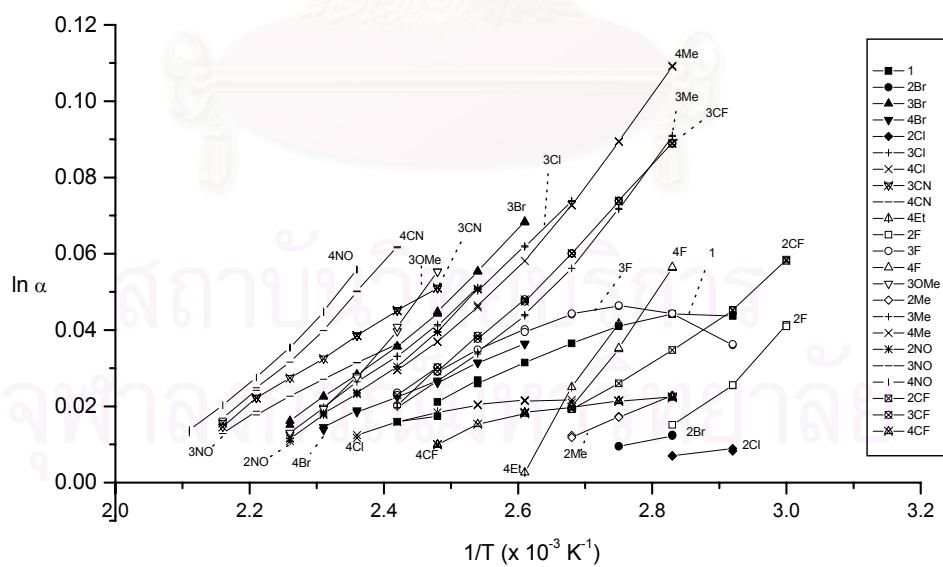
Figure C23   Plots of ln (separation factor) versus reciprocal of temperature of styrene
oxide and its derivatives on BSiAc column (part I).
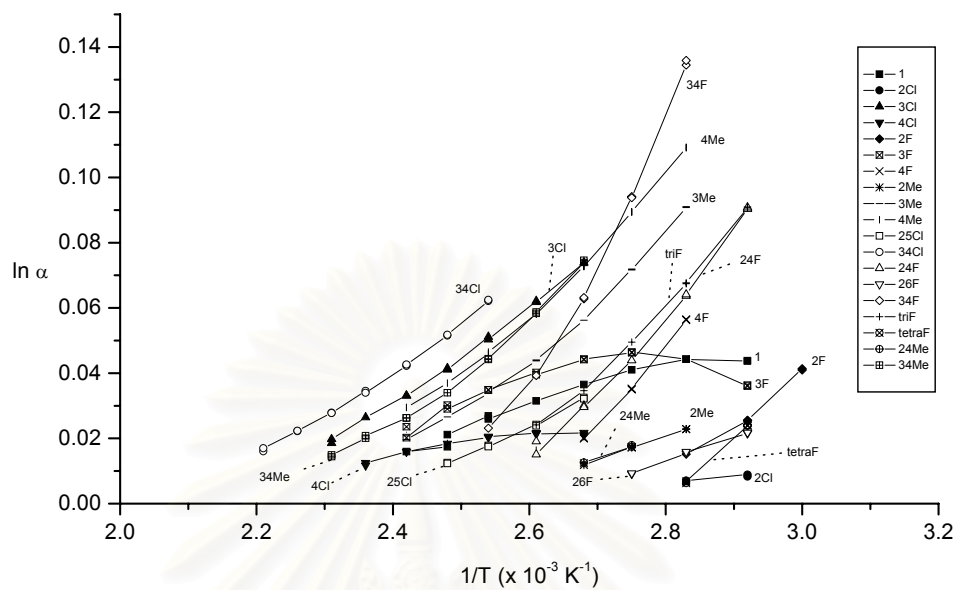
Figure C24   Plots of ln (separation factor) versus reciprocal of temperature of styrene oxide and its derivatives on BSiAc column (part II).
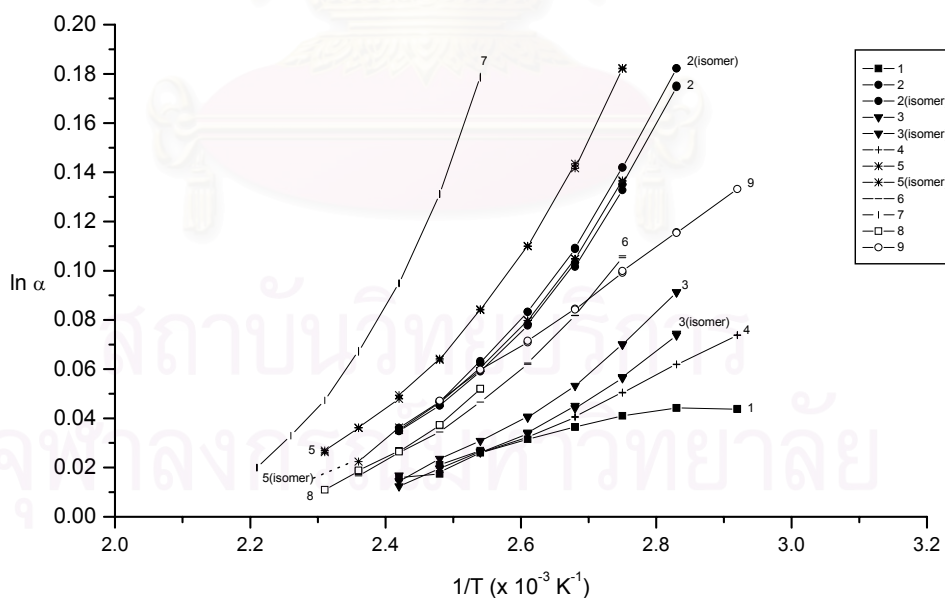
Figure C25   Plots of ln (separation factor) versus reciprocal of temperature of styrene oxide and its derivatives on BSiAc column (part III).

Table C7   Comparison of thermodynamic parameters of all epoxides on BSiMe
         column obtained from *van't Hoff approach* and *Schurig approach*.

| compound	Van't Hoff approach				Schurig approach			
	$-\Delta H_2$	$-\Delta S_2$	$-\Delta(\Delta H)$	$-\Delta(\Delta S)$	$-\Delta H_2$	$-\Delta S_2$	$-\Delta(\Delta H)$	$-\Delta(\Delta S)$
1	11.74	38.52	0.24	0.53	3.73	11.44	0.32	0.72
2Br	13.63	40.64	0.39	0.84	5.03	14.22	0.42	0.85
3Br	13.65	40.15	-	-	4.14	12.28	-	-
4Br	14.11	40.90	0.25	0.54	4.58	12.89	0.44	0.53
2Cl	13.00	40.16	0.29	0.62	4.47	13.11	0.39	0.86
3Cl	13.17	39.99	-	-	4.09	12.23	-	-
4Cl	13.57	40.65	0.32	0.71	4.47	12.78	0.37	0.81
3CN	15.10	42.24	0.22	0.46	5.39	14.91	0.28	0.57
4CN	15.40	42.64	0.28	0.58	5.51	14.88	0.34	0.70
4Et	13.43	40.56	-	-	4.14	12.33	-	-
2F	11.43	38.20	0.24	0.54	3.60	11.38	0.22	0.54
3F	11.93	39.01	0.05	0.12	3.51	10.93	0.07	0.16
4F	12.09	39.17	0.24	0.54	4.01	11.91	0.32	0.72
3OMe	13.77	40.90	0.14	0.33	3.51	10.84	0.20	4.453
2Me	12.88	40.18	0.39	0.85	4.57	13.35	0.47	1.00
3Me	12.40	39.19	0.16	0.35	3.86	11.89	0.23	0.54
4Me	12.35	38.96	0.07	0.17	3.74	11.56	0.11	0.27

compound	Van't Hoff approach				Schurig approach			
	$-\Delta H_2$	$-\Delta S_2$	$-\Delta(\Delta H)$	$-\Delta(\Delta S)$	$-\Delta H_2$	$-\Delta S_2$	$-\Delta(\Delta H)$	$-\Delta(\Delta S)$
2NO	15.25	42.85	0.72	1.45	6.69	17.90	1.43	3.06
3NO	15.34	42.00	-	-	5.07	14.31	-	-
4NO	16.04	43.07	0.22	0.44	5.78	15.33	0.25	0.50
2CF	12.49	41.01	0.68	1.53	4.38	12.96	0.36	0.58
3CF	12.29	39.99	0.04	0.11	3.69	11.61	0.03	0.07
4CF	12.99	41.14	0.40	0.85	4.27	12.29	0.31	0.57
24Cl	14.38	41.61	0.46	0.96	5.14	14.21	0.47	0.93
25Cl	14.69	42.34	0.15	0.36	5.11	14.33	0.19	0.44
34Cl	14.87	41.92	0.19	0.41	4.80	13.61	0.25	0.55
24F	11.65	38.97	0.30	0.69	3.87	11.77	0.37	0.84
25F	11.96	39.54	0.22	0.50	4.07	12.33	0.27	0.62
26F	11.95	39.09	0.30	0.67	3.56	11.40	0.38	0.84
34F	12.19	39.41	0.06	0.15	3.83	11.63	0.08	0.18
24Me	14.07	41.95	-	-	4.90	13.98	-	-
34Me	13.66	40.78	-	-	4.08	12.27	-	-
25Me	13.86	41.64	0.45	0.96	4.74	13.79	0.52	1.05
TriF	11.70	39.17	0.01	0.02	3.78	11.68	0.01	0.02
TetraF	11.17	38.18	0.01	0.04	3.23	10.71	0.01	0.04
PentaF	11.61	39.12	0.26	0.58	3.46	11.32	0.37	0.83
2 *(cis)-*	13.01	40.20	0.50	1.123	5.16	14.64	0.58	1.29

compound	Van't Hoff approach				Schurig approach			
	$-\Delta H_2$	$-\Delta S_2$	$-\Delta(\Delta H)$	$-\Delta(\Delta S)$	$-\Delta H_2$	$-\Delta S_2$	$-\Delta(\Delta H)$	$-\Delta(\Delta S)$
2 *(trans-)*	12.14	39.20	0.06	0.09	4.89	14.68	1.21	3.13
3 *(cis)-*	13.61	42.02	0.52	1.17	5.18	14.89	0.63	1.40
3 *(trans-)*	12.88	40.05	0.03	0.69	3.73	11.59	0.36	0.84
4	12.48	40.05	0.26	0.57	4.18	12.70	0.33	0.72
5 *(cis)-*	13.71	41.89	0.50	1.13	4.98	14.22	0.60	1.36
5 *(trans-)*	13.08	40.50	0.07	0.24	2.59	8.72	0.11	0.39
6	13.06	40.60	0.11	0.26	4.52	13.15	0.14	0.32
7	14.27	42.02	0.09	0.21	4.26	12.55	0.11	0.27
8	14.46	41.85	0.17	0.38	4.57	13.42	0.23	0.51
9	8.66	34.94	-	-	2.31	7.86	-	-

Table C8   Comparison of thermodynamic parameters of all epoxides on BSiAc
column obtained from *van't Hoff approach* and *Schurig approach*.

compound	*Van't Hoff approach*				*Schurig approach*			
	$-\Delta H_2$	$-\Delta S_2$	$-\Delta(\Delta H)$	$-\Delta(\Delta S)$	$-\Delta H_2$	$-\Delta S_2$	$-\Delta(\Delta H)$	$-\Delta(\Delta S)$
1	11.78	39.30	0.10	0.23	3.66	12.46	0.13	0.26
2Br	12.29	38.42	0.03	0.07	2.11	8.88	0.04	0.10
3Br	13.60	40.58	0.30	0.67	3.34	11.32	0.41	0.88
4Br	14.35	42.08	0.18	0.40	4.13	12.78	0.16	0.34
2Cl	11.91	38.40	0.01	0.04	2.39	9.57	0.02	0.05
3Cl	13.17	40.53	0.31	0.69	3.49	11.71	0.38	0.82
4Cl	13.86	41.93	0.10	0.24	4.38	13.51	0.12	0.25
3CN	15.64	43.58	0.25	0.51	-	-	-	-
4CN	17.13	46.34	0.36	0.77	-	-	-	-
4Et	13.54	41.42	0.12	0.28	4.10	13.45	0.23	0.57
2F	11.50	38.98	0.07	0.18	3.52	12.26	0.13	0.32
3F	12.48	40.88	0.14	0.32	4.35	13.91	0.16	0.34
4F	12.88	41.65	0.14	0.34	4.83	14.87	0.29	0.60
3OMe	13.94	41.53	0.26	0.59	-	-	-	-
2Me	11.58	38.01	0.06	0.16	2.14	9.13	0.14	0.35
3Me	12.20	39.37	0.29	0.68	2.96	10.88	0.52	1.20
4Me	12.83	40.65	0.36	0.83	3.76	12.52	0.57	1.30

compound	Van't Hoff approach				Schurig approach			
	$-\Delta H_2$	$-\Delta S_2$	$-\Delta(\Delta H)$	$-\Delta(\Delta S)$	$-\Delta H_2$	$-\Delta S_2$	$-\Delta(\Delta H)$	$-\Delta(\Delta S)$
2NO	13.83	40.20	0.24	0.52	-	-	-	-
3NO	16.36	44.24	0.21	0.43	-	-	-	-
4NO	18.28	47.74	0.33	0.68	-	-	-	-
2CF	10.85	37.94	0.14	0.34	2.53	10.16	0.27	0.66
3CF	12.73	41.41	0.30	0.68	4.16	13.47	0.45	1.05
4CF	13.58	43.09	0.08	0.20	4.98	14.97	0.12	0.28
24Cl	12.74	38.77	-	-	2.15	8.80	-	-
25Cl	14.92	42.48	0.26	0.56	4.00	12.46	0.36	0.75
34Cl	12.92	39.11	0.14	0.32	2.08	7.84	0.32	0.76
24F	11.83	40.02	0.23	0.55	4.17	13.64	0.39	0.95
25F	11.35	38.74	-	-	3.11	11.23	-	-
26F	11.98	36.61	0.05	0.12	3.42	11.91	0.09	0.22
34F	14.50	45.09	0.40	0.94	6.53	18.50	0.60	1.43
24Me	12.48	39.10	0.05	0.12	2.23	9.25	0.12	0.29
34Me	13.07	40.06	0.25	0.58	2.82	10.47	0.16	0.24
25Me	12.23	38.64	-	-	1.77	8.25	-	-
TriF	12.76	42.08	0.24	0.58	5.12	15.64	0.38	0.91
TetraF	12.23	40.97	0.03	0.09	4.42	14.10	0.06	0.15
PentaF	12.75	42.03	-	-	4.72	14.75	-	-
2 (cis)-	11.67	38.98	0.55	1.28	3.37	12.06	0.97	2.25

compound	Van't Hoff approach				Schurig approach			
	$-\Delta H_2$	$-\Delta S_2$	$-\Delta(\Delta H)$	$-\Delta(\Delta S)$	$-\Delta H_2$	$-\Delta S_2$	$-\Delta(\Delta H)$	$-\Delta(\Delta S)$
2 *(trans-)*	12.66	40.90	0.58	1.35	4.21	13.69	0.92	2.13
3 *(cis)-*	11.81	38.61	0.29	0.67	2.43	9.94	0.55	1.29
3 *(trans-)*	13.06	40.97	0.23	0.53	3.59	12.28	0.36	0.84
4	11.81	39.17	0.22	0.51	2.92	11.08	0.42	0.98
5 *(cis)-*	12.47	39.83	0.49	1.12	3.36	11.95	0.88	2.01
5 *(trans-)*	13.80	42.46	0.64	1.45	4.64	14.51	0.87	1.94
6	13.77	42.83	0.38	0.88	5.62	16.77	0.55	1.26
7	16.35	46.92	0.91	2.01	7.38	20.01	1.29	2.84
8	14.79	42.83	0.24	0.53	-	-	-	-
9	17.09	53.68	0.47	1.11	10.89	26.73	0.36	0.79

VITA

Miss Jirawit Yanchinda was born on Tuesday 11th April, 1978 and brought up in Bangkok, the capital city of Thailand. She completed her undergraduate study in chemitry from the Faculty of Science, Chulalongkorn University in 2001. After graduation, she continued studying for a Master of Science degree in analytical chemistry at the same university. Her current address is 38/140 M. Sangchainivate, Pathum-Bangkok Road, Bangprok, Maung, Pathumthani 12000.